

# Osteology of the Late Triassic aetosaur *Scutarx deltatylus* (Archosauria: Pseudosuchia) (#9965)

1

First submission

Please read the **Important notes** below, and the **Review guidance** on the next page. When ready [submit online](#). The manuscript starts on page 3.

## Important notes

### Editor and deadline

Mark Young / 25 Apr 2016

### Files

Please visit the overview page to [download and review](#) the files not included in this review pdf.

### Declarations

No notable declarations are present



Please in full read before you begin

## How to review

When ready [submit your review online](#). The review form is divided into 5 sections. Please consider these when composing your review:

- 1. BASIC REPORTING**
- 2. EXPERIMENTAL DESIGN**
- 3. VALIDITY OF THE FINDINGS**
4. General comments
5. Confidential notes to the editor

 You can also annotate this **pdf** and upload it as part of your review

To finish, enter your editorial recommendation (accept, revise or reject) and submit.

### BASIC REPORTING

-  Clear, unambiguous, professional English language used throughout.
-  Intro & background to show context. Literature well referenced & relevant.
-  Structure conforms to [PeerJ standard](#), discipline norm, or improved for clarity.
-  Figures are relevant, high quality, well labelled & described.
-  Raw data supplied (See [PeerJ policy](#)).

### VALIDITY OF THE FINDINGS

-  Impact and novelty not assessed. Negative/inconclusive results accepted. *Meaningful* replication encouraged where rationale & benefit to literature is clearly stated.
-  Data is robust, statistically sound, & controlled.

### EXPERIMENTAL DESIGN

-  Original primary research within [Scope of the journal](#).
-  Research question well defined, relevant & meaningful. It is stated how research fills an identified knowledge gap.
-  Rigorous investigation performed to a high technical & ethical standard.
-  Methods described with sufficient detail & information to replicate.
-  Conclusion well stated, linked to original research question & limited to supporting results.
-  Speculation is welcome, but should be identified as such.

The above is the editorial criteria summary. To view in full visit <https://peerj.com/about/editorial-criteria/>

## **Osteology of the Late Triassic aetosaur *Scutarx deltatylus* (Archosauria: Pseudosuchia).**

William G Parker

Aetosaurs are some of the most common fossils collected from the Upper Triassic Chinle Formation of Arizona, especially at the Petrified Forest National Park. Four partial skeletons collected from the park from 2002 through 2009 represent the holotype and referred specimens of *Scutarx deltatylus*. These specimens include much of the carapace, as well as the vertebral column, and shoulder and pelvic girdles. A partial skull represents the first aetosaur skull recovered from Arizona since the 1930s. *Scutarx deltatylus* can be distinguished from closely related forms *Calyptosuchus wellsi* and *Adamanasuchus eisenhardtae* not only morphologically, but also stratigraphically. Thus, *Scutarx deltatylus* is potentially an index taxon for the upper part of the Adamanian biozone.

1  
2  
3  
4  
5  
6  
7  
8  
9  
10  
11  
12  
13  
14  
15  
16  
17  
18  
19  
20  
21  
22  
23  
24

**Osteology of the Late Triassic aetosaur *Scutarx deltatylus*  
(Archosauria: Pseudosuchia).**

William G. Parker<sup>1,2</sup>

<sup>1</sup> Division of Resource Management, Petrified Forest National Park, Petrified Forest, Arizona, U.S.A.

<sup>2</sup> Department of Geosciences, The University of Texas, Austin, Texas, U.S.A.

Corresponding Author:

William Parker

1 Park Road, #2217, Petrified Forest, Arizona, 86028, U.S.A.

Email address: [William\\_Parker@nps.gov](mailto:William_Parker@nps.gov)

## 25 Abstract

26  
27 Aetosaurs are some of the most common fossils collected from the Upper Triassic Chinle  
28 Formation of Arizona, especially at the Petrified Forest National Park. Aetosaurs collected from  
29 lower levels of the park include *Desmotosuchus spurensis*, *Paratypothorax*, *Adamanasuchus*  
30 *eisenhardtae*, *Calyptosuchus wellesi*, and *Scutarx deltatylus*. Four partial skeletons collected  
31 from the park from 2002 through 2009 represent the holotype and referred specimens of *Scutarx*  
32 *deltatylus*. These specimens include much of the carapace, as well as the vertebral column, and  
33 shoulder and pelvic girdles. A partial skull represents the first aetosaur skull recovered from  
34 Arizona since the 1930s. *Scutarx deltatylus* can be distinguished from closely related forms  
35 *Calyptosuchus wellesi* and *Adamanasuchus eisenhardtae* not only morphologically, but also  
36 stratigraphical.  Thus, *Scutarx deltatylus* is potentially an index taxon for the upper part of the  
37 Adamanian biozone.

## 38 Introduction

39 The Triassic Period is a key transitional point in Earth history, when remnants of  
40 Paleozoic biotas were replaced by a Mesozoic biota including components of recent ecosystems  
41 (e.g., Fraser 2006). Prominent in this new radiation were the archosaurs, which include the  
42 common ancestor of birds and crocodylians and all of their descendants (Gauthier 1986). The  
43 early appearance and diversification of this important clade is of interest because beginning in  
44 the Triassic, the archosaurs almost completely dominated all continental ecosystems throughout  
45 the entire Mesozoic (e.g., Nesbitt 2011). Because the Triassic globe had a coalesced  
46 supercontinent, Pangaea, the Laurasian and Gondwanan continental faunas are often considered  
47 to be cosmopolitan in their distribution, presumably because of a lack of major oceanic barriers

48 (Colbert 1971). Thus many Triassic taxa were considered widespread and widely applicable for  
49 global biostratigraphy (e.g., Lucas 1998a).

50 More recent work suggests that this is a gross oversimplification of the taxonomic  
51 diversity present at the time (e.g., Irmis et al. 2007a; Nesbitt, Irmis & Parker 2007; Nesbitt et al.  
52 2009a; Nesbitt et al. 2009b) and new research on many Triassic groups is showing evidence for  
53 endemism of species-level taxa (e.g., Martz & Small 2006; Parker 2008a; Parker 2008b; Stocker  
54 2010), with distinct patterns of radiation of more inclusive clades into new areas (e.g., Nesbitt et  
55 al. 2010). Key to this change in thinking are the utilization of testable techniques such as  
56 apomorphy-based identification of fossils (e.g., Irmis et al. 2007b; Nesbitt & Stocker 2008) and  
57 improved phylogenetic approaches to archosaur relationships and paleobiogeography (e.g., Irmis  
58 2008; Nesbitt 2011; Nesbitt et al. 2010). The apomorphy-based approach reveals hidden  
59 diversity in faunal assemblages resulting in the recognition of new distinct taxa (e.g., Nesbitt &  
60 Stocker 2008).

61 Aetosaurians are quadrupedal, heavily armored, suchian archosaurs with a global  
62 distribution, restricted to non-marine strata of the Late Triassic (Desojo et al. 2013).  
63 Aetosaurians are characterized by their specialized skull with partially edentulous ws, an  
64 upturned premaxillary tip, and laterally facing supratemporal fenestrae  another key feature of  
65 aetosaurians is a heavy carapace consisting of four columns of rectangular dermal armor, two  
66 paramedian columns that straddle the midline, and two lateral columns (Walker 1961). Ventral  
67 and appendicular osteoderms are also present in most taxa. Aetosaurian osteoderms possess  
68 detailed ornamentation on the dorsal surface, the patterning of which is diagnostic for  (Long  
69 & Ballew 1985). Thus, the type specimens of several aetosaurian taxa consist solely of  
70 osteoderms (e.g., *Typothorax coccinarum* Cope 1875; *Paratypothorax andressorum* Long and

71 Ballew 1985; *Lucasuchus hunti* Long and Murry 1995; *Rioarribasuchus chamaensis* Zeigler,  
72 Heckert & Lucas 2003; *Apachesuchus heckerti* Spielmann & Lucas 2012) or consist chiefly of  
73 osteoderms (e.g., *Calyptosuchus wellsi* Long & Ballew 1985; *Typothorax antiquus* Lucas,  
74 Heckert & Hunt 2003; *Tecovasuchus chatterjeei* Martz & Small 2006; *Adamanasuchus*  
75 *eisenhardtae* Lucas, Hunt, and Spielmann 2007; *Sierritasuchus macalpini* Parker, Stocker &  
76 Irmis 2008). Aetosaurian osteoderms and osteoderm fragments are among the most commonly  
77 recovered fossils from Upper Triassic strata (Heckert & Lucas 2000). Because of this abundance,  
78 in concert with the apparent ease of taxonomic identification, global distribution in non-marine  
79 strata, and limited stratigraphic range (e.g., Upper Triassic) aetosaurians have been proposed as  
80 key index fossils for use in regional and global non-marine biostratigraphy (e.g., Heckert et al.  
81 2007a; Heckert et al. 2007b; Long & Ballew 1985; Lucas 1998; Lucas & Heckert 1996; Lucas et  
82 al. 1997; Lucas & Hunt 1993; Lucas et al. 2007; Parker & Martz 2011). Four Land Vertebrate  
83 Faunachrons (LVF) were erected that use aetosaurians to divide the Late Triassic Epoch (Lucas  
84 & Hunt 1993), from oldest to youngest these are the Otischalkian (middle Carnian); Adamanian  
85 (late Carnian); Revueltian (Norian), and the Apachean (Rhaetian). These were redefined as  
86 biozones by Parker and Martz (2011).

87 Aetosaurians are one of the most commonly recovered vertebrate fossils in the Upper  
88 Triassic Chinle Formation at Petrified Forest National Park (PEFO), Arizona. Paleontological  
89 investigations in the park between 2001 and 2009 resulted in the discovery of four partial  
90 skeletons that are considered a new taxon (Parker 2016). The first specimen (PEFO 31217),  
91 discovered in 2001 and collected in 2002 from Petrified Forest Vertebrate Locality (PFV) 169  
92 (Battleship Quarry; Figure 1), was initially assigned to *Calyptosuchus* (= *Stagonolepis*) *wellsi*  
93 based on characters of the armor and vertebrae (Parker & Irmis 2005). The second partial

94 skeleton was collected in 2004 from PFV 304 (Milkshake Quarry), at the south end of the park  
95 (Figure 1). That specimen (PEFO 34045) was also mentioned by Parker and Irmis (2005), who  
96 noted differences in the armor from *Calyptosuchus wellesi* and suggested that might represent a  
97 distinct species. The other two specimens were collected in 2007 and 2009. The first (PEFO  
98 34616), from the Billings Gap area (PFV 355; Figure 1) is notable because it included the first  
99 aetosaurian skull to be recovered in the park. The second specimen (PEFO 34919) was recovered  
100 from the Saurian Valley area of the Devils Playground (PFV 224; Figure 1). All four of these  
101 specimens were originally assigned to *Calyptosuchus wellesi* by Parker and Martz (2011) and  
102 used to construct the stratigraphic range for that taxon. *Calyptosuchus* is considered to be an  
103 index taxon of the Adamanian biozone (Lucas & Hunt 1993; Parker & Martz 2011).

104 Subsequent preparation and more detailed examination of these four specimens led to the  
105 discovery that they all shared a key autapomorphy, the presence of a prominent, raised triangular  
106 protuberance in the posteromedial corner of the paramedian osteoderms. The protuberance is not  
107 present on any of the osteoderms of the holotype of *Calyptosuchus wellesi* (UMMP 13950). It is  
108 also absent on the numerous paramedian osteoderms of *Calyptosuchus wellesi* recovered from  
109 the *Placerias* Quarry of Arizona in collections at the UCMP and the MNA. That autapomorphy  
110 and several features of the cranium and pelvis differentiate these specimens from all other known  
111 aetosaurians and form the basis for assigning these materials to a new taxon, *Scutarx deltatylus*  
112 (Parker 2016).

113 .

114 ***Institutional abbreviations*** –DMNH, Perot Museum of Natural History, Dallas, Texas, USA;  
115 MCZD, Marischal College Zoology Department, University of Aberdeen, Aberdeen, Scotland,  
116 UK; NCSM, North Carolina State Museum, Raleigh, North Carolina, USA; NHMUK, The

117 Natural History Museum, London, United Kingdom; **NMMNH**, New Mexico Museum of  
118 Natural History and Science, Albuquerque, New Mexico, USA; **MNA**, Museum of Northern  
119 Arizona, Flagstaff, Arizona, USA; **PEFO**, Petrified Forest National Park, Petrified Forest,  
120 Arizona, USA; **PFV**, Petrified Forest National Park Vertebrate Locality, Petrified Forest,  
121 Arizona, USA; **PVL**, Paleontología de Vertebrados, Instituto ‘Miguel Lillo’, San Miguel de  
122 Tucumán, Argentina; **PVSJ**, División de Paleontología de Vertebrados del Museo de Ciencias  
123 Naturales y Universidad Nacional de San Juan, San Juan, Argentina; **TMM**, Vertebrate  
124 Paleontology Laboratory, University of Texas, Austin, Texas, USA; **TTU P**, Museum of Texas  
125 Tech, Lubbock, Texas, USA; **UCMP**, University of California, Berkeley, California, USA;  
126 **UMMP**, University of Michigan, Ann Arbor, Michigan, USA; **USNM**, National Museum of  
127 Natural History, Smithsonian Institution, Washington, D.C., USA; **VPL**, Vertebrate  
128 Paleontology Lab, University of Texas at Austin, Austin, Texas, USA; **YPM**, Yale Peabody  
129 Museum of Natural History, New Haven, Connecticut, USA; **ZPAL**, Institute of Paleobiology of  
130 the Polish Academy of Sciences in Warsaw, Warsaw; Poland.

### 131 **GEOLOGICAL SETTING**

132 The four localities from which the material of *Scutarx deltatylus* was collected all occur  
133 in the lower part of the Sonsela Member of the Chinle Formation (Martz & Parker 2010) (Figure  
134 2). In the PEFO region the Sonsela Member can be divided into five distinct beds, the Camp  
135 Butte, Lot’s Wife, Jasper Forest, Jim Camp Wash, and Martha’s Butte beds (Martz & Parker  
136 2010). The Lot’s Wife, Jasper Forest, and Martha’s Butte beds are sandstone dominated, cliff  
137 forming units with source areas to the south and west (Howell & Blakey 2013), whereas the  
138 Lot’s Wife and Martha’s Butte beds are slope forming units with a higher proportion of  
139 mudrocks than sandstones (Martz & Parker 2010). All of these localities represent proximal

140 floodplain facies associated with a braided river system (Howell & Blakey 2013; Martz & Parker  
141 2010; Woody 2006).

142 PFV 169 and PFV 224 occur in the upper part of the Lot's Wife beds, PFV 355 is  
143 situated in the base of the Jasper Forest bed, and PFV 304 marks the highest stratigraphic  
144 occurrence, located in the lower part of the Jim Camp Wash beds (Figure 2). All of these sites  
145 are below the 'persistent red silcrete,' a thick, chert, marker bed that approximates the  
146 stratigraphic boundary between the Adamanian and Revueltian biozones (Martz & Parker 2010;  
147 Parker & Martz 2011). Exact locality information is available at Petrified Forest National Park to  
148 qualified researchers. Non-disclosure of locality information is protected by the Paleontological  
149 Resources Preservation Act of 2009.

150 A high concentration of volcanic material in mudrocks of the Chinle Formation includes  
151 detrital zircons and allows for determination of high precision radioisotopic dates for studied  
152 beds (Figure 2; Ramezani et al. 2011). Zircons from the top of the Lot's Wife beds provided an  
153 age of  $219.317 \pm 0.080$  Ma (sample SBJ; Ramezani et al. 2011). The base of the unit is  
154 constrained by an age of  $223.036 \pm 0.059$  Ma for the top of the underlying Blue Mesa Member  
155 (sample TPs; Ramezani et al. 2011). Ages of  $218.017 \pm 0.088$  Ma (sample GPL) and  $213.870 \pm$   
156  $0.078$  (sample KWI) are known from the Jasper Forest bed and the overlying Jim Camp Wash  
157 beds constraining the upper age for the fossil specimens (Ramezani et al. 2011).

## 158 MATERIALS AND METHODS

159 All specimens were excavated utilizing small hand tools, although a backhoe tractor was  
160 used initially to remove overburden at PFV 304. B-15 Polyvinyl Acetate "Vinac" (Air Products  
161 & Chemicals, Inc.) and B-76 Butvar (Eastman Chemical Company) dissolved in acetone were  
162 used as a consolidant in the field. PEFO 31217 was discovered partly in unconsolidated, heavily

163 weathered sediment with numerous plant roots growing over and through the bones. Small  
164 handtools, including brushes, caused damage to the bone surface so plastic drinking straws were  
165 used to blow away sediment from the bone surface, which was then quickly hardened with a  
166 consolidant. In the lab the same specimen quickly deteriorated upon exposure, and liberal  
167 amounts of extremely thin Paleobond cyanoacrylate (Uncommon Conglomerates) was applied to  
168 stop disintegration. Because of the delicate nature of this specimen and the application of the  
169 cyanoacrylate, many of the bones cannot be prepared further or removed from the original field  
170 jackets. Furthermore, during collection the condition of the bones and surrounding matrix  
171 proved to be so poor that a portion of the jacket with the scapulocoracoid in it was lost during  
172 turning. This lost material consisted mostly of trunk vertebrae, ribs, and osteoderms.

173 The other three skeletons were consolidated in the lab using B-72 Butvar (Eastman  
174 Chemical Company), with Paleobond (Uncommon Conglomerates) cyanoacrylate used in many  
175 cases for permanent bonds. Paleobond (Uncommon Conglomerates) accelerator was originally  
176 used on some of the bones in PEFO 34045, but was halted because it was causing discoloration  
177 of the bone surface during the curing process. PEFO 34919 is coated with thin layers of hematite  
178 as is common for fossil specimens recovered from sandy facies in the Devils Playground region  
179 of PEFO. Mechanical preparation with pneumatic tools damaged the bone surface upon  
180 removing the coating and revealed that the hematite had permeated numerous microfractures in  
181 the bones, expanding them slightly, or in some bones significantly. As a result, the non-  
182 osteoderm bones from PFV 224 are highly deformed and often 'mashed' into the associated  
183 osteoderms. Further preparation to remove the hematite coating was not attempted.

184

## 185 **Naming Conventions for Aetosaurian Osteoderms**

186

187 Traditionally, identification and naming of aetosaurian osteoderms, which cover the  
188 dorsal, ventral, and appendicular areas, utilizes terms first originated by Long & Ballew (1985).  
189 In this convention the dorsal armor (carapace) consists of two midline ‘paramedian’ columns  
190 flanked laterally by two ‘lateral’ columns (Desojo et al. 2013; Long & Ballew 1985). By  
191 convention, osteoderms of the dorsal region are named from the type of vertebrae they cover  
192 (e.g., cervical, dorsal, and caudal; (Long & Ballew 1985)). However, the anteriormost  
193 paramedian osteoderms lack equivalent lateral osteoderms causing a potential numbering offset  
194 between the presacral paramedian and lateral rows (Heckert et al. 2010). Aetosaurians also  
195 possess ventral armor at the throat, as well as ventral armor (plastron) that underlies the ‘dorsal’  
196 (=trunk) and caudal vertebrae. The presence of ventral armor of the ‘dorsal’ series creates the  
197 awkward combination of ‘ventral-dorsal’ osteoderms. Therefore there is a need to standardize  
198 the positional nomenclature for aetosaurian osteoderms.

199 The term carapace properly refers only to the dorsally situated network of osteoderms,  
200 thus the term ‘dorsal carapace’ is incorrect and redundant. In this study the term carapace refers  
201 only to the dorsally situated osteoderms and the term ventral osteoderms (or in some cases,  
202 plastron) is used for all ventrally situated osteoderms.

203 The carapace can be divided into four anteroposteriorly trending columns of osteoderms  
204 (Heckert et al. 2010). Those that straddle the mid-line are referred to as the paramedians and the  
205 flanking osteoderms are called the lateral armor (Long & Ballew 1985). Each column is divided  
206 into rows and as noted above these have traditionally been given names based on the vertebral  
207 series they cover (in most taxa there is a 1:1 ratio between osteoderms and vertebrae 

208 The two anteriormost paramedian osteoderms fit into the back of the skull and are  
209 generally mediolaterally oval and lack corresponding lateral osteoderms. These osteoderms are  
210 termed the nuchal series (Figure 3; Desojo et al. 2013; Sawin 1947; Schoch & Desojo 2016).  
211 Posterior to these are roughly five, six, or nine rows of paramedian and lateral osteoderms that

212 cover the entire cervical vertebral series, termed cervical osteoderms (Figure 3; Long & Ballew  
213 1985). The patch of osteoderms beneath the cervical vertebrae in the throat area would be called  
214 the **gular osteoderms**, ed on the name given to these osteoderms in phytosaurians (Long &  
215 Murry 1995).

216 The next vertebral series initiates with the 10<sup>th</sup> presacral vertebra. On this vertebra the  
217 parapophysis has moved up to the top of the centrum, just below the level of the neurocentral  
218 suture. In the previous nine vertebrae (the cervical series), the parapophysis is situated at the base  
219 of the centrum, and in the eleventh vertebra the parapophysis is situated on the transverse process.  
220 Thus the 10<sup>th</sup> presacral is transitional in form and has been considered to be the first of the  
221 ‘dorsal’ series (Case 1922; Parker 2008a; Walker 1961), and that convention is followed here.

222 Historically in aetosaurians these vertebrae have been referred to as the dorsal series and  
223 osteoderms covering these vertebrae are the ‘dorsal osteoderms’ (e.g., Desojo et al. 2013;  
224 Heckert & Lucas 2000; Long & Ballew 1985; Long & Murry 1995); however, this term has  
225 become problematic because whereas all of the osteoderms below the vertebral column are  
226 termed the ventral osteoderms, only those of above the vertebral column in the trunk region are  
227 called the dorsals. Thus technically the osteoderms beneath the caudal vertebrae would be the  
228 caudal ventral osteoderms and those beneath the ‘dorsal’ vertebrae would be the dorsal ventral  
229 osteoderms. This is non-sensical so a new term is suggested be used for what have been known  
230 as the dorsal vertebrae and osteoderms in aetosaurians. The terms thoracic and lumbar vertebrae  
231 reflect the chest and loin areas respectively and are assigned depending on the presence or  
232 absence of free ribs. This is not readily applicable to aetosaurians ere there are ribs through  
233 the entire series. Instead the term trunk vertebrae is used, which is commonly used for  
234 amphibians and lepidosaurs, which also tend to have a ribs throughout the entire series (e.g.,  
235 Wake 1992). The osteoderms above the trunk vertebrae are the dorsal trunk paramedian and  
236 dorsal trunk lateral osteoderms. The osteoderms located beneath the trunk vertebrae are the  
237 ventral trunk osteoderms and consists of numerous columns of osteoderms (Figure 3; Walker  
238 1961). Heckert et al. (2010) utilized the term ventral thoracic osteoderms, which effectively

239 solves the ‘ventral dorsal’ problem; however, the term ventral trunk osteoderms is preferred here  
240 to maintain consistency with the term dorsal trunk osteoderms.

241 The osteoderms above the caudal vertebrae are termed the dorsal caudal osteoderms and  
242 consist of paramedian and lateral columns (Figure 3; Long & Ballew 1985). The osteoderms  
243 beneath the caudal vertebrae are the ventral caudal osteoderms (Heckert et al. 2010) and also  
244 consist of paramedian and lateral columns behind the cloacal area (fourth row) to the tip of the  
245 tail (Jepson 1948; Walker 1961), the first two lateral rows bear spines in *Typothorax coccinarum*  
246 (Heckert et al. 2010). An assemblage of irregular shaped osteoderms are located anterior to the  
247 cloacal area is preserved in *Stagonolepis robertsoni*, *Aetosaurus ferratus*, and *Typothorax*  
248 *coccinarum* (Heckert et al. 2010; Schoch 2007; Walker 1961), which can be called the cloacal  
249 osteoderms. Small masses of irregular shaped osteoderms cover the limb elements of  
250 aetosaurians (e.g., Heckert & Lucas 1999; Heckert et al. 2010; Schoch 2007). These have  
251 collectively been termed as simply appendicular osteoderms. However, when found in  
252 articulation they can be differentiated by the limb that is covered, including the humeral,  
253 radioulnar, femoral, and tibiofibular osteoderms (Hill 2010).

254  
255

## 256 SYSTEMATIC PALEONTOLOGY

257 Archosauria Cope 1869 *sensu* Gauthier & Padian 1985.

258 Pseudosuchia Zittel 1887-90 *sensu* Gauthier & Padian 1985.

259 Aetosauria Marsh 1884 *sensu* Parker, 2007.

260 Stagonolepididae Lydekker 1887 *sensu* Heckert & Lucas 2000.

261 *Scutarx deltatylus* Parker 2016

262 (Figs. 4 – 25)

263

- 264 1985 *Calyptosuchus wellesi*: Long and Ballew, p. 54, fig. 13a.  
 265 1995 *Stagonolepis wellesi*: Long and Murry, p. 82, figs. 71b, 72b, e.  
 266 2005 *Stagonolepis wellesi*: Parker and Irmis, p. 49, fig. 4a.  
 267 2005a *Stagonolepis wellesi*: Parker, p. 44.  
 268 2005b *Stagonolepis wellesi*: Parker, p. 35.  
 269 2006 *Stagonolepis wellesi*: Parker, p. 5.  
 270 2011 *Calyptosuchus wellesi*: Parker and Martz, p. 242.  
 271 2013 *Calyptosuchus wellesi*: Martz et al., p. 342, figs. 7a-d.  
 272 2014 *Calyptosuchus wellesi*: Roberto-Da-Silva et al., p. 247.  
 273 2016 *Scutarx deltatylus*: Parker, p. 27, figs. 2-5.  
 274

275 ***Holotype*** – PEFO 34616, posterior portion of skull with braincase, cervical and dorsal  
 276 trunk paramedian and dorsal trunk lateral osteoderms, ventral osteoderms, rib fragments, and  
 277 paired gastral ribs.

278 ***Paratypes*** -- PEFO 31217, much of a postcranial skeleton including vertebrae, pectoral and pelvic girdles, osteoderms; PEFO 34919, much of a postcranial skeleton including  
 279 pectoral and pelvic girdles, osteoderms; PEFO 34919, much of a postcranial skeleton including  
 280 vertebrae, ribs, osteoderms, girdle fragments, ilium; PEFO 34045, much of a postcranial skeleton  
 281 including vertebrae, ribs, and osteoderms.

282 ***Referred Specimens*** -- UCMP 36656, UCMP 35738, dorsal trunk paramedian and dorsal  
 283 trunk lateral osteoderms (lower part of the Chinle Formation, Nazlini, Arizona); TTU P-09240,  
 284 left and right dorsal trunk paramedian osteoderms (Cooper Canyon Formation, Dockum Group,  
 285 Post, Texas).

286 ***Locality, Horizon, and Age*** -- PFV 255 (The Sandcastle), Petrified Forest National Park,  
 287 Arizona; lower part of the Sonsela Member, Chinle Formation; Adamanian biozone, Norian,  
 288 ~217 Ma (Ramezani et al. 2011).

289 ***Diagnosis*** – From Parker (2016): Medium-sized aetosaurian diagnosed by the following  
 290 autapomorphies; the cervical and dorsal trunk paramedian osteoderms bear a strongly raised,  
 291 triangular tuberosity in the posteromedial corner of the dorsal surface of the osteoderm; the

292 occipital condyle lacks a distinct neck because the condylar stalk is mediolaterally broad; the  
293 base of the cultriform process of the parabasisphenoid bears deep lateral fossae; the frontals and  
294 parietals are very thick dorsoventrally; and there is a distinct fossa or recess on the lateral surface  
295 of the ilium between the supraacetabular crest and the posterior portion of the iliac blade. *Scutarx*  
296 *deltatylus* can also be differentiated from other aetosaurs a unique combination of characters  
297 including moderately wide dorsal trunk paramedian osteoderms with a strongly raised anterior  
298 bar that possesses anteromedial and anterolateral processes (shared with all aetosaurians except  
299 *Desmotosuchini*); osteoderm surface ornamentation of radiating ridges and pits that emanate  
300 from a posterior margin contacting a dorsal eminence (shared with *Calyptosuchus wellsi*,  
301 *Stagonolepis robertsoni*, *Adamanasuchus eisenhardtae*, *Neoaetosauroides engaeus*, and  
302 *Aetosauroides scagliai*); lateral trunk osteoderms with an obtuse angle between the dorsal and  
303 lateral flanges (shared with non-desmotosuchines); a dorsoventrally short pubic apron with two  
304 proximally located ‘obturator’ fenestrae (shared with *Stagonolepis robertsoni*); and an  
305 extremely anteroposteriorly short parabasisphenoid, with basal tubera and basiptyergoid  
306 processes almost in contact and a reduced cultriform process (shared with *Desmotosuchus*).

## 307 DESCRIPTION

### 308 Skull

309 Much of the posterodorsal portion of the skull is present in PEFO 34616 (Figures 4-10).

310 Elements preserved include much of the left nasal, both frontals (the right is incomplete), both

311 postfrontals, the left parietal (badly damaged), the left and right squamosals, the right postorbital,

312 a portion of the left postorbital, and a nearly complete occipital region and braincase. The skull

313 was already heavily eroded when discovered and although the skull roof/braincase portion was

314 collected *in situ*, the remaining elements had to be carefully pieced back together from many  
315 fragments collected as float. Accordingly many of the skull roof elements are incomplete.

316 Much of the skull appears to have separated originally along some of the sutures, notably  
317 those between the prefrontal-frontal, squamosal-quadrato, and postorbital-quadratojugal contacts  
318 The left frontoparietal suture is also visible because of bone separation, and the sockets in the  
319 squamosals for reception of the proximal heads of the quadrates are well-preserved. Thus, the  
320 skull appears to have mostly fallen apart before burial and many of the anterior and ventral  
321 elements were presumably scattered and lost during disarticulation, with the exception of the left  
322 nasal, which is represented as an isolated piece. Similar preservation exists for the skull roof of  
323 the holotype of *Stagonolepis olenkae* (ZPAL AbIII/466/17) in which the frontal, parietals,  
324 occipital, and braincase are preserved as a single unit. This may suggest that the posterodorsal  
325 portion of the skull fuses earlier in ontogeny in these taxa. The skull of *Scutarx deltatylus*  
326 features a well-preserved braincase, which is described in detail below. Sutures are difficult to  
327 observe because of the state of preservation of the specimen, and the skull of *Longosuchus*  
328 *meadei* (TMM 31185-98) was used to infer the locations of various sutures, based on observable  
329 landmarks present in PEFO 34616.

### 330 *Nasal*

331 The proximal half of the left nasal is preserved, consisting of the main body and the  
332 posterior portion of the anterior projection through the mid-point of the external naris (Figure 4).  
333 The main body is dorsoventrally thick and the entire element is slightly twisted dorsomedially so  
334 that the dorsal surface is noticeably concave. Any surface ornamentation is obscured by a thin  
335 coating of hematite. The midline symphysis is straight and slightly rugose (Figure 4). The lateral  
336 surface is damaged along the lacrimal suture; however, more anteriorly, the sutural surface for

337 the ascending process of the maxilla is preserved and is strongly posteroventrally concave  
338 (Figure 4). Anteriorly the nasal narrows mediolaterally where it forms the dorsal margin of the  
339 external naris. The ventral process of the nasal that borders the posterior edge of the naris is  
340 missing its tip but it is clear from what is preserved that it was not elongate as in *Aetosauroides*  
341 *scagliai* but rather short as in *Stagonolepis olenkae* (ZPAL AbIII/346). 

342

### 343 ***Frontal***

344 Both frontals are present, with the left nearly complete and the right missing the posterior  
345 portion (Figure 5). The extreme dorsoventral thickness of the element is evident, as the  
346 dorsoventral thickness is 0.35 times the midline length of the element. The frontals appear to be  
347 hollow; however, this is most likely from damage during deposition and subsequent weathering  
348 before the skull roof was collected and pieced back together. In dorsal view the posterior margin  
349 of the frontal is slanted posterolaterally as in *Stagonolepis robertsoni* (Walker 1961) so that the  
350 lateral margin of the frontal is longer than the medial margin, forming a distinct posterolateral  
351 process (Figure 5)  the anterior portion of that process meets the postfrontal laterally and the  
352 parietal posteriorly as in *Stagonolepis olenkae* (Sulej 2010). Just anterior to the posterolateral  
353 process the frontal forms the dorsal margin of the orbit. The position of the suture with the  
354 postfrontal is not clear, but it should have been present as in all other aetosaurians.

355 The dorsal surfaces of the frontals are rugose, ornamented with deep pits, some  
356 associated with more elongate grooves. Laterally above the round orbits and anteriorly there is  
357 are wider, anteroposteriorly oriented grooves as in *Stagonolepis olenkae* (Sulej 2010). These  
358 grooves demarcate a raised central portion of the frontals as described for *Stagonolepis*  
359 *robertsoni* by Walker (1961). The anterolateral margins of the frontals are dorsoventrally thick,

360 rugose, anteromedially sloping areas that are bounded posteriorly by a thin curved ridge. These  
361 are the sutures for the prefrontals (Figures 5-6). There is no clear evidence for articulation of a  
362 palpebral bone at this position as in *Stenomyti huangae* (Small & Martz 2013), but the  
363 posteriormost portion of the articular surface (Figure 6) is probably a suture for a palpebral as in  
364 *Longosuchus meadei* (TMM 31184-98). The anterior margins of the frontals are thick and rugose  
365 for articulation with the nasals (Figures 5, 7). The frontal/nasal suture is nearly transverse. The  
366 frontal also lacks the distinct, raised midline ridge present in *Stenomyti huangae* (Small & Martz  
367 2013).

368         The ventral surfaces of the frontals are broadly ventrally concave and smooth (Figure 7).  
369 Medial to the orbital fossa is a distinct, slightly curved ridge that is the articulation point with the  
370 laterosphenoid.

### 371 ***Postfrontal***

372         The postfrontals are roughly triangular bones that form the posterodorsal margin of the  
373 orbit. Both are certainly preserved in PEFO 34616, as in all aetosaurians, but the positions of  
374 their sutures are not clear.

### 375 ***Parietal***

376         The dorsal portions of both parietals are mostly missing, although the posterolateral  
377 corner of the left one remains as well as a small fragment of the posterior portion of the right  
378 where it contacts the dorsal process of the squamosal (Figure 5). The frontal/parietal suture is  
379 visible along the posterior margin of the frontals, so it is clear that these elements were not fused.  
380 The posterolateral portion forms the dorsal border of the supratemporal fenestra, but few other  
381 details are visible.

382           The posterior flanges of both parietals are preserved (Figure 8). Their posteroventrally  
383 sloping surfaces form the upper portion of the back of the skull. Ventrally, they contact the  
384 paroccipital processes of the opisthotics. There is no evidence for a posttemporal fenestrae,  
385 which may have been obliterated by slight ventral crushing of the skull roof. The parietal flanges  
386 contact the supraoccipital medially and the posterior process of the squamosal laterally. The  
387 upper margins are damaged so that the presence of a shelf for articulation of the nuchal  
388 paramedian osteoderms cannot be confirmed.

389

### 390 *Squamosal*

391           The majority of both squamosals is present. As is typical for aetosaurians the squamosals  
392 are elongate bones that are fully exposed in lateral view, forming the posterior corner of the  
393 skull, as well as the posteroventral margin of the oval supratemporal fenestra (Figure 6). The  
394 anterior and posterior portions are separated by a dorsoventrally thin neck. The anterior portion  
395 divides into two distinct rami, a large, but mediolaterally thin, ventral lobe that presumably  
396 contacted the upper margin of the quadratojugal, and a much smaller triangular dorsal ramus that  
397 forms much of the anteroventral margin of the supratemporal fenestra. These two rami are  
398 separated by a posterior process of the postorbital. On the right side of PEFO 34616, the dorsal  
399 ramus is broken, clearly showing the articulation with the postorbital and exposing the prootic in  
400 this view (Figure 6). The ventral margin of the main body is concave and bears a flat surface that  
401 is the articulation surface with the quadrate (s.qu; Figure 7). Anterior to that articular surface the  
402 ventral margin of the anterior portion of the squamosal is confluent with the ventral margin of  
403 the postorbital. This arrangement suggests that the squamosal contributed little if anything to the  
404 margin of the lateral temporal fenestra. This is similar to the condition in *Stagonolepis robertsoni*

405 (Walker 1961) and differs from that in *Stenomyti huangae* (Small & Martz 2013) in which the  
406 ventral margin of the squamosal is situated much lower than the ventral margin of the postorbital,  
407 and the squamosal contributes significantly to the margin of the infratemporal fenestra.

408 The posterior portion of the squamosal expands dorsally into dorsal and ventral posterior  
409 processes. The dorsal process forms the posterior border of the supratemporal fenestra and is  
410 mediolaterally thickened with a smooth anterior concave area that represents the supratemporal  
411 fossa. The apex of the upper process contacts the parietal. The ventral posterior process forms a  
412 small hooked knob that projects off of the back of continued the  
sentences  
413 ~~the~~ skull. Medial to this is a deep pocket in the medial surface of the squamosal that receives the  
414 dorsal head of the quadrate. Dorsomedial to this pocket is the contact between the squamosal  
415 and the distal end of the paroccipital process of the opisthotic (Figure 

#### 416 ***Postorbital***

417 A portion of the left and almost the complete right postorbital are preserved in PEFO  
418 34616 (Figures ). They are mediolaterally thin, triradiate bones that contact the postfrontal  
419 and parietal dorsally, the jugal anteriorly, and the squamosal posteriorly. The upper bar forms the  
420 posterior margin of the orbit and the anterior margin of the supratemporal fenestra. The posterior  
421 process is triangular and inserts into a slot in the anterior portion of the squamosal. The ventral  
422 margin is flat, and forms the dorsal border of the infratemporal fenestra and more anteriorly that  
423 edge bears an articular surface with the jugal. The tip of the anterior process is broken, but it  
424 would have overlain the posterior process of the jugal and formed the posteroventral margin of  
425 the orbit. 

426 ***Supraoccipital***

427         The supraoccipital is present but poorly preserved (Figure  A median element, it forms  
428 much of the dorsal portion of the occiput and roofs the foramen magnum. Laterally it contacts  
429 the parietal flanges and ventrally the otooccipitals.

430 ***Exoccipital/opisthotic***

431         The exoccipitals and opisthotics are indistinguishably fused into a single structure, the  
432 otooccipital. The exoccipital portions form the lateral margins of the foramen magnum (Figure  
433 8). A protuberance is present on the left exoccipital at the dorsolateral corner of the foramen  
434 magnum (Figures 5, 8). The presence of similar structures in *Neoaetosauroides engaeus* (e.g.,  
435 PVL 5698) was noted by Desojo and Báez (2007), and interpreted by them to be facets for  
436 reception of the proatlantes. Those authors considered the facets located on the supraoccipital   
437 however, in *Longosuchus meadei* (TMM 31185-84) they are located on the exoccipital and the  
438 same appears to be true for PEFO 34616.

439         Anteriorly, a strong lateral ridge forms the posteroventral margin of the ‘stapedial  
440 groove’ as is typical for aetosaurs (Gower & Walker 2002). In aetosaurians there are typically  
441 two openings for the hypoglossal nerve (XII) that straddle the lateral ridge (Gower & Walker  
442 2002); however, they are not apparent in PEFO 34616, and where the posterior opening of the  
443 left side should be situated there is a fragment of bone missing.

444         Both paroccipital processes are present and well-preserved (Figures 5-8). They are  
445 mediolaterally short (14 mm) and stout, dorsoventrally taller than anteroposteriorly long (8 mm  
446 tall, 4 mm long), and contact the parietal flanges dorsally and the squamosal laterally. The distal  
447 end expands slightly dorsoventrally (Figure 8). The posterior surface is flat and distally the  
448 process forms the posterior border of the pocket for reception of the quadrate head, therefore  
449 there was a sizeable contact between the opisthotic and the quadrate.

450           The proximoventral portion of the paroccipital process opens into the ‘stapedial groove’.  
451   That groove continues into the main body of the opisthotic, bounded by the lateral ridge of the  
452   exoccipital posteroventrally and the crista prootica anterodorsally (Figure 9). Here there is a large  
453   opening for the fenestra ovalis and the metotic foramen; however, the two cannot be  
454   distinguished because the ventral ramus of the opisthotic that divides the two openings in  
455   aetosaurians (Gower & Walker 2002) is not preserved (Figure 9). It is not clear if the ventral  
456   ramus was never originally preserved or if it was removed during preparation of the braincase.  
457   Thus the perilymphatic foramen is not preserved as well. The embryonic metotic fissure is  
458   undivided in aetosaurs and therefore the glossopharyngeal, vagal, and accessory (IX, X, XI)  
459   nerves and the jugular vein would have exited the braincase via a single opening, the metotic  
460   foramen (Gower & Walker 2002; Rieppel 1985; Walker 1990). Just lateral to the metotic  
461   foramen on the ventral surface of the crista prootica there should be a small opening for the  
462   facial nerve (VII); however, it is not visible through the hematite build-up on the lateral wall of  
463   the cranium.

464           A second distinct groove extends from the ventral border of the fenestra ovalis  
465   anteroventrally along the lateral face of the parabasisphenoid to the posterodorsal margin of the  
466   basipterygoid process, and is bordered anterodorsally by the anteroventral continuation of the  
467   crista prootica (Figure 9). The termination of that groove houses the entrance of the cerebral  
468   branch of the internal carotid artery (Gower & Walker 2002; Sulej 2010).

#### 469   ***Prootic***

470           The entire braincase is slightly crushed and rotated dorsolaterally so that the left side of  
471   the otic capsule is easier to view (Figure 9). Both prootics are preserved. Posteriorly, the prootic  
472   overlaps the opisthotic medially, and ventrolaterally forms a thin ridge (crista prootica), which is

473 bounded ventrally by the upper part of the ‘stapedial groove’ and the groove in the  
474 parabasisphenoid leading to an opening for the internal carotid. Anteroventrally, the prootic  
475 meets the anterior portion of the parabasisphenoid, just posterior to the hypophyseal fossa.  
476 Anteriorly and anterodorsally, the prootic meets the laterosphenoid and dorsally it is bounded by  
477 the parietal. The uppermost margin is deformed by a thick anteroposteriorly oriented mass of  
478 bone, which could represent crushing of the parietal margin. Just posterior to the anterior suture  
479 with the laterosphenoid is the opening for the trigeminal nerve (V) which is deformed and closed  
480 by crushing (Figure 9). In PEFO 34616 the opening for the trigeminal nerve is completely  
481 enclosed by the prootic 

#### 482 ***Laterosphenoid***

483 The laterosphenoids are ossified but poorly preserved. On the left side anterodorsal to the  
484 opening for the trigeminal nerve (V), there is the cotylar crest, which is crescentic and opens  
485 posteriorly (Figure 9). No other details of the laterosphenoid can be determined.

#### 486 ***Basioccipital/Parabasisphenoid***

487 The basioccipital and parabasisphenoid are complete and together comprise the best  
488 preserved and most distinctive portion of the braincase in *Scutarx deltatylus* (Figure 10). The  
489 occipital condyle is transversely ovate in posterior view rather than round like in other aetosaurs  
490 such as *Longosuchus meadei* (TMM 31185-98). The dorsal surface is broad with a wide shallow  
491 groove for the spinal cord.

492 The condylar stalk is also broad (25 mm wide), and wider than the condyle. Thus there is  
493 no distinct ‘neck,’ nor does a sharp ridge delineate the condyle from the stalk as in *Longosuchus*  
494 *meadei* (TMM 31185-98; Parrish 1994) or *Desmotosuchus smalli* (TTU P-9024; Small 2002).   
495 The ventral surface of the condylar stalk bears two low rounded ‘keels’ separated by a shallow,

496 but distinct, oblong pit. The broad stalk, lack of a distinct neck, and ventral keels all appear to be  
497 autapomorphic for *Scutarx deltatylus*. Anterolaterally the condylar stalk expands laterally to  
498 form the ventral margin of the metotic fissure. The contacts with the exoccipitals are dorsal and  
499 posterior to that margin 

500         The right basal tuber of the basioccipital is present, but the left is missing. The  
501 basioccipital tuber is separated from the crescentic basal tuber of the parabasisphenoid by an  
502 unossified cleft, typical for aetosaurians and other suchians (Figure 10; Gower & Walker 2002).  
503 The basal tubera of the basioccipital are divided medially by an anteroposteriorly oriented bony  
504 ridge that bifurcates anteriorly to form the crescentic basal tubera of the parabasisphenoid and  
505 enclose the posterior portion of the basisphenoid recess (sensu Witmer 1997). Posteriorly that  
506 bony ridge is confluent with the posteriorly concave posterior margin of the basioccipital basal  
507 tubera (Figure 10). The short, anterolaterally directed basipterygoid processes are located  
508 anteriorly and in contact posteriorly with the anterior margin of the basal tubera of the  
509 parabasisphenoid. The upper portion of the distal end of the left basipterygoid process is broken,  
510 but the right is complete and bears a slightly expanded and slightly concave distal facet that faces  
511 anterolaterally to contact the posterior process of the pterygoid.

512         The basipterygoid processes and the basal tubera are positioned in the same horizontal  
513 plane (Figure 9), which is typical for aetosaurians and differs significantly from the condition in  
514 *Revueltosaurus callenderi* (PEFO 34561) and *Postosuchus kirkpatricki* (TTU P-9000;  
515 Weinbaum 2011) in which the basicranium is oriented more vertically, with the  
516 basipterygoid processes situated much lower dorsoventrally than the basal tubera.

517         *Scutarx deltatylus* differs from aetosaurians such as *Stagonolepis robertsoni* (MCZD 2)  
518 and *Aetosauroides scagliai* (PVSJ 326)  that there is a broad contact between the basal tubera

519 and the basiptyergoid processes and that the basiptyergoid processes are not elongate (Figure  
520 10). This is nearly identical to the condition in *Desmotosuchus smalli* (TTU P-9023) and  
521 *Desmotosuchus spurensis* (UMMP 7476; Case 1922). There are two basicrania (UCMP 27414,  
522 UCMP 27419) from the *Placerias* Quarry with widely separated (anteroposteriorly) basal tubera  
523 and (elongate) basiptyergoid processes that apparently do not pertain to either *Desmotosuchus* or  
524 *Scutarx deltatylus*, and may belong to *Calyptosuchus welllesi*. This would demonstrate a potential  
525 important braincase difference between *Calyptosuchus welllesi* and *Scutarx deltatylus*, despite the  
526 nearly identical structure of the osteoderms shared between these two taxa. 

527 In the anteroposteriorly short area between the basal tubera and the basiptyergoid  
528 processes, a deep, subrounded fossa (Figure 10) represents the basisphenoid recess (=median  
529 pharyngeal recess of Gower and Walker, 2002; =parabasisphenoid recess of Nesbitt, 2011),  
530 which is formed by the median pharyngeal system (Witmer 1997). The presence of a ‘deep  
531 hemispherical fontanelle’ (= basisphenoid recess) between the basal tubera and the basiptyergoid  
532 processes has been proposed as a synapomorphy of *Desmotosuchus* and *Longosuchus* (Parrish  
533 1994), but as discussed by Gower and Walker (2002), that condition is present in many  
534 archosauriforms. The number of aetosaurian taxa with this feature was expanded by Heckert and  
535 Lucas (1999), who also reported that a ‘hemispherical fontanelle’ is absent in *Typothorax* and  
536 *Aetosaurus*. Unfortunately they did not list catalog numbers for examined specimens, and  
537 scoring of character occurrences cannot be replicated. The basisphenoid recess is actually present  
538 in *Aetosaurus* (Schoch 2007) and *Typothorax* (TTU P-9214; Martz 2002) , the presence of  
539 that recess is an aetosaurian synapomorphy.

540 Small (2002) found the shape and size of the basisphenoid recess to be variable in his  
541 hypodigm of *Desmotosuchus haplocerus*, and recommended that the character be dropped from

542 phylogenetic analysis pending further review. However, rather than utilizing the presence or  
543 absence of the structure, it has been proposed that the shape and depth may be of phylogenetic  
544 significance (Gower & Walker 2002). As noted above, it appears that there are two types of  
545 aetosaurian basicrania, those with anteroposteriorly short parabasisphenoids and those with long  
546 parabasisphenoids. These differences were used as rationale for splitting *Desmotosuchus*  
547 *haplocerus* into two species (Parker 2005b). Among taxa with short parabasisphenoids, *Scutarx*  
548 *deltatylus* (PEFO 34616) and *Desmotosuchus spurensis* (UMMP 7476) have deep, more or less  
549 round basisphenoid recesses, and *Desmotosuchus smalli* has a shallow subtriangular recess. In  
550 *Longosuchus meadei* (TMM 31185-98) the recess is round and shallow. Among taxa with  
551 elongate basisphenoids, *Aetosauroides scagliai* (PVSJ 326) has a shallow, round recess and  
552 *Tecovasuchus chatterjeei* (TTU P-545) has a deep, round recess. However, in *Coahomasuchus*  
553 *kahleorum* (NMMNH P-18496; TMM 31100-437), which has an elongate basisphenoid, the  
554 recess has the form of a moderately deep, anteroposteriorly elongate oval (Desojo & Heckert  
555 2004; pers. obs. of TMM 31100-437). Thus, the shape of this structure is highly variable and  
556 most likely not phylogenetically informative, although the elongate form of the recess in *C.*  
557 *kahleorum* may prove autapomorphic. 

558 Anterior to the basisphenoid recess and between the bases of the basiptyergoid processes  
559 there is another shallow, anteroventrally opening recess (Figure 10). This recess is at the base of  
560 the parasphenoid process, in the same position as the subsellar recess in theropod dinosaurs  
561 (Rauhut 2004; Witmer 1997) and may be homologous to the latter. However, the function and  
562 origin of the recess are not understood (Witmer 1997). 

563 Dorsal to the basiptyergoid processes, two crescentic and dorsally expanding clinoid  
564 processes flank the circular, concave hypophyseal fossa, which housed the pituitary gland

565 (Figure 9). No openings are visible because of poor preservation, but the dorsum sellae should be  
566 pierced by two canals for the abducens (VI) nerves (Gower & Walker 2002; Hopson 1979). At  
567 the base of the hypophyseal fossa in *Stagonolepis robertsoni* (MCZD 2) and *Longosuchus*  
568 *meadei* (TMM 31185-98) there is a triangular flange of bone termed the parabasisphenoid pro-  
569 (Gower & Walker 2002). This structure is mostly eroded in PEFO 34616, although its base is  
570 preserved as a small dorsal protuberance.

571 Anterior to this, the cultriform process of the parasphenoid is completely preserved  
572 (Figures 9-10). This structure is delicate and usually missing or **obscured in the few known**  
573 aetosaur skulls, making comparisons difficult. However, the process is notably short in PEFO  
574 34616, barely extending past the anterior margins of the orbits (Figure 9). In PEFO 34616 the  
575 basisphenoid has a length of 34.2 mm, whereas the cultriform process measures 20.2 mm in  
576 length (cultriform process/basisphenoid ratio = 0.59). This is noticeably different from the  
577 parabasisphenoid in *Aetosauroides scagliai* (PVSJ 326) which has a basisphenoid length of 51  
578 mm and a cultriform process length of at least 63 mm, although the anterior end of the process is  
579 concealed (ratio = 1.23) beneath the left pterygoid. The cultriform process is also preserved in  
580 *Desmotosuchus spurensis* (UMMP 7476), which has a relatively short parabasisphenoid and a  
581 cultriform process/basisphenoid ratio of 0.96.

582 The cultriform process is elongate and tapers anteriorly. It is Y-shaped in cross-section  
583 with a ventral ridge, and dorsal trough for the ethmoid cartilage. Its posterolateral margins bear  
584 distinct oval recesses bound posterodorsally by strong ridges that are confluent with the  
585 posterodorsal edge of the process (Figures 9-10). Thus the process is broader posteriorly, with  
586 these recesses contributing greatly to the thinning of the element anteriorly. **The parasphenoid**

587 recesses appear to be unique to PEFO 34616, although the general lack of known aetosaurian  
588 cultriform processes makes it difficult to determine this with certainty.

## 589 **Postcranial skeleton**

### 590 *Vertebrae*

#### 591 *Cervical Series*

##### 592 *Axis/Atlas*

593 The axis and atlas are not preserved in any presently known specimens of *Scutarx*  
594 *deltatylus*.

##### 595 *Post-axial Cervicals*

596 Two articulated cervical vertebrae are preserved in PEFO 31217 (Figure 11). Although  
597 both are crushed mediolaterally, they are nearly complete and preserve many details. The centra  
598 are taller than long (Figure 11a) suggesting they represent part of the anterior (post-axial) series  
599 (i.e., positions 3-6). Most notably, the difference in dimensions is not as pronounced as in  
600 *Typhothorax coccinarum* and *Neoaetosauroides engaeus*, in which the centra are greatly reduced  
601 in length (Desojo & Báez 2005; Long & Murry 1995). The centrum faces are subcircular in  
602 anterior and posterior views and slightly concave, with slightly flared rims (Figures 11b-c). The  
603 ventral surface of each centrum consists of two concave, ventromedially inclined, rectangular  
604 surfaces divided by a sharp and deep mid-line keel (Figure 11d).

605 The short parapophyses are oval in cross-section and situated at the anteroventral corners  
606 of the centrum. The parapophyses are directed posteriorly, and each forms the beginning of a  
607 prominent ridge that continues posteriorly to the posterior margin of the centrum. The lateral  
608 faces of the centra are concave mediolaterally and dorsoventrally forming discrete, but shallow,  
609 lateral fossae that contact the neural arch dorsally (Figure 11a). However, PEFO 31217 lacks the

610 deep lateral fossae, which are considered an autapomorphy of *Aetosauroides scagliai* (Desojo &  
611 Ezcurra 2011). The neurocentral sutures are not apparent on this specimen, suggesting closure of  
612 the sutures and that this individual is osteologically ‘mature’ although this cannot be completely  
613 confirmed without histological sectioning of the sutural contact (Brochu 1996; Irmis 2007).

614 The diapophyses are centrally located at the base of the neural arch (Figure 11b). The  
615 best preserved vertebra shows that they are slightly elongate, oval in cross-section, and curved  
616 ventrolaterally. Because none of the diapophyses appears to be complete their exact length  
617 cannot be determined. The neural canal is round in posterior view (Figure 11c) rather than  
618 rectangular as in *Desmotosuchus spurensis* (UMMP 7504). The entire neural arch is taller than  
619 the corresponding centrum face. The zygapophyses are well-formed, elongate, and oriented at  
620 approximately 45 degrees from the horizontal.

621 Aetosaurian vertebrae bear several vertebral laminae and associated fossae. The  
622 terminology for these structures follows Wilson (1999) and Wilson et al. (2011). There is a  
623 weakly developed posterior centrodiaepophyseal lamina (pcdl) that originates at the  
624 posteroventral corner of the diapophysis and continues posteroventrally to the posterior edge of  
625 the neurocentral suture. The only other apparent vertebral laminae are paired  
626 intrapostzygapophyseal laminae (tpol) that originate on the posteroventral surface of the  
627 postzygapophyses and form two sharp ridges (laminae) that meet at the dorsomedial margin of  
628 the neural canal (Figure 11b). Those laminae delineate the medial margins of a pair of distinct  
629 subzygapophyseal fossae, called the postzygapophyseal centrodiaepophyseal fossae (pocdf), as  
630 well as a sizeable intrazygapophyseal fossa, called the spinopostzygapophyseal fossa (spof). This  
631 represents the first recognition of distinct intrapostzygapophyseal laminae in an aetosaurian.  
632 *Desmotosuchus spurensis* (MNA V9300) has struts of bone from the dorsomedial margins of the

633 postzygapophyses that join medially and then extend ventrally as a single thickened unit to form  
634 a Y-shaped hyposphene (Parker 2008a: fig. 10a), similar to the pattern formed by the  
635 intrapostzygapophyseal laminae in *Scutarx deltatylus*. Thus, it is possible that the structure of the  
636 hyposphene in aetosaurians is homologous (i.e., the hyposphene is actually formed by paired  
637 vertebral laminae) with the presence of paired (but not joined) intrapostzygapophyseal laminae,  
638 but this interpretation requires further investigation.

639         The neural spines are not complete; however, the base of the one on the second preserved  
640 vertebra shows that the spine was anteroposteriorly elongate, with prominent  
641 spinopostzygapophyseal laminae (spol) that are confluent with the dorsal surfaces of the  
642 postzygapophyses (Figure 11b). Spinopostzygapophyseal laminae are also present on the  
643 cervical vertebrae of *Desmotosuchus spurensis* (Parker 2008a).

#### 644 ***Trunk Series***

##### 645 ***Mid-trunk vertebrae***

646         Four mid-trunk vertebrae are preserved in PEFO 34045. In aetosaurs the cervical to trunk  
647 transition occurs when the parapophysis fully migrates from the base of the neural arch, laterally  
648 onto the ventral surface of the transverse process (Case 1922; Parker 2008a). PEFO 34045/FF-51  
649 is well preserved, missing only the postzygapophyses (Figures 12a-c). The articular faces of the  
650 centra are round and slightly concave with broad flaring rims. The centrum is longer (45.78 mm)  
651 than tall (41.81 mm), its lateral faces are deeply concave, and its ventral surface is narrow and  
652 smooth. The neural canal is large and in anterior view, the margins of the neural arch lateral to  
653 the canal are mediolaterally thin with sharp anterior edges.

654         The prezygapophyses are inclined at about 45 degrees from the horizontal and are  
655 confluent laterally with a short horizontally oriented prezygadiapophyseal lamina (prdl) that

656 terminates laterally at the parapophysis (Figure 12b). Between the prezygapophyses and ventral  
657 to the base of the neural spine there is a well-developed broad, sub-triangular  
658 spinoprezygapophyseal fossa (sprf). In combination with the flat prezygapophyses this creates a  
659 broad shelf for reception of the posterior portion of the neural arch of the preceding vertebra  
660 (Figure 12b). There is a horizontal, ventral bar that roofs the opening of the neural canal between  
661 the ventromedial edges of the prezygapophyses (Figure 12d); thus, there is no developed  
662 hypantrum as in *Desmotosuchus spurensis* or *Aetobarbakinoides brasiliensis* (Desojo, Ezcurra &  
663 Kischlat 2012; Parker 2008a). The ventral bar also occurs in *Stagonolepis robertsoni* (Walker  
664 1961: fig 7j). Ventrolateral to the prezygapophysis there is a deep fossa termed the  
665 centroprezygapophyseal fossa (cprf), which is bordered posteriorly by the main strut of the  
666 transverse process (Figure 12b). Although the positions of these fossae are homologous with  
667 those of saurischian dinosaurs because they share distinct topological landmarks, it is not clear if  
668 these features are similarly related to the respiratory system (Butler, Barrett & Gower 2012;  
669 Wilson et al. 2011).

670 In posterior view, the postzygapophyses (best preserved in PEFO 34045/14-R) are also  
671 oriented about 45 degrees above the horizontal. They are triangular in posterior view with a well-  
672 developed lateral postzygodiapophyseal lamina (podl). That lamina extends laterally to the  
673 diapophysis and forms a broad dorsal shelf of the transverse process in dorsal view (Figure 12a).  
674 The shelf is wider proximally and significantly narrows distally along the transverse process.  
675 Along the dorsal surface of the shelf, between the postzygapophyses and the neural spine is a  
676 pair of shallow postzygapophyseal spinodiapophyseal fossae (posdf).

677 The neural spine is short (32.3 mm) relative to the centrum height as in *Desmotosuchus*  
678 *spurensis* (MNA V9300) and *Tyothorax coccinarum* (TTU P-9214). The spine is

679 anteroposteriorly elongate, equal in length to the proximal portion of the neural arch, and the  
680 distal end is mediolaterally expanded (spine table). The anterior and posterior margins of the  
681 neural spine possess paired vertical spinoprezygapophyseal (sprl) and spinopostzygapophyseal  
682 (spol) laminae as in *Desmotosuchus spurensis* (MNA V9300).

683         The postzygapophyses bound deep oval spinopostzygapophyseal fossa (spof). This fossa  
684 is much taller than wide and is bounded laterally by thin, nearly vertical intrapostzygapophyseal  
685 laminae (tpol). These laminae meet medially at a thickened triangular area dorsal to the neural  
686 canal. Here the vertebra bears a strong posteriorly pointed projection that inserts into the ventral  
687 portion of the spinoprezygapophyseal fossa just above the ventral bar. That projection is also  
688 present in *Calyptosuchus wellsi* (e.g., UCMP 139795). Ventrolateral to the postzygapophyses  
689 there are two deep centropostzygapophyseal fossae (cpof) in the proximal portions of the  
690 transverse processes.

691         The transverse processes extend laterally with a length of 81.6 mm in PEFO 34045/FF-  
692 51. However, in two of the other vertebrae (PEFO 34045/14-R; PEFO 34045/19-V) the  
693 transverse processes are directed more dorsolaterally (Figures 12d-e). This difference also occurs  
694 in *Stagonolepis robertsoni* (Walker 1961) and occurs in the more anteriorly positioned trunk  
695 vertebrae. Furthermore, the ventral surface of the centrum in these two vertebra (PEFO  
696 34045/14-R; 19-V) is more constricted forming a blunt ventral 'keel'. The keel and the  
697 orientation of the transverse process are the only visible differences between and anterior and  
698 mid-trunk vertebrae in *Scutarx deltatylus*.

### 699 ***Posterior trunk vertebrae***

700         The currently available material of *Scutarx deltatylus* includes seven posterior trunk  
701 vertebrae; three from PEFO 34045, three from PEFO 31217, and one from PEFO 34919. As in

702 *Desmotosuchus spurensis* (MNA V9300; Parker 2008a), the posterior trunk vertebrae are much  
703 more robust than the anterior and mid-trunk vertebrae (Figures 12g-h; 13a-c). Notable  
704 differences between the mid- and posterior trunk vertebrae in *Scutarx deltatylus* include an  
705 increase in the height of the neural spines and a lengthening of the transverse processes, which  
706 coincide with the loss of distinct parapophyses and diapophyses along the series. Furthermore,  
707 the centra become anteroposteriorly shorter than they are dorsoventrally tall (Figure 12h). The  
708 neural spine characteristics are identical to those of the mid-trunk vertebrae with regard to the  
709 presence of the various vertebral laminae and associated fossae. An isolated posterior trunk  
710 vertebra from PEFO 31217 (Figure 13c) shows that the prezygodiapophyseal laminae are even  
711 more strongly developed and extend farther laterally than in the more anterior trunk vertebrae. In  
712 the more posterior vertebra, the length ratio between the transverse process length (86.84 mm)  
713 and centrum width (53.26 mm) equals 1.63, thus the process is more than 1.5 times the width of  
714 the centrum. This is comparable to a ratio of 1.58 for the mid-trunk vertebrae.

715 This same vertebra from PEFO 31217 also lacks distinct diapophyses and parapophyses  
716 and a single-headed rib is fused onto the distal end of the process (Figure 13c). This is also seen  
717 in *Desmotosuchus spurensis* (Parker 2008a), *Stagonolepis robertsoni* (Walker 1961), and  
718 *Calyptosuchus wellesi* (UMMP 13950). An isolated posterior trunk vertebra from PEFO 34045  
719 (Figures 13a-b) preserves the entire transverse processes and the associated fused ribs. However,  
720 the specimen differs from the previously described vertebra from PEFO 31217 in that the  
721 parapophysis and diapophysis are distinct and the rib is double-headed (Figures 13a-b). Although  
722 the ribs and transverse processes are fused, the fusion is incomplete; gaps are present within the  
723 individual articulations and a gap is apparent between the anterior surface of the distal end of the  
724 transverse process and the medial surface of the capitulum of the rib (Figure 13b). This suggests

725 that several vertebrae in the posterior trunk series fuse with the ribs, and loss of a distinct  
726 parapophysis and diapophysis of the transverse process and of the tuberculum and capitulum of  
727 the dorsal ribs only occurred in the last one or two presacrals. Examination of UMMP 13950  
728 (Case 1932; Long & Murry 1995) suggests that this loss occurs in the last three presacrals. In  
729 *Stagonolepis robertsoni* that condition occurs in the final two presacral vertebrae (Walker 1961).  
730 There is no evidence in *Scutarx deltatylus* that the last presacral was incorporated into the  
731 sacrum as in *Desmotosuchus spurensis* (Parker 2008a). The last presacral in PEFO 31217 also  
732 shows a distinct vertical offset in the ventral margins of the articular faces of the centra with the  
733 anterior face situated more ventrally. This is also the case in *Stagonolepis robertsoni* (Walker  
734 1961) and *Desmotosuchus spurensis* (Parker 2008a).

735 Another posterior trunk vertebra, PEFO 34045/22 (Figures 12g-h), lacks the transverse  
736 processes, but preserves other key characteristics of the posterior presacrals. Its neural spine is  
737 taller (81.94 mm) than the height of the centrum (61.24 mm), differing from the condition in the  
738 anterior and mid-trunk vertebrae where the neural spine is shorter than the centrum (Figure 12g).  
739 This transition occurs at the beginning of the posterior trunk vertebrae series, because the  
740 specimen from PEFO 34045 with the fused ribs, but distinct rib facets (Figures 13a-b), has a  
741 centrum and neural spine of equal height. PEFO 34045/22 also preserves the pointed posterior  
742 projection above the neural arch that is present throughout the trunk series (Figure 12h).

#### 743 ***Sacral vertebrae***

744 A sacral vertebra, probably the second, is visible in ventral view in PEFO 31217 in  
745 articulation with the rest of the pelvis (Figure 14). It is recognizable by the presence of a strong,  
746 broad sacral rib that laterally expands anterodorsally to contact the posterodorsal margin of the  
747 left ilium. Unfortunately no other details are available for that specimen.

748 *Caudal series.*

749 *Vertebrae*

750 Eight vertebrae occur in semi-articulation in PEFO 31217 posterior to the sacral vertebra

751 described above (Figure 14). The first two are robust with thick flaring rims on the centra. The  
752 first vertebra has a length of 57.3 mm, and its anterior face is indistinguishable from the posterior  
753 face of the preceding sacral vertebra. Furthermore, the centrum is constricted which is unusual  
754 for an aetosaur, because the sacrals and anterior caudals usually have wide ventral surfaces (e.g.,  
755 *Desmotosuchus spurensis*, MNA V9300). The vertebra in PEFO 31217 lacks a ventral groove  
756 and chevron facets. It is possible that this is a sacral vertebra that has been forced backwards, but  
757 the poor preservation of the specimen does not allow a firm determination. The second caudal  
758 vertebra (assuming the first described is from the caudal series) has a centrum length of 52.2 mm  
759 and a width of 61.6 mm, thus it is wider than long as is typical for the anterior caudals of  
760 aetosaurians (Long & Murry 1995). The centrum is ventrally broad and a chevron is articulated  
761 to the posterior margin. The base of the caudal rib originates from the base of the neural arch, but  
762 laterally the rib is incomplete.

763 Two anterior caudal vertebrae are also known from PEFO 34045, which roughly  
764 correspond in morphology to the second and third caudal centra of PEFO 31217 (Figures 15a-f).  
765 These two vertebrae have blocky centra that are wider (flared centrum faces) than long. The  
766 ventral surfaces are broad, with a deep median trough bordered by two lateral ridges. These  
767 ridges terminate posteriorly into two posteroventrally facing hemispherical chevron facets  
768 (Figures 15d-e). The articular faces of the centra are round in anterior and posterior views, and in  
769 lateral view these faces are offset from each other (Figure 15f). The ventral margin of the  
770 posterior face is situated much farther ventrally than that of the anterior face, as is typical for  
771 aetosaurs (e.g., *Desmotosuchus spurensis*, MNA V9300) although the neural spines are

772 missing, it is apparent that the neural arch complex was much taller than the height of the  
773 centrum (Figure 15c). The neural canal is oval with a taller dorsoventral axis.

774 The pre- and postzygapophyseal stalks are thickened and the facets are closely situated  
775 medially. They are oriented at about 30 degrees from the horizontal. The neural arch is directed  
776 posterodorsally and the postzygapophyses project posteriorly significantly beyond the posterior  
777 centrum face (Figure 15c). The caudal vertebrae lack diapophyseal and zygapophyseal laminae,  
778 but spinozygapophyseal fossae occur between the prezygapophyses (Figures 15a-b). The caudal  
779 ribs are fully fused to the centrum. They are anteroposteriorly broad and dorsoventrally thin with  
780 flat dorsal surfaces and buttressed ventral margins. The ribs are directed slightly posteriorly and  
781 laterally they arc ventrally (Figures 15a-c). Unfortunately their lateral extent is unknown.

782 The third and fourth caudal vertebrae in PEFO 31217 are longer than wide, with the  
783 centrum narrowing mediolaterally and with reduced flaring of the rims as in the previous  
784 vertebrae (Figure 14). The posteroventral margins possess chevron facets. The caudal ribs are  
785 broad, flat, and were elongate, as in *Desmotosuchus spurensis* (MNA V9300), even though the  
786 distal ends are not preserved. The third centrum has a length of 56.4 mm and the fourth has a  
787 length of 56.4 mm. Details of the neural arches and spines are buried in the block and  
788 irretrievable by mechanical preparation.

789 The fifth and sixth caudal vertebrae are mostly concealed beneath armor, bone fragments,  
790 and what are probably the eighth and ninth caudal vertebrae. Only the left caudal ribs are  
791 apparent, jutting out of the block. They are dorsoventrally flat and laterally elongate, typical for  
792 aetosaurs, but they are poorly preserved and no other details are apparent.

793 The anterior face of what is probably the seventh caudal vertebra is visible underneath  
794 matrix and an osteoderm about six centimeters behind where the sixth caudal vertebra is buried

795 in the block, breaking the line of articulation. The neural canal is prominent on this vertebra and  
796 what is visible of the neural arch shows that it was tall. The centrum is amphicoelous and  
797 mediolaterally constricted. The ventral surface consists of a median ventral groove bounded  
798 laterally by two sharp ridges. The ridges would terminate posteriorly with the chevron facets,  
799 but the relevant area is obliterated. A vertebra from approximately the same position is  
800 preserved in PEFO 34919 (Figures 16a-c) and provides more details.

801 The centrum is much longer than wide (57 mm to ~30 mm), mediolaterally compressed,  
802 and grooved ventrally. Its rims flare minimally, but the articular faces are deeply concave (Figure  
803 16b-c). The neural arch is dorsoventrally shorter than in the more anteriorly positioned caudal  
804 vertebrae, but the neural spine was certainly tall in this position as well (Figure 16b). The  
805 zygapophyses are reduced and each pair is closely situated medially. The postzygapophyses do  
806 not project far posteriorly. The caudal rib is situated anteroventrally on the neural arch. It is  
807 broad and flat, extends laterally (~50 mm), and is slightly arcuate in anterior view (Figure 16b).

808 What are probably the eighth and ninth caudal vertebrae are well-preserved at the edge of  
809 the block in PEFO 31217 (Figure 14). The centra are much longer than wide. The ninth centrum  
810 has a length of 66.3 mm and a width of 40.2 mm. The lateral faces of the centrum are concave  
811 and, as on the preceding centra, the ventral face is narrow with a deep median groove terminating  
812 at the chevron facets. The neural arches and spines are complete and tall, with a height of 100.9  
813 mm in the eighth vertebra and 98.4 mm in the ninth. The neural spines are tall and roughly  
814 triangular in lateral view, with an anteroposteriorly broad base and tapering distally. The  
815 zygapophyses are closely situated medially and extend anteriorly and posteriorly beyond the  
816 articular faces of the centra. The caudal ribs are greatly reduced in lateral length.

817 An isolated vertebra from PEFO 34045 represents the mid-caudal series (Figure 16d).  
818 The centrum is longer than tall (65 mm to 35 mm) and mediolaterally compressed. Its articular  
819 faces are deeply concave and oval with the longest axis situated dorsoventrally. The neural arch  
820 is dorsolaterally reduced and mediolaterally compressed. The caudal ribs are greatly reduced and  
821 eroded. The neural spine is elongate, but its full dorsal extent is unknown (Figure 16d).

## 822 ***Chevrons***

823 Only half of a single chevron and part of the head of a second are preserved in PEFO  
824 34045 (Figures 17a-b). A few are smashed beneath other elements in PEFO 34919 and a badly  
825 preserved chevron is present beneath the second caudal vertebra of PEFO 31217. Although the  
826 details are poor the latter suggests, in accordance with the lack of facets on the first caudal  
827 vertebra of PEFO 31217, that chevrons started on the second centrum. This is different from the  
828 condition in *Desmatosuchus spurensis*, in which they first appear on the third caudal centrum  
829 (Parker 2008a), but similar to the condition in *Typhothorax coccinarum* (Heckert et al. 2010). The  
830 two preserved chevrons in PEFO 34045 are of the ‘slim’ elongate type and, therefore, from the  
831 anterior portion of the tail (Parker 2008a).

## 832 ***Ribs***

### 833 ***Presacral***

834 No cervical ribs are preserved in any of the specimens, but trunk ribs are common. The  
835 sacral and caudal ribs have been described above along with their associated vertebrae. The  
836 anterior and mid-trunk ribs are double-headed (Figure 17c-d). They extend laterally for the first  
837 quarter of their total length and then sharply turn ventrolaterally, are straight for another two  
838 quarters of the length, and then gently turn more ventrally. Proximally the rib body is oval in

839 cross-section, becoming ovate and then flattened more distally; it is broadest at the point of the  
840 sharp ventrolateral turn.

841 The capitulum is oval in cross-section, with a sharp posterior projection. The capitulum  
842 and tuberculum are separated along the neck by 44 mm. The dorsal surface of the neck is marked  
843 by a transverse groove that terminates at a fossa on the proximal surface of the tuberculum  
844 (Figure 17e). That groove probably hosted the ventral portion of the vertebrarterial canal as in  
845 *Alligator* (Reese 1915). A thin flange of bone originates on the dorsal surface of the tuberculum  
846 and extends laterally, becoming confluent with the rib body just lateral to the ventrolateral hook.  
847 That flange forms a deep, elongate groove along the posterodorsal surface of the rib. Dorsally the  
848 rib is flattened and forms a thin anterior blade. The posteriormost ribs are single headed and fused  
849 with the transverse processes of the trunk vertebrae (Figure 13c).

### 850 ***Gastralia***

851 It has been suggested that aetosaurians lack gastralia (Nesbitt 2011), but they are present  
852 in *Typhothorax coccinarum* (Heckert et al. 2010) that taxon (e.g., NMMNH P-56299), the  
853 gastralia are preserved in the posteroventral portion of the thoracic region, are medially fused  
854 and laterally elongate. A single gastralia set is preserved in PEFO 34616 demonstrating that they  
855 were present in *Scutarx deltatylus* as well (Figure 17f). This set consists of incomplete but  
856 medially fused ribs with a short anterior projection.

### 857 ***Appendicular Girdles***

#### 858 ***Scapulocoracoid***

859 The left scapulocoracoid is preserved in PEFO 31217; unfortunately the coracoid is  
860 covered by osteoderms that cannot be removed without causing significant damage, so only the  
861 dorsal-most portion of the coracoid where it sutures to the scapula, is visible lateral view the

862 general outline of the scapula of PEFO 31217 (Figure 18a) strongly resembles the  
863 scapulocoracoid of *Stagonolepis robertsoni* (Walker 1961: fig. 12a). The proximal end is  
864 expanded anterolaterally with the posterior projection situated more dorsally than the anterior  
865 projection. The posterior projection has a rounded posterior margin, as in *Stagonolepis*  
866 *robertsoni* (Walker 1961) differing from the pointed projection in *Stagonolepis olenkae* (ZPAL  
867 AbIII/694). The anterior projection is poorly preserved but appears to be pointed as in  
868 *Stagonolepis robertsoni* (Walker 1961). The scapular blade is gently bowed medially and the  
869 posterior edge is straight except for a slight posterior projection (the triceps tubercle) about 62  
870 mm above the glenoid lip (Figure 18a). The anterior edge of the blade is straight for most of its  
871 length until it strongly flares anteriorly, forming a prominent deltoid ridge (=acromion process;  
872 Brochu 1992; Martz 2002). Below this there is a prominent foramen, although its anterior edge is  
873 broken away. Likewise the ventral margin of the posterior edge of the scapular blade strongly  
874 flares posteriorly forming the supraglenoid buttress. The glenoid facet opens posteriorly.  
875 Laterally there is a sharp ridge, which probably represents deformation and crushing along the  
876 scapulocoracoid suture. 

### 877 *Ilium*

878 Iliac are preserved in PEFO 34919 (right ilium) and PEFO 31217 (both ilia). The ilia of *Scutarx*  
879 *deltatylus* were oriented in life so that the acetabula faced ventrally; however, to avoid confusion  
880 in this description, the anatomical directions will be provided as if the reader is viewing the  
881 ventral surface laterally (see Figure 18b-c). The right ilium of PEFO 34919 is nearly complete,  
882 missing only a portion of the anterior margin of the acetabulum (Figures 18b-c)  usual for the  
883 bones from this specimen, the ilium is covered with a thin layer of weathered hematite that  
884 cannot be removed without damaging the underlying bone.  iliac blade is complete with a

885 length of 196 mm and a mid-height of 66.8 mm. The ‘dorsal’ margin of the iliac blade is  
886 mediolaterally narrow, expanding anteriorly so that the dorsal margin of the anterior process is  
887 thicker and more robust than the rest of the blade. The anterior portion of the iliac blade is  
888 triangular in lateral view, and does not extend anteriorly beyond the edge of the pubic peduncle.  
889 There is a prominent recess on the dorsal surface between the supraacetabular crest and the  
890 posterior iliac blade (Figure 18b) that appears to be unique to *Stagonolepis deltatylus*.

891 The posterior portion of the iliac blade quickly narrows in its dorsoventral height  
892 posteriorly, terminating in a point. From there the posteroventral margin slopes anteroventrally  
893 into a curving posterior margin that distally hooks posteriorly and thickens to form the ischiadic  
894 peduncle. The posterior projection of the ischiadic peduncle is proportionally larger and more  
895 pointed than the same structure in *Aetosauroides scagliai* (PVL 2073) and *Stagonolepis*  
896 *robertsoni* (NHMUK R4789a), and more like that of TMM 31100-1, which represents a  
897 desmotosuchine aetosaurine. The ventral margins of the pubic and ischiadic peduncles meet at an  
898 angle of 90 degrees ventral to the acetabulum, with the ilium contributing to the majority of the  
899 acetabulum. In ventral view the margins of the peduncles are comma-shaped, thinning into the  
900 ventral margin of the broadly concave acetabulum. The medial side of the acetabulum is smooth  
901 and slightly convex.

902 Dorsal to the iliac neck, the medial side of the posterior portion of the iliac blade bears a  
903 prominent ventral ridge that forms a shelf for sacral rib articulation (Figure 18c). The rib scar is  
904 situated just above the ridge and forms a concave sulcus that extends anteriorly to just dorsal to  
905 the anterior margin of the neck.

906 Both ilia are present in PEFO 31217 as portions of a complete sacrum. Of the two the left  
907 is the better preserved. The acetabula are deeply concave and oriented ventrally (Figure 14).

908 Originally this was thought to be the result of crushing of the pelvis; however, the acetabula are  
909 oriented ventrally in many other uncrushed aetosaurian specimens including *Aetosauroides*  
910 *scagliai* (PVL 2073) and the holotype of *Typothorax antiquus* (Lucas, Heckert & Hunt 2003).  
911 The supraacetabular ridge in these ilia is strongly produced, but not as strong as in rauisuchids.  
912 As in PEFO 34919 there is a **deep fossa/recess on the dorsal surface** between the supraacetabular  
913 ridge and the posterior portion of the iliac blade, a condition that appears to be autapomorphic  
914 for this taxon. That fossa is bordered posteroventrally by the thickened margin of the neck, a  
915 feature which is ventrally confluent with the ischiadic peduncle. The left iliac blade measures  
916 188.6 mm in length and 67.4 mm in height, producing a relatively tall iliac blade. The posterior  
917 portion of the iliac blade has a posterior margin that projects well beyond the iliac peduncle. The  
918 extent of the ventral portions of the ilia is hard to determine because they are indistinguishably  
919 fused to the ischia and pubes; however, the left acetabulum is more or less rounded, 116.5 mm  
920 tall and 111 mm wide.

### 921 *Ischium*

922 The left ischium and part of the right are present, but poorly preserved. The ischium  
923 consists of the main body with a sharp, rounded acetabular rim, and an elongate posterior  
924 process.  The upper margin of the posterior process slopes gradually from the posterior margin of  
925 the ischiadic peduncle, and the entire ischium measures 183 mm in length. The anteroventral  
926 margin is flat where the two ischia are fused, forming a wide, slightly concave ventral shelf.  
927 Overall the ischium is similar to that of other aetosaurians such as *Stagonolepis robertsoni*  
928 (Walker 1961), but lacks the prominent ventral kink found in *Desmotosuchus spurensis* (MNA  
929 V9300; Parker 2008a).

930 ***Pubis***

931 Both pubes are present and in articulation with the pelvis although they are moderately  
932 distorted by crushing and were damaged by weathering before collection. The body of the pubis  
933 consists of an elongate, narrow 'tube' that curves anteroventrally and expands medially into two  
934 broad sheets of bone that meet in a median symphysis. This pubic apron is convex anteriorly and  
935 concave posteriorly. It is dorsoventrally short, barely extending past the ventral margin of the  
936 puboischiadic plate, more like the condition in *Typothorax coccinarum* (Long & Murry 1995)  
937 rather than the extremely deep pubic apron found in *Desmotosuchus spurensis* (MNA V9300).  
938 Two distinct oval foramina pierce the pubic apron in the proximal part of the element. The bone  
939 is broken around the more anterior foramen of the right pubis, but it is clear that it was the larger  
940 of the two openings (Figure 14). Two pubic foramina are also described for *Stagonolepis*  
941 *robertsoni* (Walker 1961), and the upper (anterior) opening considered homologous to the single  
942 foramen found in other aetosaurs, MNA V9300, *Desmotosuchus spurensis*). The distal ends  
943 of the pubes are shaped like elongate commata, narrow and curving into the symphysis (Figure  
944 14), different from the strong, knob-like projections (pubic boots) found in *Desmotosuchus*  
945 *spurensis* (MNA V9300).

946 **Osteoderms**

947 ***Paramedian osteoderms***

948 ***Cervical***

949 Cervical osteoderms are present in PEFO 31217, PEFO 34045, and PEFO 34616. All of the  
950 osteoderms are wider than long (w/l ratio of 1.85). The cervical osteoderms are dorsoventrally  
951 thick with well-developed anterior bars (sensu Long and Ballew, 1985), which bear prominent  
952 anteromedial projections. The lateral edges are strongly sigmoidal, and lack anterolateral  
953 projections (Figures 19a, c; 20a).

954 The dorsal surface is relatively featureless, with the ornamentation poorly developed. The  
955 dorsal eminence is low, broad, and mounded, contacting the posterior plate margin (Figures 19a,  
956 c). The eminence is also offset medially, closer to the midline margin. The characteristic  
957 triangular protuberance that diagnoses *Scutarx deltatylus* is present in the posteromedial corner  
958 of the osteoderm, but is greatly reduced in area (Figure 19c). In the cervical paramedian  
959 osteoderms the shape of that protuberance is more of a right triangle than the equilateral triangles  
960 found in the trunk series (see below).

961 In posterior view, the osteoderms are gently arched (Figures 19b, d). The median margins  
962 are sigmoidal in medial view and dorsoventrally thick as is typical for aetosaurians. *Scutarx*  
963 *deltatylus* lacks the ‘tongue-and-groove’ lateral articular surfaces present in *Desmatosuchus*  
964 (e.g., MNA V9300) and *Longosuchus meadei* (TMM 31185-84b).

965 The more posterior cervical paramedian osteoderms are similar, but increase in width  
966 (w/l ratio of 2.05) and lack the strongly sigmoidal lateral margin. The margin is still sigmoidal  
967 but bears a strong anterolateral projection (Figure 20a). Moreover, the anterior and posterior  
968 plate margins are gently curved anterolaterally. In posterior view, these osteoderms have a lesser  
969 degree of arching and are dorsoventrally thinner than the more anteriorly situated osteoderms.  
970 The dorsal eminence is strongly offset medially and slightly more developed, becoming raised  
971 and more pyramidal in shape, although this could be an individual variation (see description of  
972 caudal paramedian osteoderms).

### 973 ***Trunk***

974 The osteoderm transition between the cervical and trunk series is difficult to identify, but  
975 anterior dorsal trunk osteoderms are considered here to have higher width/length ratios and be  
976 dorsoventrally thinner than the cervical paramedian osteoderms. Furthermore, the triangular  
977 protuberance is more equilateral. However, it is difficult to differentiate these osteoderms from  
978 those of the anterior caudal region.

979 Osteoderms with the maximum width/length ratio (2.72) are found in the mid-trunk  
980 region. They bear a strongly raised anterior bar with prominent anteromedial and anterolateral  
981 projections. The dorsal eminence is medially offset, and forms a broad, low mound. Anterior to  
982 this on the anterior bar is a prominent, pointed anterior projection. The area of the anterior bar  
983 medial to this process is 'scalloped out,' and is deeply concave. The length of the anterior bar  
984 decreases significantly within the arc of this concavity. The triangular protuberance is equilateral  
985 (Figures 19e-k).

986  
987 The lateral margin is sigmoidal, and the anterior portion just posterior to the anterior bar  
988 is slightly embayed for slight overlap of the associated lateral osteoderm. In posterior view the  
989 osteoderm is only slightly arched (Figure 19h). In what are presumed to be more posteriorly  
990 positioned osteoderms, the osteoderme is more strongly arched (Figures 19l-m). The ventral  
991 surface of the dorsal trunk paramedian osteoderms are smooth, with a slight embayment situated  
992 on the underside of the dorsal eminence.

993 The surface ornamentation of the dorsal trunk paramedian osteoderms is barely apparent  
994 in PEFO 34045, but much better developed in the other specimens. The ornament consists of  
995 pitting surrounding the dorsal eminence and radiating grooves and ridges over the rest of the  
996 surface.

997 There is no direct evidence for a constriction ('waist') in the carapace anterior to the  
998 pelvis as in *Aetosaurus ferratus* (Schoch 2007), and *Calyptosuchus welllesi* (Case 1932);  
999 however, because the lateral osteoderm shapes in *Scutarx deltatylus* are identical to those of  
1000 *Calyptosuchus welllesi*, it is probable that *Scutarx deltatylus* also possessed a 'waisted' carapace  
1001 although this cannot be confirmed.

1002

1003 ***Caudal***

1004 Like the cervical-trunk transition, the trunk-caudal transition is also difficult to determine  
1005 in unarticulated aetosaurian carapaces (Parker 2008a). The latter transition is generally  
1006 characterized by reduction of osteoderm width-length ratios and greater development of the  
1007 dorsal eminences. The extreme is found in *Rioarribasuchus chamaensis*, in which the barely  
1008 visible dorsal eminences in the mid-dorsal region transition posteriorly to elongate,  
1009 anteromedially curved spines in the anterior caudal region (Parker 2007).

1010 The trunk-caudal transition for *Scutarx deltatylus* is best preserved in PEFO 34919 in  
1011 which the dorsal eminences show a marked increase in height from 16.35 in the mid-trunkregion  
1012 to 40.07 mm in the anterior dorsal caudal region. Width/length ratios across this same transition  
1013 are 2.54 to 2.16, showing the corresponding decrease. The dorsal eminence is a tall pyramid,  
1014 with a posterior vertical keel (Figure 21). In all other respects the anterior caudal osteoderms are  
1015 similar to those of the trunk region.

1016 Dorsal mid-caudal paramedians are relatively equal in width and length (w/l ratio = 1.08).  
1017 Those osteoderms still possess the pronounced dorsal eminence (Figures 22a-j), as well as the  
1018 anteromedial and anterolateral projections of the anterior bar. In PEFO 34045 these osteoderms  
1019 are extremely thickened (Figures 22a-b, e-f).

1020 The posterior dorsal caudal paramedians (Figures 22k-n) become longer than wide (w/l  
1021 ratios of 0.73 and 0.66), and the dorsal eminence is reduced to a raised, anteroposteriorly  
1022 elongate keel with a posterior projection that extends beyond the posterior margin of the  
1023 osteoderm. Presumably these continue until they become elongate strips of bone as in *Aetosaurus*  
1024 *ferratus* (Schoch 2007).

1025

1026 ***Lateral osteoderms***

1027 The best guide for the distribution of the lateral osteoderms is UMMP 13950, the  
1028 holotype of *Calyptosuchus wellesi*, which preserves the posterior dorsal armor and much of the

1029 caudal lateral armor in articulation (Case 1932). *Scutarx deltatylus* possesses lateral plates that  
1030 are identical in shape to those of *Calyptosuchus wellesi* allowing for determination of caudal and  
1031 posterior dorsal osteoderms. Therefore, any lateral osteoderms falling outside of those  
1032 morphotypes probably are from more anterior regions. Anterior dorsal lateral osteoderms are  
1033 preserved in the articulated holotype of *Aetosauroides scagliai* (PFV 2073), which can be used to  
1034 help assign isolated osteoderms.

1035 Lateral osteoderms can be distinguished from paramedian osteoderms primarily by the  
1036 lack of the prominent anterolateral projection. Furthermore, the anteromedial corner of the  
1037 osteoderm is ‘cut-off’ and beveled for reception of the anterolateral projection of the associated  
1038 adjacent paramedian osteoderm (poa; Figure 23).

1039

#### 1040 *Cervical*

1041 There are no lateral osteoderms in the material present that can unequivocally be assigned  
1042 to the cervical region.

1043

#### 1044 *Trunk*

1045 Anterior lateral trunk osteoderms are not preserved in the holotype of *Calyptosuchus*  
1046 *wellesi*, but they are preserved in *Aetosaurus ferratus* (Schoch 2007). In *Aetosaurus* those  
1047 osteoderms are strongly asymmetrical with the dorsal flanges roughly half the dimensions of the  
1048 lateral flanges. Furthermore, the dorsal flanges are triangular or trapezoidal in dorsal view rather  
1049 than rectangular, with a slight, medially projecting posterior tongue.

1050 Two osteoderms from the left side in PEFO 34616 and a third from the right side in  
1051 PEFO 34045 match this anatomy and are probably from the anterior portion of the carapace  
1052 (Figures 23a-d). In addition to the features just mentioned, those osteoderms possess a distinct  
1053 anterior bar. The anteromedial corner of the anterior bar is beveled for articulation with the  
1054 anterolateral process of the paramedian osteoderm. The dorsal eminence of the lateral osteoderm

1055 is a prominent pyramidal boss that contacts the posterior plate margin and extends anteriorly,  
1056 covering two-thirds of the osteoderm length. Surface ornamentation consists of elongate grooves  
1057 and ridges radiating from the dorsal eminence. In posterior view, the osteoderms are only slightly  
1058 angulated, with the angle between flanges strongly obtuse (Figures 23b, d). Similarly shaped  
1059 osteoderms are found in the anterior lateral trunk region of *Aetosauroides scagliai* (PVL 2073).

1060         Posterior-mid trunk osteoderms (from roughly the ninth through 12<sup>th</sup> positions) are sub-  
1061 rectangular with a distinct, posteromedially sloping lateral edge (Figures 23e-h; Case 1932). The  
1062 dorsal flange is sub-rectangular in dorsal view. The medial edge of the dorsal flange is beveled  
1063 and slightly sigmoidal with a ‘cut-off’ anterior corner for the anterolateral projection of the  
1064 paramedian plate. The osteoderm is moderately flexed with the lateral flange extending at about  
1065 45 degrees relative to the dorsal flange (Figures 23f, h). Both flanges are roughly the same  
1066 size although the sloping lateral edge produces a small anteromedial ‘wing’ that extends that  
1067 edge a bit farther laterally and provides a trapezoidal shape for the lateral flange (alw; Figures  
1068 23e, g). The dorsal eminence is pyramidal, and the degree of its development differs between  
1069 specimens, from a low mound in PEFO 34045 to a distinct tall, triangular boss in PEFO 34919.  
1070 On the dorsal surface a distinct anterior bar is present and the surface ornamentation consists of  
1071 small pits and elongate grooves radiating from the dorsal eminence. Ventrally the osteoderms are  
1072 smooth, except for longitudinal striations along the posterior margin where this margin would  
1073 overlap the anterior bar of the preceding lateral osteoderm.

1074         The posteriormost lateral trunk osteoderms (15<sup>th</sup> and 16<sup>th</sup> positions) are similar to the  
1075 posterior mid-trunk osteoderms but lack the anterolateral ‘wing’ and are much more strongly  
1076 flexed, enclosing an angle of approximately 90 degrees in posterior view (Figures 23i-j). They  
1077 are similar to the posterior lateral trunk osteoderms in *Calypotosuchus wellsi* (Case 1932).

1078

1079 ***Caudal***

1080 Caudal lateral osteoderms are more equal in dimension, and bear rectangular dorsal  
1081 flanges (Figures 23k-p). The angle enclosed between the dorsal and lateral flanges is about 45-50  
1082 degrees (Figures 23l, n, p). Overall these osteoderms possess some of the same surficial features  
1083 as the other osteoderms, such as an anterior bar, radial ornamentation, and a posteriorly placed  
1084 dorsal eminence. However, the anterior caudal osteoderms in some specimens (e.g., PEFO  
1085 34919) possess some of the tallest dorsal eminences in the carapace (Figures 21; 23n). The  
1086 caudal lateral osteoderms also decrease in width posteriorly (Figure 23m-n). The height of the  
1087 dorsal eminence is gradually reduced and becomes an elongate sharp ridge.  
1088

1089 ***Ventral trunk osteoderms***

1090 Ventral trunk osteoderms are preserved in all of the PEFO specimens, including an  
1091 articulated, but badly preserved, set in PEFO 31217. They consist mainly of square to  
1092 rectangular osteoderms, with reduced anterior bars, no dorsal eminence and a surface  
1093 ornamentation of pits and elongated pits in a radial pattern (Figures 24a-f). Because no complete  
1094 set is preserved the exact numbers of rows and column cannot be determined. 

1095 ***Appendicular osteoderms***

1096 A few irregular, small, rounded osteoderms most likely represent appendicular  
1097 osteoderms that covered the limbs. There are two types: one featureless except for a distinct  
1098 raised keel, and the other with a surface ornamentation of radial pits (Figures 24g, i). A  
1099 triangular osteoderm (Figure 24h) from PEFO 34616 could represent a different type of  
1100 appendicular osteoderm, or it could also be an irregularly shaped osteoderm from the ventral  
1101 carapace. 

1102

1103 ***Broken osteoderms?***

1104 An interesting aspect of PEFO 34045 is the presence of many irregularly shaped  
1105 osteoderms recovered with the specimen (Figure 25). All of the edges on these osteoderms are  
1106 compact bone and do not represent recent breaks. Close examination shows that these specimens  
1107 are the lateral ends of dorsal paramedian osteoderms because they possess anterior bars with  
1108 strong anterolateral projections and sigmoidal edges (Figures 25a-d). It is unclear why these  
1109 osteoderms are incomplete but two possibilities exist. The first possibility is that these  
1110 osteoderms were incompletely ossified. Alternatively, they were broken and then the edges  
1111 rehealed during the life of the animal. However, there is no visible sign of pathology because the  
1112 edges are smooth and the dorsoventral thickness of the osteoderms remains constant. The  
1113 osteoderms are also from opposite sides of the body precluding a cause from a single injury if  
1114 they are pathologic in nature. Histological examination could help determine the ontogeny of  
1115 these elements. If growth rings are uniform throughout the specimen, it would demonstrate that  
1116 either damage occurred at a young age or that the remainder of the element did not ossify. If the  
1117 osteoderms were broken at a later ontogenetic stage and healed, then that should be reflected in  
1118 the bone histology showing a disruption in the growth rings, or establishment of new rings along  
1119 the broken edge 

1120

1121 **DISCUSSION**

1122 *Scutarx deltatylus* represents another good example of the importance of utilizing a  
1123 detailed apomorphy-based approach to differentiate Late Triassic archosauromorph taxa (e.g.,  
1124 Nesbitt, Irmis & Parker 2007; Nesbitt & Stocker 2008; Stocker 2010). The material here referred  
1125 to *Scutarx deltatylus* was originally assigned to *Calypotosuchus welllesi* (Long & Murry 1995;  
1126 Martz et al. 2013; Parker & Irmis 2005), which was differentiated from *Stagonolepis robertsoni*  
1127 by the presence of the triangular protuberance on the paramedian osteoderms (Martz et al. 2013).

1128 However, reexamination of the holotype of *Calyptosuchus wellesi* (UMMP 13950) as well as  
1129 referred material from the *Placerias* Quarry of Arizona shows that material of *Calyptosuchus*  
1130 *wellesi* actually lacks the triangular protuberance. Moreover, the skull of *Scutarx deltatylus*  
1131 possesses characters of the braincase (e.g., foreshortened parabasisphenoid) that are more similar  
1132 to *Desmatosuchus* than to other aetosaurians that are similar to *Stagonolepis*. Unfortunately, the  
1133 skull of *Calyptosuchus wellesi* is still mostly unknown. The *Placerias* Quarry contains a number  
1134 of isolated aetosaurian skull bones, most notably basicrania, with differing anatomical  
1135 characteristics, but none of these can be referred with certainty to *Calyptosuchus wellesi* (Parker  
1136 2014). Nonetheless, prior to the discovery of the skull of *Scutarx deltatylus*, *Calyptosuchus*  
1137 *wellesi* was assumed to have a skull more like that of *Stagonolepis robertsoni* and *Aetosauroides*  
1138 *scagliai* (i.e., with an elongate parabasisphenoid). That assumption can no longer be maintained.  
1139 A phylogenetic analysis (Parker, 2016) recovers *Scutarx deltatylus* as the sister taxon to  
1140 *Adamanasuchus eisenhardtae* and forming a clade with *Calyptosuchus wellesi*. The unnamed  
1141 clade formed by these three taxa is the sister taxon of Desmatosuchini (Parker, 2016) within  
1142 Desmatosuchinae (Figure 26). The presence of a aetosaurian with armor similar to *Stagonolepis*  
1143 *robertsoni* (sensu Heckert and Lucas, 2000), but with a skull more like that of desmatosuchins  
1144 provides further support that certain characteristic of the armor that were once used to unite taxa,  
1145 such as paramedian osteoderm ornamentation (Heckert & Lucas 2000; Long & Ballew 1985;  
1146 Long & Murry 1995), may have wider distributions across Aetosauria than previously  
1147 recognized (Parker 2008b).

1148

1149

1150

### 1151 **Implications for Late Triassic Vertebrate Biochronology**

1152 The holotype and all of the referred specimens of *Scutarx deltatylus* were originally  
1153 assigned to *Calyptosuchus wellesi* (Long & Murry 1995; Martz et al. 2013; Parker & Irmis 2005;

1154 Parker & Martz 2011), a proposed index taxon of the Adamanian biozone (Parker & Martz  
1155 2011), which is earliest Norian in age (Irmis et al. 2011). However, all of the recognized  
1156 specimens of *Scutarx deltatylus* originate only from the Adamanian portion of the Sonsela  
1157 Member of the Chinle Formation and the middle part of the Cooper Canyon Formation of Texas  
1158 (Martz et al. 2013; Parker & Martz 2011). The reassignment of this material restricts the  
1159 stratigraphic range of *Calyptosuchus wellesi* to the Bluewater Creek and Blue Mesa members of  
1160 the Chinle Formation as well as the Tecovas Formation of Texas (Heckert 1997; Long & Murry  
1161 1995), which are stratigraphically lower than the Sonsela Member and middle part of the Cooper  
1162 Canyon (Martz et al. 2013).

1163         It has been suggested that the Adamanian biozone (*sensu* Martz & Parker In Press; Parker  
1164 & Martz 2011) could possibly be subdivided into sub-zones (Martz et al. 2013). That hypothesis  
1165 was supported by a list of Adamanian taxa of the Chinle Formation that noted which are known  
1166 solely from the Blue Mesa Member and which are known only from the lower part of the  
1167 Sonsela Member. The list of taxa shared by both units is small and consists of *Placerias*  
1168 *hesternus* (a dicynodont synapsid), the archosauromorph *Trilophosaurus dornorum*, the  
1169 poposaurid *Poposaurus gracilis*, a paratypothoracin aetosaur similar to *Tecovasuchus*  
1170 *chatterjeei*, and *Calyptosuchus wellesi* (Martz et al. 2013). The reassignment of the Sonsela  
1171 material previously placed in *Calyptosuchus wellesi* to *Scutarx deltatylus* further reduces that  
1172 list. *Scutarx deltatylus* also occurs in the upper Adamanian Post Quarry of Texas, which contains  
1173 taxa elsewhere only found in the lower part of the Sonsela Member (e.g., *Desmotosuchus smalli*,  
1174 *Trilophosaurus dornorum*, *Typothorax coccinarum*, *Paratypothorax* sp.; Martz et al. 2013).  
1175 Thus, *Scutarx deltatylus* can presently be considered an index taxon of the upper part of the

1176 Adamanian biozone, which is presently considered to be middle Norian in age (Figure 26; Irmis  
1177 et al., 2011).

1178

## 1179 CONCLUSIONS

1180 *Scutarx deltatylus* is a new taxon of aetosaurian from the middle Norian (late  
1181 Adamanian) of the American Southwest, based on material that was originally assigned to  
1182 *Calyptosuchus wellsi*. This taxon is known from several carapaces and includes rare skull  
1183 material from western North America. *Scutarx deltatylus* differs from all other aetosaurians in  
1184 the presence of a raised triangular boss in the posteromedial corner of the presacral paramedian  
1185 osteoderms, a dorsoventrally thickened skull roof, and an anteroposteriorly shortened  
1186 parabasisphenoid. A phylogenetic analysis places it as the sister taxon of *Adamanasuchus*  
1187 *eisenhardtae* near the base of Desmatosuchinae (Parker, 2016). *Scutarx deltatylus* appears to  
1188 have utility as an index taxon for the late Adamanian biozone.

1189

## 1190 ACKNOWLEDGEMENTS

1191 Much of this manuscript was a part of a doctoral dissertation submitted to the University  
1192 of Texas at Austin. Reviews of that earlier version were provided by Tim Rowe, Chris Bell,  
1193 Sterling Nesbitt, and Hans-Dieter Sues. Thank you to the management and staff of Petrified  
1194 Forest National Park (PEFO) for their support of this project. For fieldwork assistance at the  
1195 Petrified Forest I thank Daniel Woody, David Gillette, Sue Clements, Dan Slais, Randall Irmis,  
1196 Sterling Nesbitt, Jeff Martz, Michelle Stocker, Raul Ochoa, Lori Browne, Chuck Beightol,  
1197 Rachel Guest, Matt Smith, and Kenneth Bader. Raul Ochoa discovered the type specimen of  
1198 *Scutarx deltatylus*. I also greatly appreciate the assistance provided by the Maintenance Division  
1199 staff of PEFO in the final collection of many of these specimens. Preparation of PEFO specimens

1200 was completed by Pete Reser, Matt Brown, Matt Smith, and Kenneth Bader. All specimens were  
1201 collected under a natural resources permit from the National Park Service.

1202 Access to specimens under their care was provided by T. Scott Williams and Matt Smith  
1203 (PEFO); Pat Holroyd, Mark Goodwin, and Kevin Padian (UCMP); David and Janet Gillette  
1204 (MNA); Julia Desojo (MACN); the late Jaime Powell (PVL); Ricardo Martinez (PVSJ); Sandra  
1205 Chapman, Lorna Steel, and David Gower (NHMUK); Lindsay Zanno and Vince Schneider  
1206 (NCSM); Sankar Chatterjee and Bill Mueller (TTUP); Matthew Carrano (USNM); Tony Fiorillo  
1207 and Ron Tykoski (DMNH); Alex Downs (GR); Charles Dailey and Dick Hilton (Sierra College);  
1208 Tim Rowe, Lyndon Murray, Matt Brown, and Chris Sagebiel (VPL).

1209 Financial assistance for this project was provided by the Jackson School of Geosciences,  
1210 the Lundelius Fund, the Francis L. Whitney Endowed Presidential Scholarship, the Ronald K. DeFord  
1211 Scholarship Fund, the Petrified Forest Museum Association, Petrified Forest National Park, the Friends of  
1212 the Petrified Forest, the Museum of Northern Arizona, the GSA Geocorp program, the Samuel and Doris  
1213 Welles Fund, and the Systematics Association. This is Petrified Forest National Park Paleontological  
1214 Contribution **number xx**.

1215

## 1216 REFERENCES

- 1217 Brochu CA. 1992. Ontogeny of the postcranium in crocodylomorph archosaurs M.S. University  
1218 of Texas
- 1219 Brochu CA. 1996. Closure of neurocentral sutures during crocodylian ontogeny: implications for  
1220 maturity assessment in fossil archosaurs. *Journal of Vertebrate Paleontology* 16:49-62.
- 1221 Butler RJ, Barrett PM, and Gower DJ. 2012. Reassessment of the evidence for postcranial  
1222 skeletal pneumaticity in archosaurs, and the early evolution of the avian respiratory  
1223 system. *PLoS One* 7(3):e34094.

- 1224 Case EC. 1922. New reptiles and stegocephalians from the Upper Triassic of western Texas. .  
1225 *Carnegie Institute of Washington Publication* 321:1-84.
- 1226 Case EC. 1932. A perfectly preserved segment of the armor of a phytosaur, with associated  
1227 vertebrae. *Contributions from the Museum of Paleontology, University of Michigan* 4:57-  
1228 80.
- 1229 Colbert EH. 1971. Tetrapods and continents. *Quarterly Review of Biology* 46:250-269.
- 1230 Cope ED. 1869. Synopsis of the extinct Batrachia, Reptilia, and Aves of North America. .  
1231 *Transactions of the American Philisophical Society, ns* 14:1-252.
- 1232 Cope ED. 1875. Appendix LL: Report on the geology of that part of northwestern New Mexico  
1233 examined during the field season of 1874. In: Wheeler GM, ed. *Appendix GI: Annual*  
1234 *Report upon the Geographical Explorations and Surveys West of the One Hundredth*  
1235 *Meridian, Annual Report of the Chief of Engineers for 1875*. Washington, D.C.: Engineer  
1236 Department, U.S. Army, 61-116.
- 1237 Desojo JB, and Báez AM. 2005. El esqueleto postcraneano de *Neoaetosauroides* (Archosauria:  
1238 Aetosauria) del Triásico Superior del centro-oeste de Argentina. *Ameghiniana* 42:115-  
1239 126.
- 1240 Desojo JB, and Báez AM. 2007. Cranial morphology of the Late Triassic South American  
1241 archosaur *Neoaetosauroides engaeus*: evidence for aetosaurian diversity. *Palaeontology*  
1242 50:267-276.
- 1243 Desojo JB, and Ezcurra MD. 2011. A reappraisal of the taxonomic status of *Aetosauroides*  
1244 (Archosauria, Aetosauria) specimens from the Late Triassic of South America and their  
1245 proposed synonymy with *Stagonolepis*. *Journal of Vertebrate Paleontology* 31:596-609.

- 1246 Desojo JB, Ezcurra MD, and Kischlat E-E. 2012. A new aetosaur genus (Archosauria:  
1247 Pseudosuchia) from the early Late Triassic of southern Brazil. *Zootaxa* 3166:1-33.
- 1248 Desojo JB, and Heckert AB. 2004. New information on the braincase and mandible of  
1249 Coahomasuchus (Archosauria: Aetosauria) from the Otischalkian (Carnian) of Texas.  
1250 *Neues Jahrbuch für Geologie und Paläontologie Monatshefte* 2004:605-616.
- 1251 Desojo JB, Heckert AB, Martz JW, Parker WG, Schoch RR, Small BJ, and Sulej T. 2013.  
1252 Aetosauria: a clade of armoured pseudosuchians from the Upper Triassic continental  
1253 beds. In: Nesbitt SJ, Desojo JB, and Irmis RB, editors. *Anatomy, Phylogeny, and*  
1254 *Paleobiology of Early Archosaurs and their Kin: Special Publications of the Geological*  
1255 *Society of London* p203-239.
- 1256 Fraser NC. 2006. *Dawn of the Dinosaurs: Life in the Triassic*. Bloomington: Indiana University  
1257 Press.
- 1258 Gauthier J. 1986. Saurischian monophyly and the origin of birds. *Memoirs of the California*  
1259 *Academy of Sciences* 8:1-55.
- 1260 Gauthier J, and Padian K. 1985. Phylogenetic, functional, and aerodynamic analyses of the origin  
1261 of birds and their flight. In: Hecht MK, Ostrom JH, Viohl G, and Wellnhofer P, eds. *The*  
1262 *Beginning of Birds: Proceedings of the International Archaeopteryx Conference*.  
1263 Eichstätt: Freunde des Jura Museums, 185-197.
- 1264 Gower DJ, and Walker AD. 2002. New data on the braincase of the aetosaurian archosaur  
1265 (Reptilia: Diapsida) *Stagonolepis robertsoni* Agassiz. *Zoological Journal of the Linnean*  
1266 *Society* 136:7-23.

- 1267 Heckert AB. 1997. The tetrapod fauna of the Upper Triassic lower Chinle Group (Adamanian:  
1268 latest Carnian) of the Zuni Mountains, west-central New Mexico. *New Mexico Museum*  
1269 *of Natural History and Science Bulletin* 11:29-39.
- 1270 Heckert AB, and Lucas SG. 1999. A new aetosaur (Reptilia: Archosauria) from the Upper  
1271 Triassic of Texas and the phylogeny of aetosaurs. *Journal of Vertebrate Paleontology*  
1272 19:50-68.
- 1273 Heckert AB, and Lucas SG. 2000. Taxonomy, phylogeny, biostratigraphy, biochronology,  
1274 paleobiogeography, and evolution of the Late Triassic Aetosauria (Archosauria:  
1275 Crurotarsi). *Zentralblatt für Geologie und Paläontologie Teil I* 1998 1539-1587.
- 1276 Heckert AB, Lucas SG, Hunt AP, and Spielmann J. 2007a. Late aetosaur biochronology  
1277 revisited. *New Mexico Museum of Natural History & Science Bulletin* 41:49-50.
- 1278 Heckert AB, Lucas SG, Rinehart LF, Celeskey MD, Spielmann JA, and Hunt AP. 2010.  
1279 Articulated skeletons of the aetosaur *Tyothorax coccinarum* Cope (Archosauria:  
1280 Stagonolepididae) from the Upper Triassic Bull Canyon Formation (Revueltian: early-  
1281 mid Norian), eastern New Mexico, USA. *Journal of Vertebrate Paleontology* 30:619-  
1282 642.
- 1283 Heckert AB, Spielmann J, Lucas SG, and Hunt AP. 2007b. Biostratigraphic utility of the Upper  
1284 Triassic aetosaur *Tecovasuchus* (Archosauria: Stagonolepididae), an index taxon of St.  
1285 Johnian (Adamanian: Late Carnian) time. In: Lucas SG, and Spielmann J, eds. *The*  
1286 *Global Triassic*. Albuquerque: New Mexico Museum of Natural History and Science, 51-  
1287 57.
- 1288 Hill RV. 2010. Osteoderms of *Simosuchus clarki* (Crocodyliformes: Notosuchia) from the Late  
1289 Cretaceous of Madagascar. *Journal of Vertebrate Paleontology Memoir* 10:154-176.

- 1290 Hopson JA. 1979. Paleoneurology. In: Gans C, Northcutt RG, and Ulinsky P, eds. *Biology of the*  
1291 *Reptilia 9, neurology A*. London: Academic Press, 39-146.
- 1292 Howell ER, and Blakey RC. 2013. Sedimentological constraints on the evolution of the  
1293 Cordilleran arc: New insights from the Sonsela Member, Upper Triassic Chinle  
1294 Formation, Petrified Forest National Park (Arizona, USA). *Geological Society of*  
1295 *America Bulletin* 125:1349-1368. 10.1130/B30714.1
- 1296 Irmis RB. 2007. Axial skeleton ontogeny in the Parasuchia (Archosauria: Pseudosuchia) and its  
1297 implications for ontogenetic determination in archosaurs. *Journal of Vertebrate*  
1298 *Paleontology* 27:350-361.
- 1299 Irmis RB. 2008. Perspectives on the origin and early diversification of dinosaurs PhD. University  
1300 of California.
- 1301 Irmis RB, Mundil R, Martz JW, and Parker WG. 2011. High-resolution U-Pb ages from the  
1302 Upper Triassic Chinle Formation (New Mexico, USA) support a diachronous rise of  
1303 dinosaurs. *Earth and Planetary Science Letters* 309:258-267.
- 1304 Irmis RB, Nesbitt SJ, Padian K, Smith ND, Turner AH, Woody D, and Downs A. 2007a. A Late  
1305 Triassic dinosauromorph assemblage from New Mexico and the rise of dinosaurs.  
1306 *Science* 317:358-361.
- 1307 Irmis RB, Parker WG, Nesbitt SJ, and Liu J. 2007b. Early ornithischian dinosaurs: the Triassic  
1308 record. *Historical Biology* 19:3-22.
- 1309 Jepson GL. 1948. A Triassic armored reptile from New Jersey. In: Johnson ME, ed. *State of New*  
1310 *Jersey Department of Conservation Miscellaneous Geologic Paper*. Trenton: New Jersey  
1311 Geologic Survey, 5-20.

- 1312 Long RA, and Ballew KL. 1985. Aetosaur dermal armor from the Late Triassic of Southwestern  
1313 North America, with special reference to material from the Chinle Formation of Petrified  
1314 Forest National Park. *Museum of Northern Arizona Bulletin* 54:45-68.
- 1315 Long RA, and Murry PA. 1995. Late Triassic (Carnian and Norian) tetrapods from the  
1316 southwestern United States. *New Mexico Museum of Natural History & Science Bulletin*  
1317 4:1-254.
- 1318 Lucas SG. 1998. Global Triassic tetrapod biostratigraphy and biochronology. *Palaeogeography,*  
1319 *Palaeoclimatology, Palaeoecology* 143:347-384.
- 1320 Lucas SG, and Heckert AB. 1996. Late Triassic aetosaur biochronology. *Albertiana* 17:57-64.
- 1321 Lucas SG, Heckert AB, Estep JW, and Anderson OJ. 1997. Stratigraphy of the Upper Triassic  
1322 Chinle Group, Four Corners Region. *New Mexico Geological Society Guidebook* 48:81-  
1323 108.
- 1324 Lucas SG, Heckert AB, and Hunt AP. 2003. A new species of the aetosaur *Tyothorax*  
1325 (Archosauria: Stagonolepididae) from the Upper Triassic of east-central New Mexico.  
1326 *New Mexico Museum of Natural History and Science Bulletin* 21:221-233.
- 1327 Lucas SG, and Hunt AP. 1993. Tetrapod biochronology of the Chinle Group (Upper Triassic),  
1328 western United States. *New Mexico Museum of Natural History and Science Bulletin*  
1329 3:327-329.
- 1330 Lucas SG, Hunt AP, Heckert AB, and Spielmann JA. 2007. Global Triassic tetrapod  
1331 biostratigraphy and biochronology: 2007 status. *New Mexico Museum of Natural History*  
1332 *and Science Bulletin* 41:229-240.
- 1333 Lucas SG, Hunt AP, and Spielmann J. 2007. A new aetosaur from the Upper Triassic  
1334 (Adamanian: Carnian) of Arizona. In: Lucas SG, and Spielmann J, eds. *Triassic of the*

- 1335 *American West*. Albuquerque: New Mexico Museum of Natural History and Science,  
1336 241-247.
- 1337 Lydekker R. 1887. The fossil vertebrata of India. *Records of the Geological Survey of India*  
1338 20:51-80.
- 1339 Marsh OC. 1884. The classification and affinities of dinosaurian reptiles. *Nature*:68-69.
- 1340 Martz JW. 2002. The morphology and ontogeny of *Typosuchus coccinarum* (Archosauria,  
1341 Stagonolepididae) from the Upper Triassic of the American Southwest M.S. Texas Tech  
1342 University.
- 1343 Martz JW, Mueller BD, Nesbitt SJ, Stocker MR, Atanassov M, Fraser NC, Weinbaum JC, and  
1344 Lehane J. 2013. A taxonomic and biostratigraphic re-evaluation of the Post Quarry  
1345 vertebrate assemblage from the Cooper Canyon Formation (Dockum Group, Upper  
1346 Triassic) of southern Garza County, western Texas. . *Earth and Environmental Science*  
1347 *Transactions of the Royal Society of Edinburgh* 103:339-364.
- 1348 Martz JW, and Parker WG. 2010. Revised lithostratigraphy of the Sonsela Member (Chinle  
1349 Formation, Upper Triassic) in the southern part of Petrified Forest National Park,  
1350 Arizona. *PLoS One* 5:e9329, 9321-9326.
- 1351 Martz JW, and Parker WG. In Press. Revised formulation of the Late Triassic land vertebrate  
1352 "faunachrons" of western North America. In: Zeigler KE, and Parker WG, eds.  
1353 *Deciphering Complex Depositional Systems*: Elsevier.
- 1354 Martz JW, and Small BJ. 2006. *Tecovasuchus chatterjeei*, a new aetosaur (Archosauria:  
1355 Stagonolepididae) from the Tecovas Formation (Carnian, Upper Triassic) of Texas.  
1356 *Journal of Vertebrate Paleontology* 26:308-320.

- 1357 Nesbitt SJ. 2011. The early evolution of archosaurs: relationships and the origin of major clades.  
1358 *Bulletin of the American Museum of Natural History* 352:1-292.
- 1359 Nesbitt SJ, Irmis RB, and Parker WG. 2007. A critical re-evaluation of the Late Triassic dinosaur  
1360 taxa of North America. *Journal of Systematic Palaeontology* 5:209-243.
- 1361 Nesbitt SJ, Sidor CA, Irmis RB, Angielczyk KD, Smith RMH, and Tsuji LA. 2010. Ecologically  
1362 distinct dinosaurian sister group shows early diversification of Ornithodira. *Nature*  
1363 464:95-98.
- 1364 Nesbitt SJ, Smith ND, Irmis RB, Turner AH, Downs A, and Norell MA. 2009a. A complete  
1365 skeleton of a Late Triassic saurischian and the early evolution of dinosaurs. *Science*  
1366 326:1530-1533.
- 1367 Nesbitt SJ, and Stocker MR. 2008. The vertebrate assemblage of the Late Triassic Canjilon  
1368 Quarry (northern New Mexico, USA), and the importance of apomorphy-based  
1369 assemblage comparisons. *Journal of Vertebrate Paleontology* 28:1063-1072.
- 1370 Nesbitt SJ, Stocker MR, Small BJ, and Downs A. 2009b. The osteology and relationships of  
1371 *Vancleavea campi* (Reptilia: Archosauriformes). *Zoological Journal of the Linnean*  
1372 *Society* 157:814-864.
- 1373 Parker WG. 2005a. Faunal review of the Upper Triassic Chinle Formation of Arizona. *Mesa*  
1374 *Southwest Museum Bulletin* 11:34-54.
- 1375 Parker WG. 2005b. A new species of the Late Triassic aetosaur *Desmotosuchus* (Archosauria:  
1376 Pseudosuchia). *Comptes Rendus Palevol* 4:327-340.
- 1377 Parker WG. 2007. Reassessment of the aetosaur '*Desmotosuchus*' *chamaensis* with a reanalysis  
1378 of the phylogeny of the Aetosauria (Archosauria: Pseudosuchia). *Journal of Systematic*  
1379 *Palaeontology* 5:41-68. 10.1017/S1477201906001994

- 1380 Parker WG. 2008a. Description of new material of the aetosaur *Desmatosuchus spurensis*  
1381 (Archosauria: Suchia) from the Chinle Formation of Arizona and a revision of the genus  
1382 *Desmatosuchus*. *PaleoBios* 28:1-40.
- 1383 Parker WG. 2008b. How many valid aetosaur species are there? Reviewing the alpha-taxonomy  
1384 of the Aetosauria (Archosauria: Pseudosuchia) and its implications for Late Triassic  
1385 global biostratigraphy. *Journal of Vertebrate Paleontology* 28:125A.
- 1386 Parker WG. 2014. Taxonomy and phylogeny of the Aetosauria (Archosauria: Pseudosuchia)  
1387 including a new species from the Upper Triassic of Arizona Ph.D. The University of  
1388 Texas at Austin.
- 1389 Parker WG. 2016. Revised phylogenetic analysis of the Aetosauria (Archosauria: Pseudosuchia);  
1390 assessing the effects of incongruent morphological character sets. *PeerJ* 4:e1583.  
1391 10.7717/peerj.1583
- 1392 Parker WG, and Irmis RB. 2005. Advances in Late Triassic vertebrate paleontology based on  
1393 new material from Petrified Forest National Park, Arizona. *New Mexico Museum of*  
1394 *Natural History and Science Bulletin* 29:45-58.
- 1395 Parker WG, and Martz JW. 2011. The Late Triassic (Norian) Adamanian-Revuelitian tetrapod  
1396 faunal transition in the Chinle Formation of Petrified Forest National Park, Arizona.  
1397 *Earth and Environmental Science Transactions of the Royal Society of Edinburgh*  
1398 101:231-260.
- 1399 Parrish JM. 1994. Cranial osteology of *Longosuchus meadei* and the phylogeny and distribution  
1400 of the Aetosauria. *Journal of Vertebrate Paleontology* 14:196-209.
- 1401 Ramezani J, Hoke GD, Fastovsky DE, Bowring SA, Therrien F, Dworkin SI, Atchley SC, and  
1402 Nordt LC. 2011. High-precision U-Pb zircon geochronology of the Late Triassic Chinle

- 1403 Formation, Petrified Forest National Park (Arizona, USA): temporal constraints on the  
1404 early evolution of dinosaurs. *Geological Society of America Bulletin* 123:2142-2159.
- 1405 Rauhut OWM. 2004. Braincase structure of the Middle Jurassic theropod dinosaur  
1406 *Piatnitzkysaurus*. *Canadian Journal of Earth Sciences* 41:1109-1122.
- 1407 Reese AM. 1915. *The Alligator and its Allies*. New York: Knickerbocker Press.
- 1408 Reichgelt T, Parker WG, Martz JW, Conran JG, Van Konijnenburg-Van Cittert JHA, and  
1409 Kürschner WM. 2013. The palynology of the Sonsela Member (Late Triassic, Norian) at  
1410 Petrified Forest National Park, Arizona, USA. *Review of Palaeobotany and Palynology*  
1411 189:18-28.
- 1412 Rieppel O. 1985. The recessus scalae tympani and its bearing on the classification of lizards.  
1413 *Journal of Herpetology* 19:373-384.
- 1414 Roberto-Da-Silva L, Desojo JB, Cabrera SF, Aires ASS, Müller ST, Pacheco CP, and Dias-da-  
1415 Silva S. 2014. A new aetosaur from the Upper Triassic of the Santa Maria Formation,  
1416 southern Brazil. *Zootaxa* 3764:240-278.
- 1417 Sawin HJ. 1947. The pseudosuchian reptile *Typothorax meadei*. *Journal of Paleontology* 21:201-  
1418 238.
- 1419 Schoch RR. 2007. Osteology of the small archosaur *Aetosaurus* from the Upper Triassic of  
1420 Germany. *Neues Jahrbuch für Geologie und Paläontologie Abhandlungen* 246:1-35.  
1421 10.1127/0077-7749/2007/0246-0001
- 1422 Schoch RR, and Desojo JB. 2016. Cranial anatomy of the aetosaur *Paratypothorax andressorum*  
1423 Long & Ballew, 1985, from the Upper Triassic of Germany and its bearing on aetosaur  
1424 phylogeny. *Neues Jahrbuch für Geologie und Paläontologie Abhandlungen* 279:73-95.

- 1425 Small BJ. 2002. Cranial anatomy of *Desmotosuchus haplocerus* (Reptilia: Archosauria:  
1426 Stagonolepididae). *Zoological Journal of the Linnean Society* 136:97-111.
- 1427 Small BJ, and Martz JW. 2013. A new basal aetosaur from the Upper Triassic Chinle Formation  
1428 of the Eagle Basin, Colorado, USA. In: Nesbitt SJ, Desojo JB, and Irmis RB, eds.  
1429 *Anatomy, Phylogeny and Palaeobiology of Early Archosaurs and their Kin*. Bath: The  
1430 Geological Society Publishing House, 393-412.
- 1431 Spielmann J, and Lucas SG. 2012. Tetrapod fauna of the Upper Triassic Redonda Formation,  
1432 east-central New Mexico: the characteristic assemblage of the Apachean land-vertebrate  
1433 faunachron. *New Mexico Museum of Natural History & Science Bulletin* 55:1-119.
- 1434 Stocker MR. 2010. A new taxon of phytosaur (Archosauria: Pseudosuchia) from the Late  
1435 Triassic (Norian) Sonsela Member (Chinle Formation) in Arizona, and a critical  
1436 reevaluation of *Leptosuchus* Case 1922. *Palaeontology* 53:997-1022.
- 1437 Sulej T. 2010. The skull of an early Late Triassic aetosaur and the evolution of the  
1438 stagonolepidid archosaurian reptiles. *Zoological Journal of the Linnean Society* 158:860-  
1439 881.
- 1440 Wake MH. 1992. *Hyman's comparative vertebrate anatomy, revised third edition*. Chicago:  
1441 University of Chicago Press.
- 1442 Walker AD. 1961. Triassic Reptiles from the Elgin Area: *Stagonolepis*, *Dasygnathus* and Their  
1443 Allies. *Philosophical Transactions of the Royal Society of London Series B, Biological*  
1444 *Sciences* 244:103-204.
- 1445 Walker AD. 1990. A revision of *Sphenosuchus acutus* Houghton, a crocodylomorph reptile from  
1446 the Elliott Formation (Late Triassic or Early Jurassic) of South Africa. *Philosophical*  
1447 *Transactions: Biological Sciences* 330:1-120.

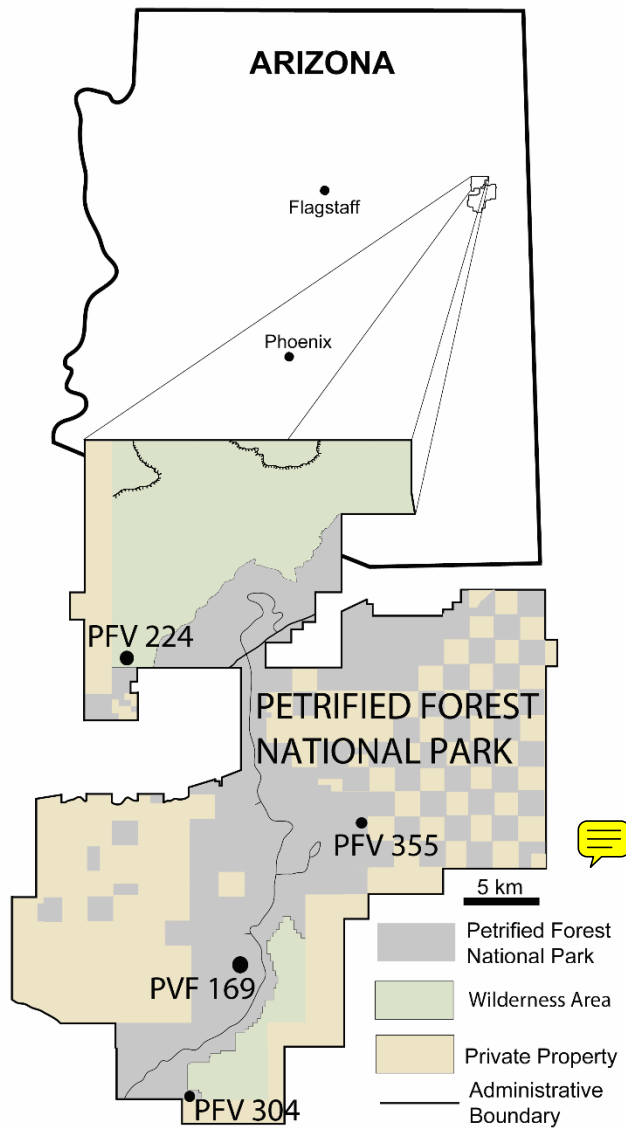
- 1448 Weinbaum JC. 2011. The skull of *Postosuchus kirkpatricki* (Archosauria: Paracrocodyliformes)  
1449 from the Upper Triassic of the United States. *PaleoBios* 30:18-44.
- 1450 Wilson JA. 1999. A nomenclature for vertebral laminae in sauropods and other saurischian  
1451 dinosaurs. *Journal of Vertebrate Paleontology* 19:639-653.
- 1452 Wilson JA, D'Emic MD, Ikejiri T, Moacdieh EM, and Whitlock JA. 2011. A nomenclature for  
1453 vertebral fossae in sauropods and other saurischian dinosaurs. *PLoS One* 6(2):e17114.
- 1454 Witmer LM. 1997. Craniofacial air sinus systems. In: Currie PJ, and Padian K, eds.  
1455 *Encyclopedia of Dinosaurs*. San Diego: Academic Press.
- 1456 Woody DT. 2006. Revised stratigraphy of the lower Chinle Formation (Upper Triassic) of  
1457 Petrified Forest National Park, Arizona. *Museum of Northern Arizona Bulletin* 62:17-45.
- 1458 Zeigler KE, Heckert AB, and Lucas SG. 2003 [imprint 2002]. A new species of *Desmotosuchus*  
1459 (Archosauria: Aetosauria) from the Upper Triassic of the Chama Basin, north-central  
1460 New Mexico. *New Mexico Museum of Natural History and Science Bulletin* 21:215-219.
- 1461 Zittel KA. 1887-1890. *Handbuch der Palaeontologie. 1. Abteilung: Palaeozoologie, 3*. München  
1462 & Leipzig.
- 1463
- 1464
- 1465
- 1466

1467

1468

1469

1470

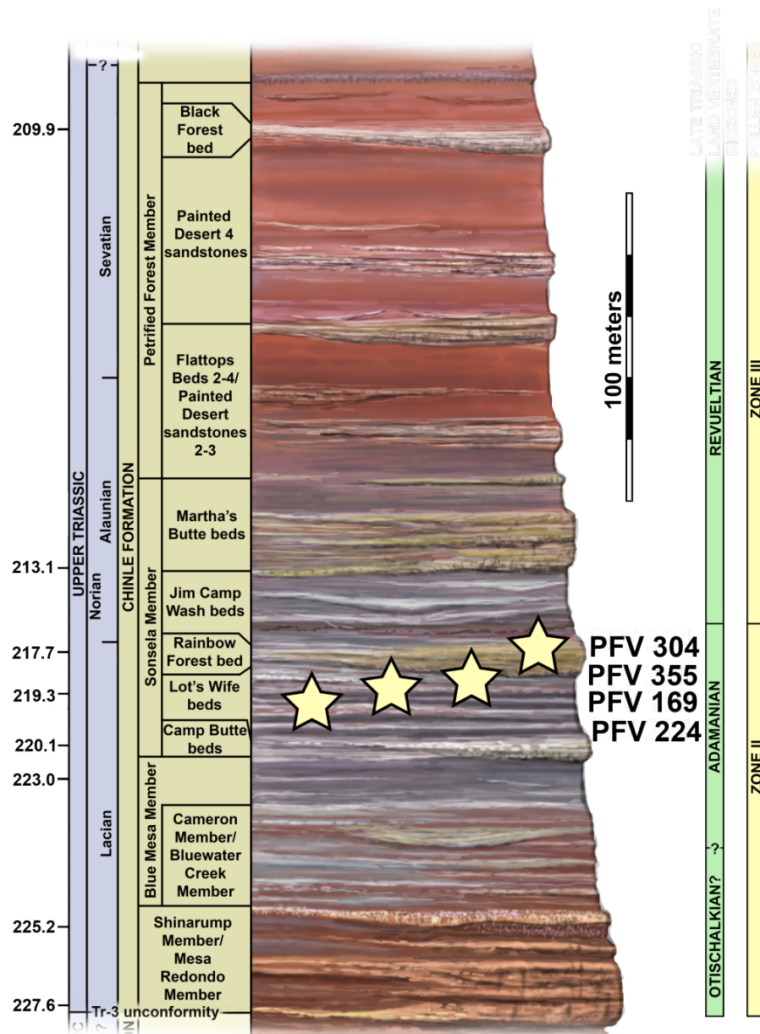


1471

1472

1473 Figure 1. Map of Petrified Forest National Park showing relevant vertebrate fossil localities.  
1474 Modified from Parker & Irmis (2005).

1475

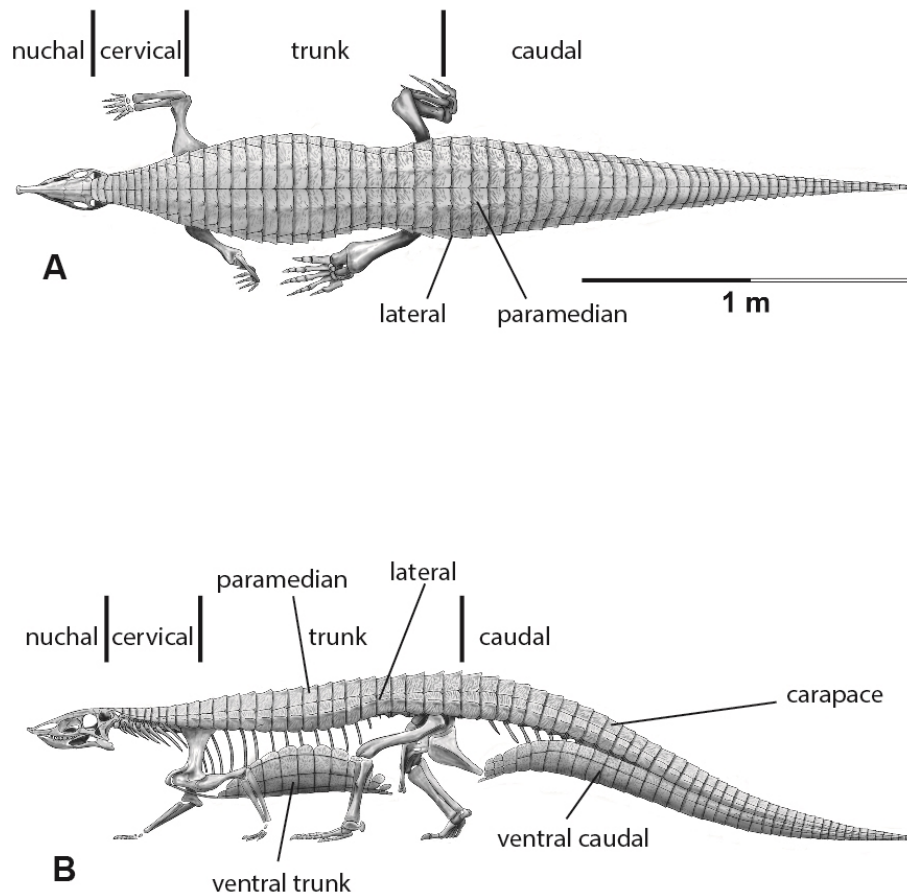


1476

1477

1478 Figure 2. Regional stratigraphy of the Petrified Forest area showing the stratigraphic position of  
 1479 the localities discussed in the text. All occurrences are in the lower part of the  
 1480 Sonsela Member of the Chinle Formation and are within the Adamanian biozone.  
 1481 Stratigraphy from Martz & Parker, 2010. Biozones from Parker & Martz (2011) and  
 1482 Reichgelt et al. (2013). Ages from Ramezani et al. (2011) and Atchley et al. (2013).

1483

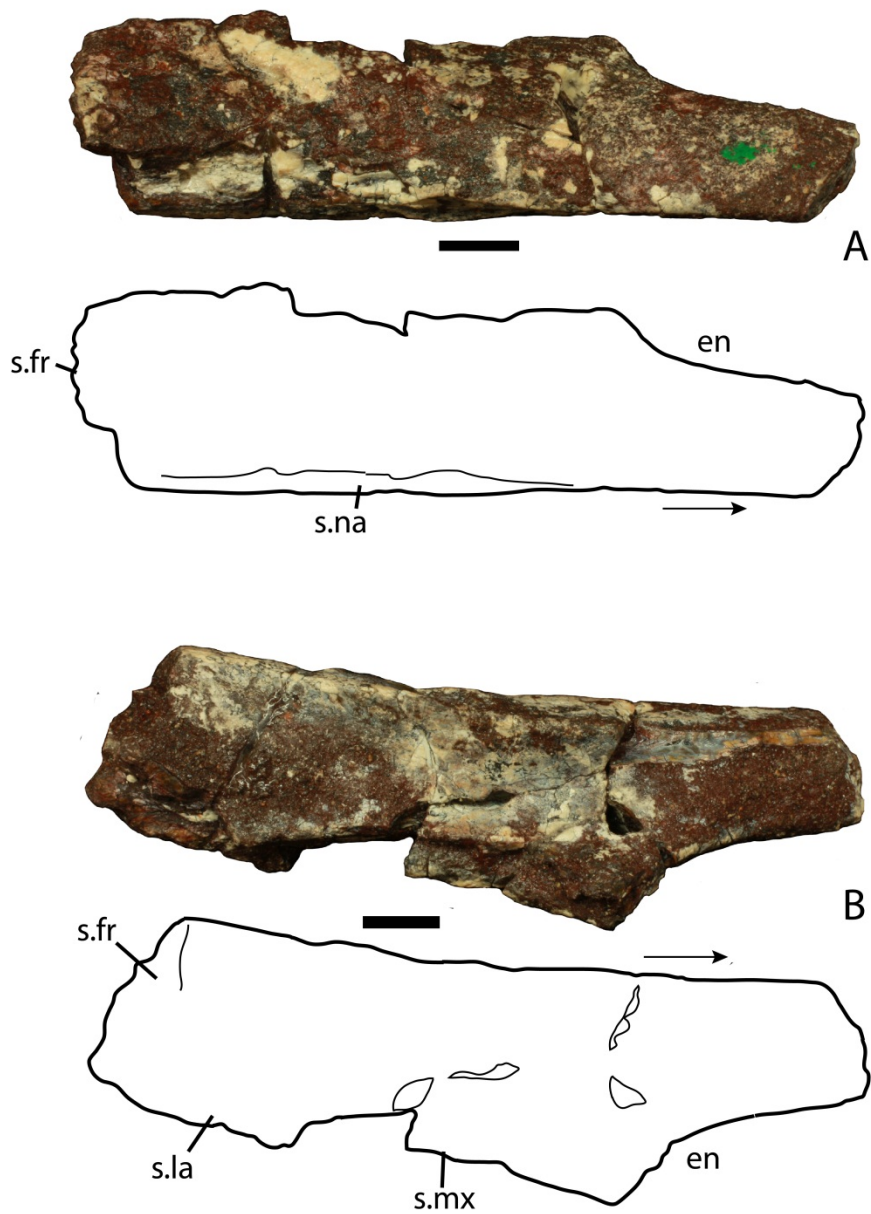


1484

1485 Figure 3. Differentiation and terminology for aetosaurian osteoderms. Reconstruction

1486 courtesy of Jeffrey Martz. 

1487

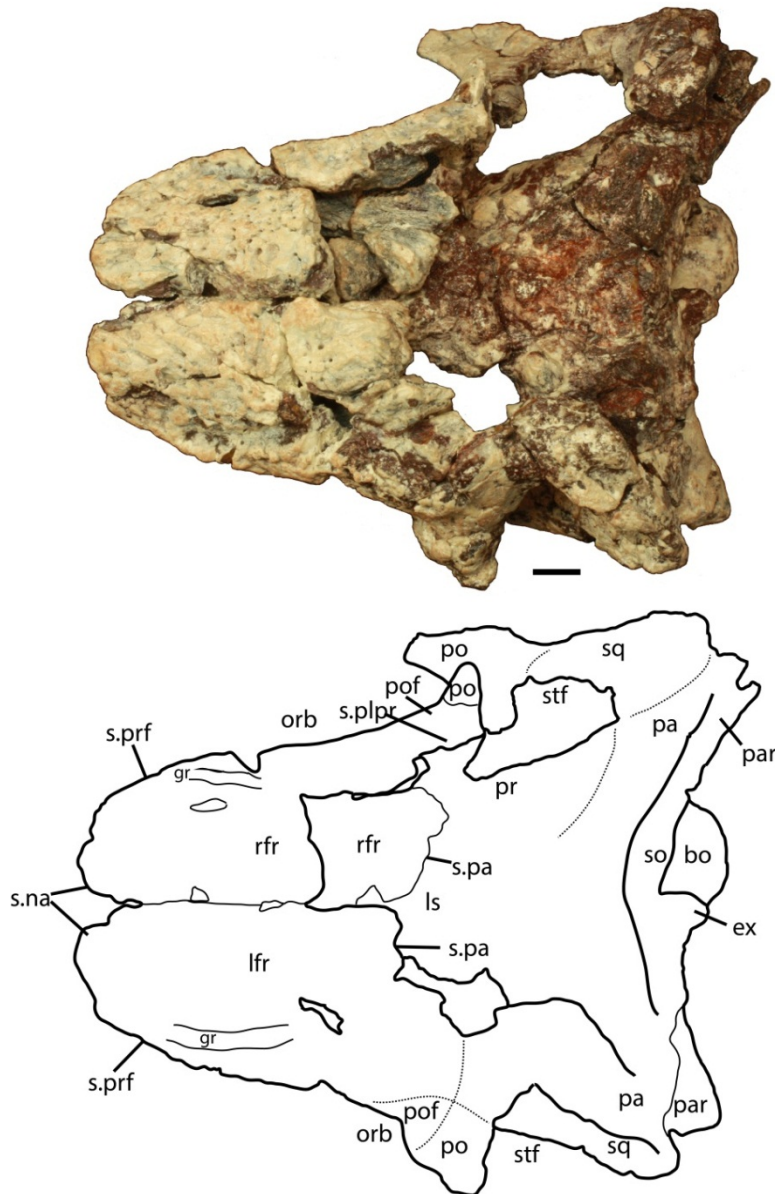


1488

1489

1490 Figure 4. Photos and interpretive sketches of the left nasal (PEFO 34616) in dorsal (A) and  
 1491 ventral (B) views. Arrows point anteriorly and scale bars equal 1 cm.  
 1492 Abbreviations: en, external nares; fr, frontal; la, lacrimal; mx, maxilla; s., suture  
 1493 with listed element.

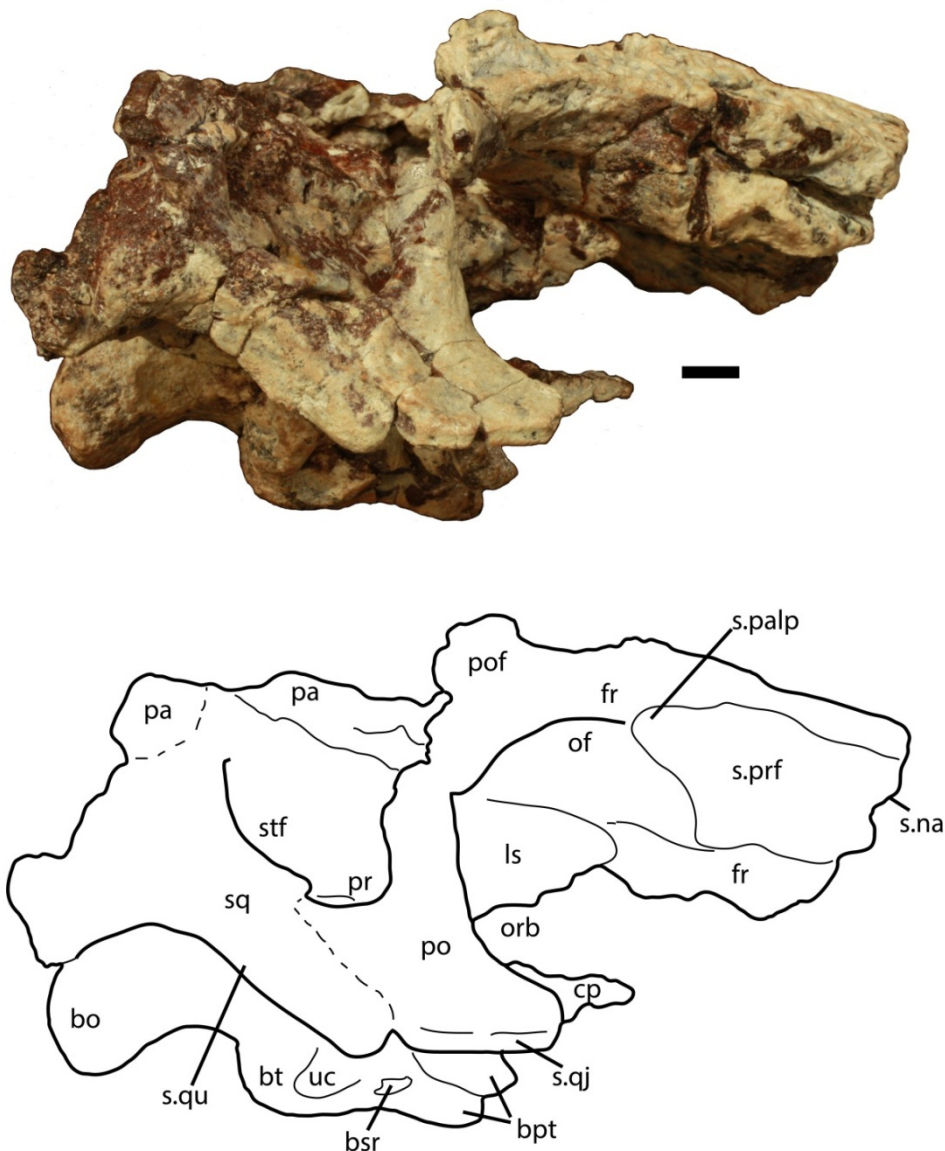
1494



1495

1496

1497 Figure 5. Photo and interpretive sketch of posterodorsal portion of the skull of *Scutarx deltatylus*   
 1498 in dorsal view. Scale bar equals 1 cm. Abbreviations: bo, basioccipital; gr, groove;  
 1499 ex, exoccipital; lfr, left frontal; ls, laterosphenoid; na, nasal; orb, orbit; pa, parietal;  
 1500 par, paroccipital process of the opisthotic; plpr, palpebral; po, postorbital; pof,  
 1501 postfrontal; pr, prootic; prf, prefrontal; rfr, right frontal; s., suture with listed  
 1502 element; so, supraoccipital; sq, squamosal; stf, supratemporal fenestra.



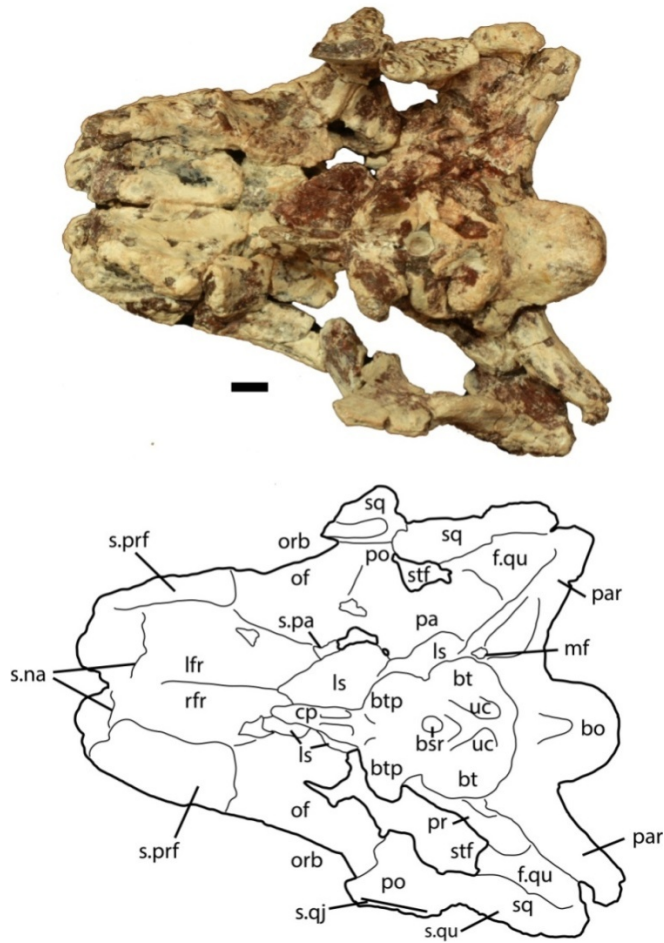
1503

1504

1505 Figure 6. Partial skull of *Scutarx deltatylus* (PEFO 34616) in right lateral view. Scale bar  
 1506 equals 1 cm. Abbreviations: bo, basioccipital; bpt, basipterygoid processes; bsr, basisphenoid  
 1507 recess; bt, basal tubera; cp, cultriform process; fr, frontal; ls, laterosphenoid; na, nasal; of, orbital  
 1508 fossa; orb, orbit; pa, parital; palp, palpebral; po, postorbital; pof, postfrontal; pr, prootic; prf,  
 1509 prefrontal; qj, quadratojugal; qu, quadrate; sq, squamosal; stf, supratemporal fenestra; uc,  
 1510 unossified cleft of the basal tubera.

1511

1512

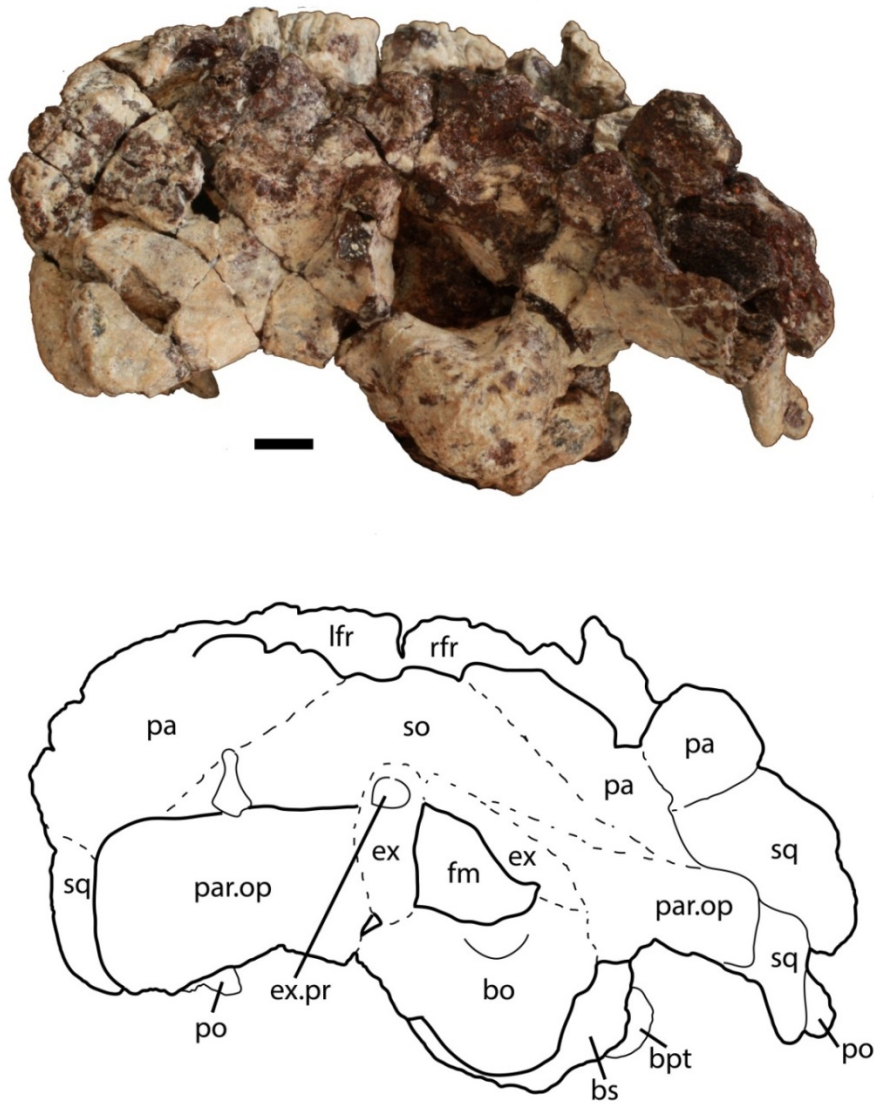


1513

1514

1515 Figure 7. Partial skull of *Scutarx deltatylus* (PEFO 34616) in ventral view. Scale bar  
 1516 equals 1 cm. Abbreviations: bo, basioccipital; btp, basipterygoid processes; bsr, basisphenoid  
 1517 recess; bt, basal tubera; cp, cultriform process; f., fossa for specified element; lfr, left frontal; ls,  
 1518 laterosphenoid; mf, metotic fissure; na, nasal; of, orbital fossa; orb, orbit; pa, parietal; palp,  
 1519 palpebral; par, paroccipital process of the opisthotic; po, postorbital; pof, postfrontal; pr, prootic;  
 1520 prf, prefrontal; qj, quadratojugal; qu, quadrate; rfr, right frontal; sq, squamosal; stf,  
 1521 supratemporal fenestra; uc, unossified cleft of the basal tubera.

1522



1523

1524

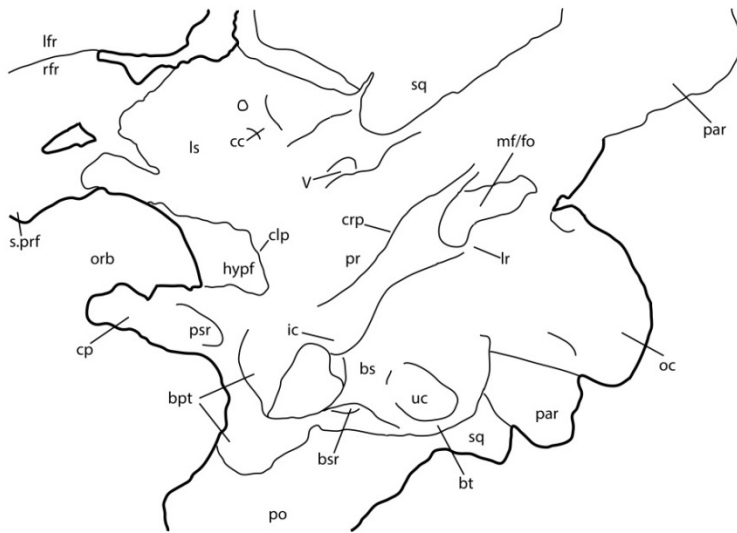
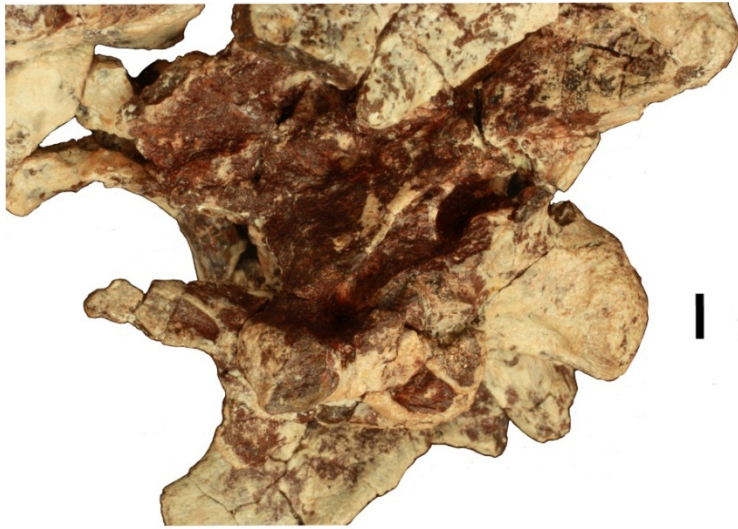
1525 Figure 8. Partial skull of *Scutarx deltatylus* (PEFO 34616) in posterior view. Scale bar

1526 equals 1 cm. Abbreviations: bo, basioccipital; bpt, basipterygoid processes; bs, basisphenoid; ex,

1527 exoccipital; ex.pr; exoccipital prong; fm, foramen magnum; lfr, left frontal; pa, parietal; par.op,

1528 paroccipital process of the opisthotic; po, postorbital; rfr, right frontal; sq, squamosal.

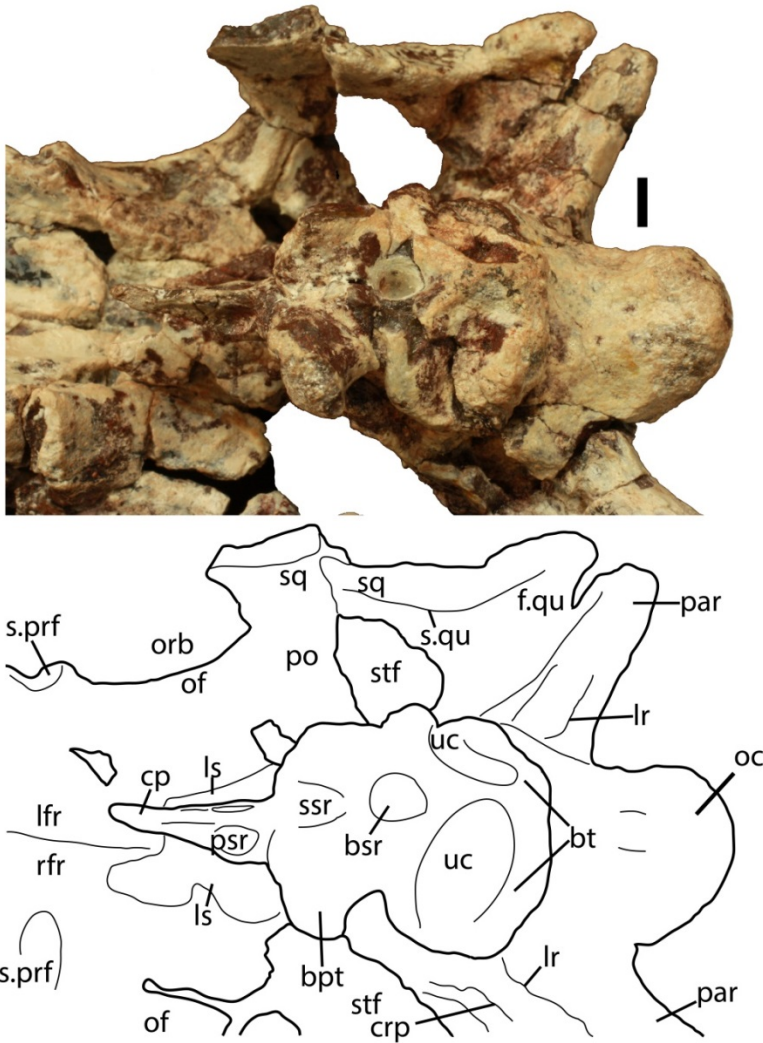
1529



1530

1531

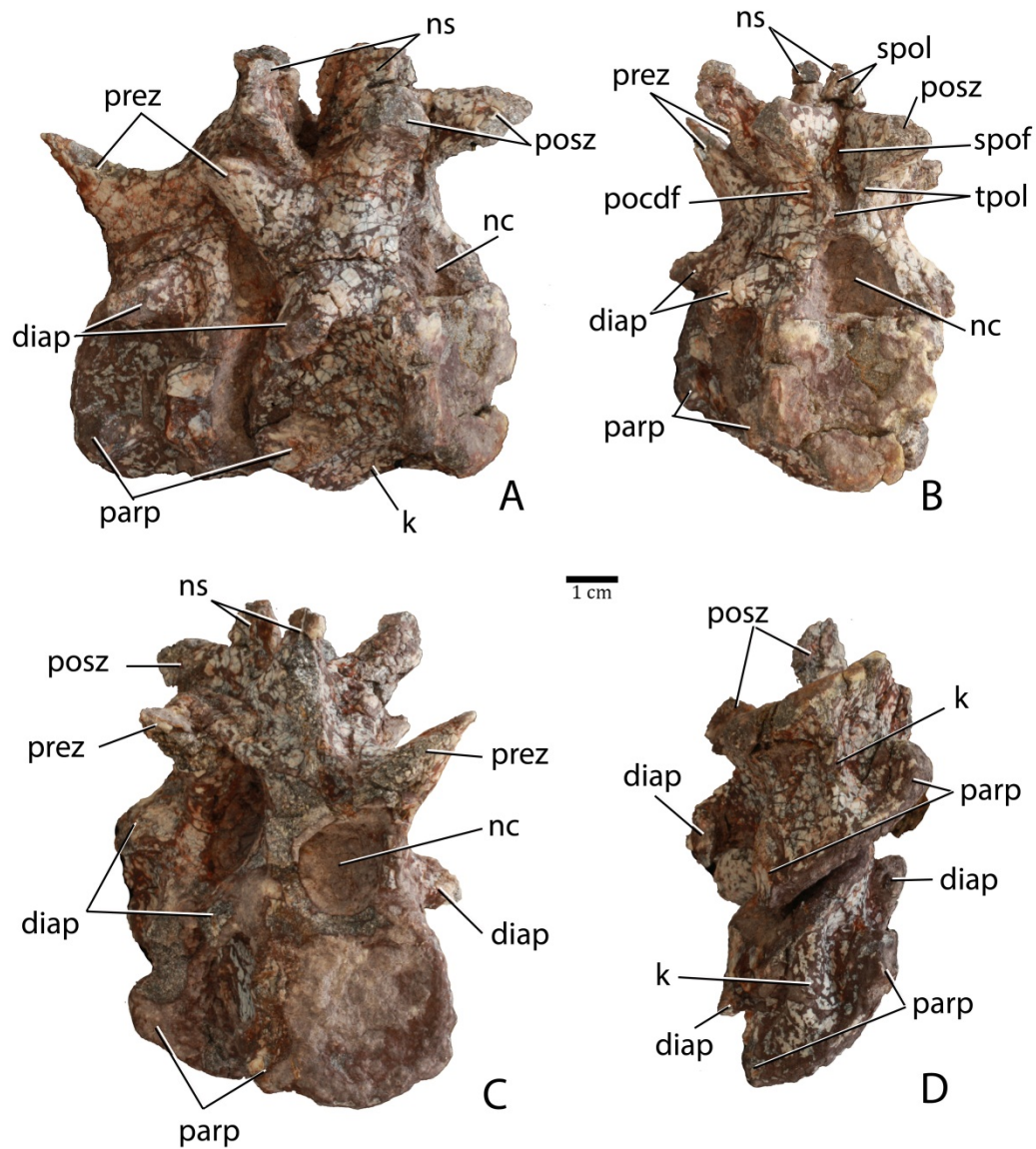
1532 Figure 9. Braincase of *Scutarx deltatylus* (PEFO 34616) in ventrolateral view. Scale bar equals 1  
 1533 cm. Abbreviations: bpt, basiptyergoid processes; bsr, basisphenoid recess; bt, basal  
 1534 tubera; cc, cotylar crest; clp, clinoid process; cp, cultriform process; crp, crista  
 1535 prootica; fo, foramen ovale; hypf, hypophyseal fossa; ic, exit area of the internal  
 1536 carotid artery; lfr, left frontal; lr, lateral ridge; ls, laterosphenoid; mf, metotic  
 1537 foramen; na, nasal; oc, occipital condyle; orb, orbit; pa, parietal; par, paroccipital  
 1538 process of the opisthotic; po, postorbital; pr, prootic; prf, prefrontal; psr,  
 1539 parasphenoid recess; rfr, right frontal; s., suture with designated element; sq,  
 1540 squamosal; uc, unossified cleft of the basal tubera; V, passageway for the  
 1541 Trigeminal nerve.



1542

1543

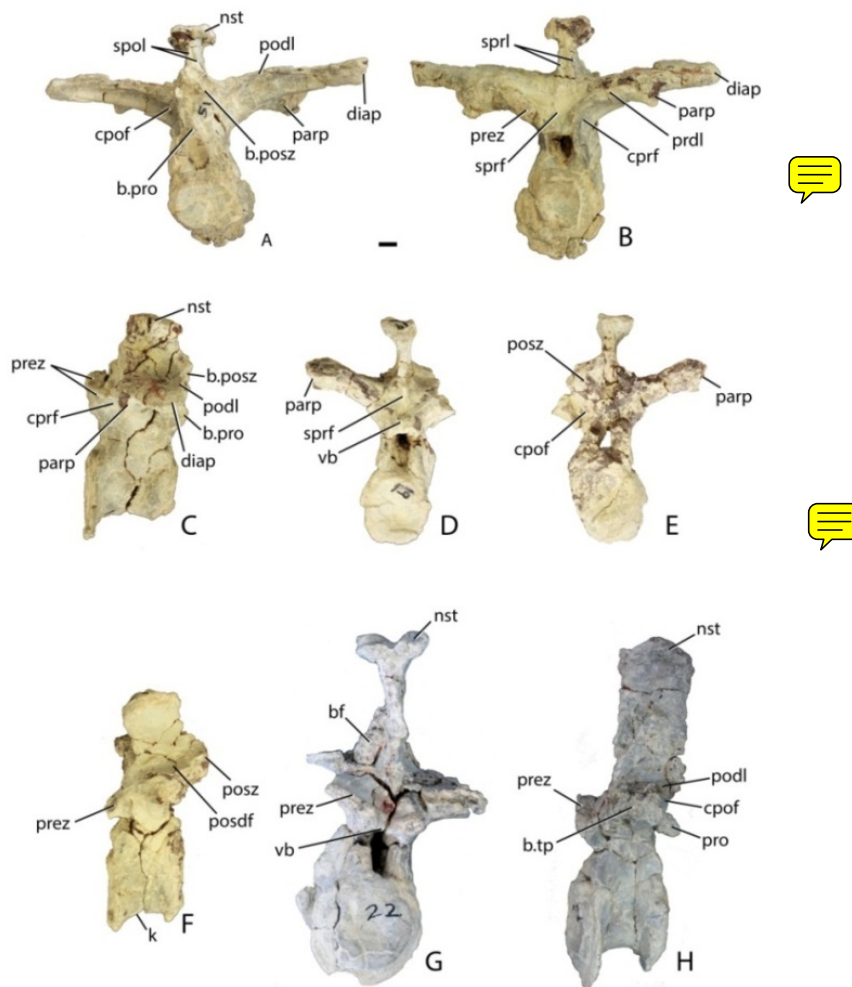
1544 Figure 10. Parabasisphenoid of *Scutarx deltatylus* (PEFO 34616) in ventral view. Scale bar  
 1545 equals 1 cm. Abbreviations: **bpt**, basiptyergoid processes; **bsr**, basisphenoid recess;  
 1546 **bt**, basal tubera; **cp**, cultriform process; **crp**, crista prootica; **f.**, fossa for specified  
 1547 element; **lfr**, left frontal; **lr**, lateral ridge; **ls**, laterosphenoid; **of**, orbital fossa; **orb**,  
 1548 orbit; **par**, paroccipital process of the opisthotic; **po**, postorbital; **prf**, prefrontal; **pr**,  
 1549 prootic; **psr**, parasphenoid recess; quadrate; **rfr**, right frontal; **sq**,  
 1550 squamosal; **ssr**, subsellar recess; **stf**, supratemporal fenestra; **uc**, unossified cleft of  
 1551 the basal tubera.



1552

1553

1554 Figure 11. Articulated anterior post-axial vertebrae of *Scutarx deltatylus* (PEFO 31217) in  
 1555 posterolateral (A), posterior (B), anterior (C), and ventral (D) views. Scale bar  
 1556 equals 1 cm. Abbreviations: diap, diapophysis; k, keel; nc, neural canal; ns, neural  
 1557 spine; parp, parapophysis; pocdf, postzygapophyseal centrodiapophyseal fossa;  
 1558 posz, postzygapophysis; prez, prezygapophysis; spof, spinopostzygapophyseal  
 1559 fossa; spol, spinopostzygapophyseal lamina; tpol, intrapostzygapophyseal lamina.



1560

1561

1562 Figure 12. Trunk vertebrae of *Scutarx deltatylus*. A-C, PEFO 34045/FF-51, mid-trunk

1563 vertebra in posterior (A), anterior (B), and lateral (C) views. D-F, PEFO 34045/19, Anterior

1564 trunk vertebra in anterior (D), posterior (E), and lateral (F) views. G-H, PEFO 34045/22,

1565 Posterior trunk vertebra in anterior (G) and lateral (H) views. Scale bar equals 1 cm.

1566 Abbreviations: b., broken designated element; bf, bone fragment; cpor, centropostzygapophyseal

1567 fossa.; cpor, centroprezygapophyseal fossa; diap, diapophysis; k, keel; nst, neural spine table;

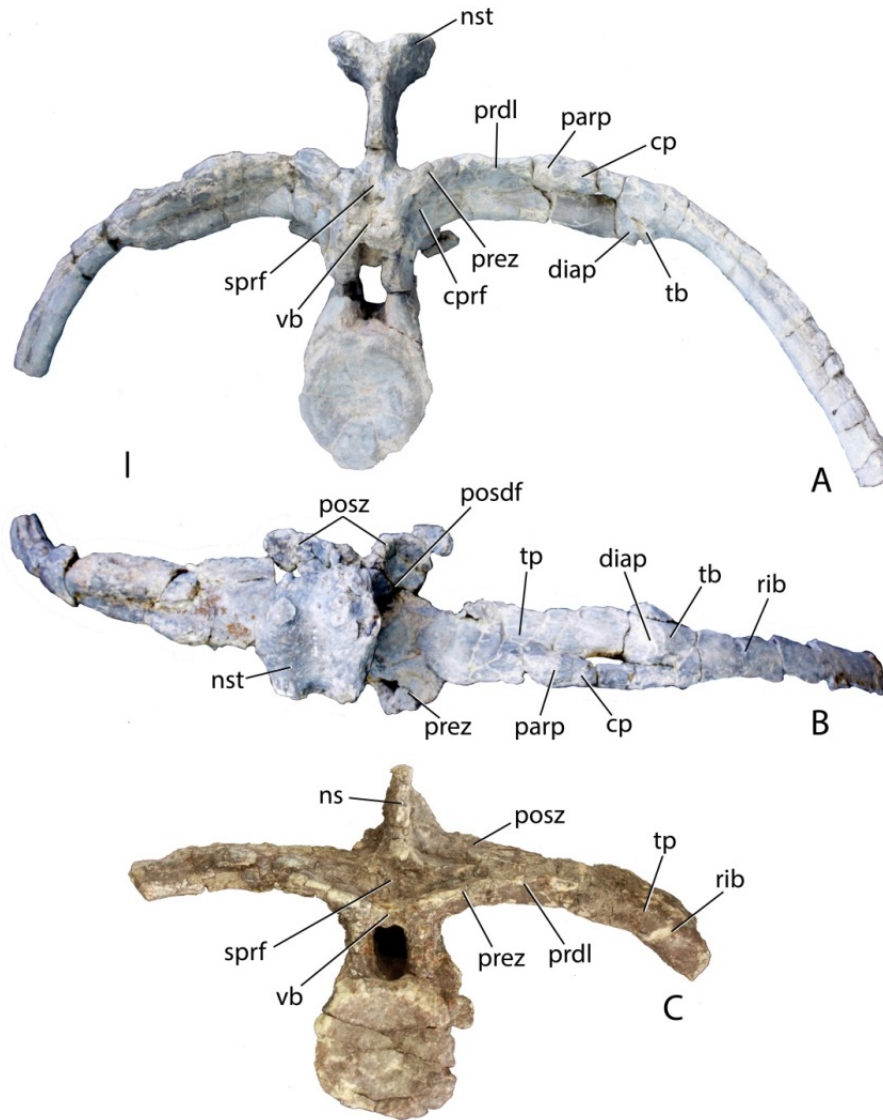
1568 parp, parapophysis; podl, postzygodiapophyseal lamina; posdf, postzygapophyseal

1569 spinodiapophyseal fossa; posz, postzygapophysis; prez, prezygapophysis; pro, projection; sprf,

1570 spinoprezygapophyseal fossa; spol, spinopostzygapophyseal lamina; tp, transverse process; vb,

1571 ventral bar.

1572



1573

1574

1575

1576 Figure 13. Posterior trunk vertebrae of *Scutarx deltatylus*. A-B, PEFO 34045 in anterior

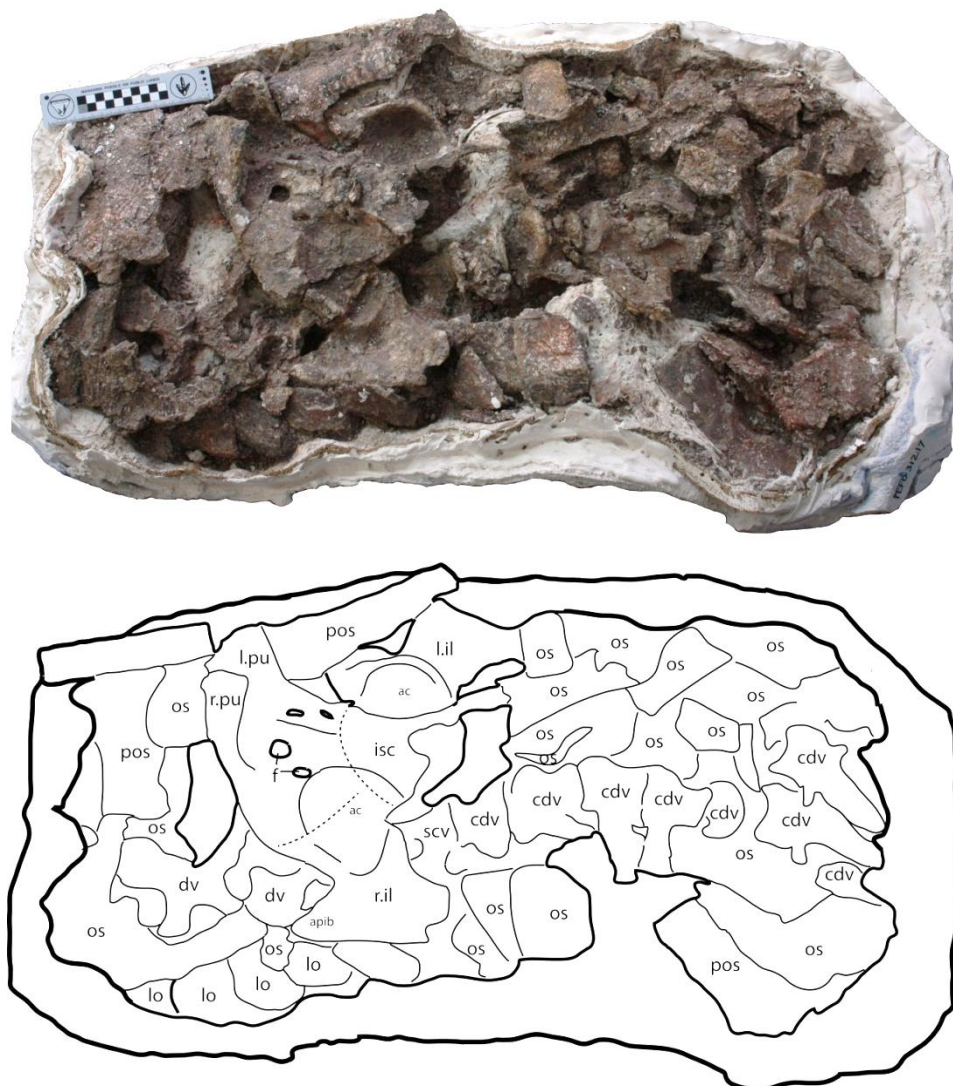
1577 (A) and dorsal (B) view. C, PEFO 31217 in anterior view. Scale bar equals 1 cm. Abbreviations:

1578 cp, capitulum; cprf, centroprezygapophyseal fossa; diap, diapophysis; ns, neural spine; nst,

1579 postzygapophyseal spinodiapophyseal fossa; posz, postzygapophysis; prez, prezygapophysis;

1580 sprf, spinoprezygapophyseal fossa; tb, tuberculum; tp, transverse process; vb, ventral bar.

1581



1582

1583

1584

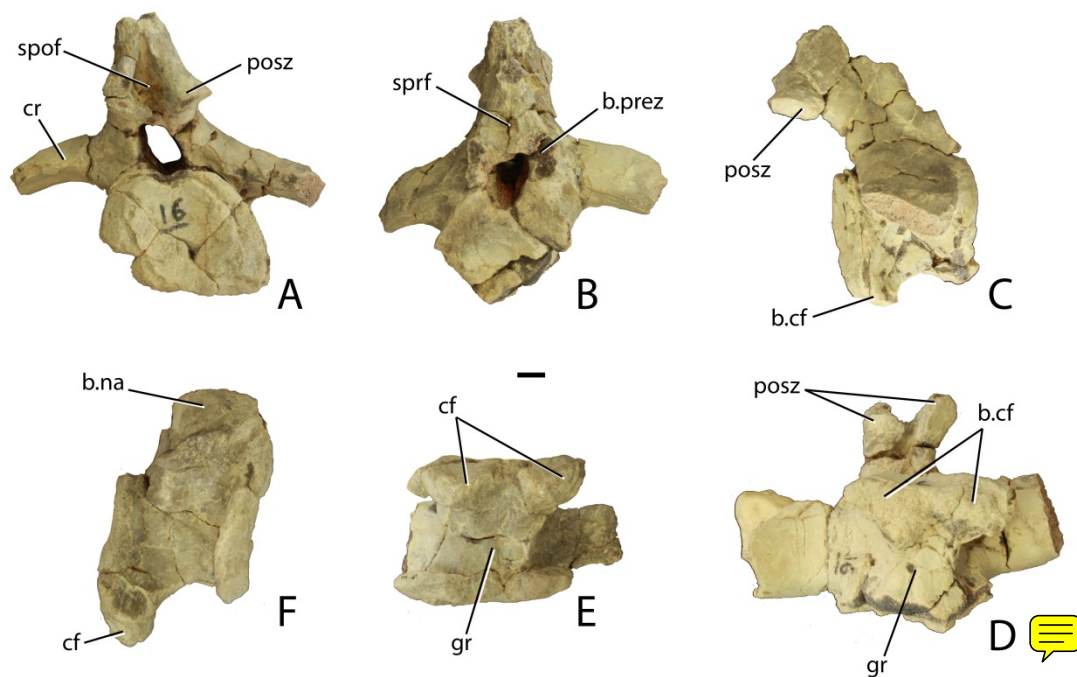
1585 Figure 14. Photo and interpretive sketch of a partially articulated sacrum and anterior

1586 portion of the tail of *Scutarx deltatylus* (PEFO 31217). Scale bar equals 10 cm. Abbreviations:

1587 ac, acetabulum; apib, anterior process of the iliac blade; cdv, caudal vertebra; dv, trunk vertebra;

1588 f, foramen; isc, ischia; l.il, left ilium; l.pu, left pubis; lo, lateral osteoderm; os, osteoderm; pos,

paramedian osteoderm; r.il, right ilium; r.pu, right pubis; scv, sacral vertebra.

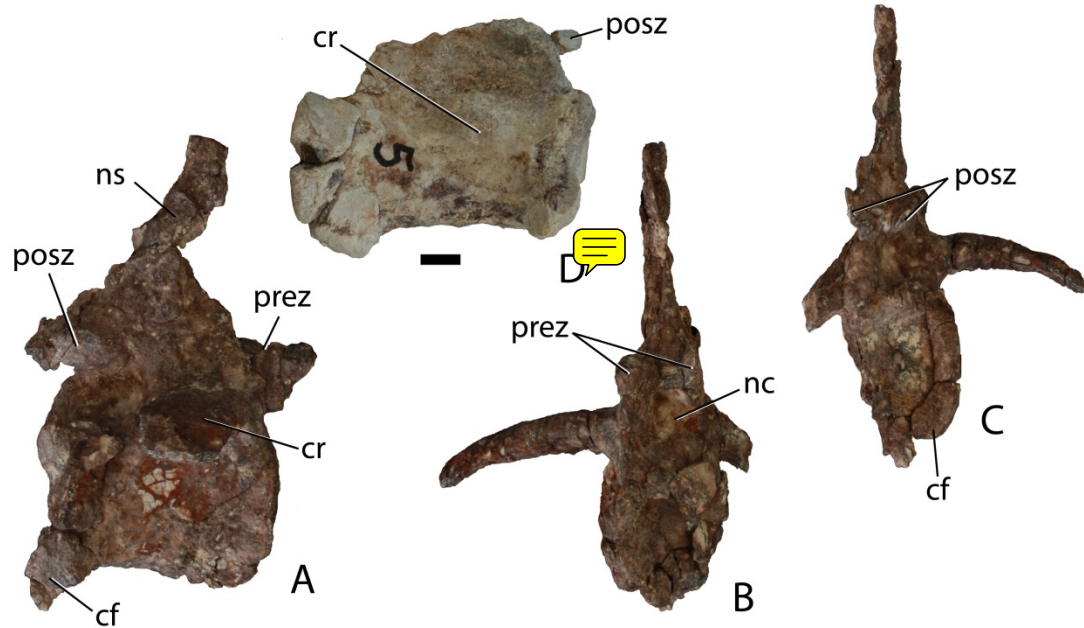


1589

1590

1591 Figure 15. Anterior caudal vertebrae of *Scutarx deltatylus* (PEFO 34045). A-D, anterior caudal in  
 1592 posterior (A), anterior (B), lateral (C), and ventral (D). E-F, Anterior caudal  
 1593 vertebra in ventral (E) and lateral (F). Scale bar equals 1 cm. Abbreviations: b.,  
 1594 broken designated element; cf, chevron facet; cr, caudal rib; gr, ventral groove;  
 1595 posz, postzygapophysis; prez, prezygapophysis; spof, spinopostzygapophyseal fossa,  
 1596 ; sprf, spinoprezygapophyseal fossa.

1597

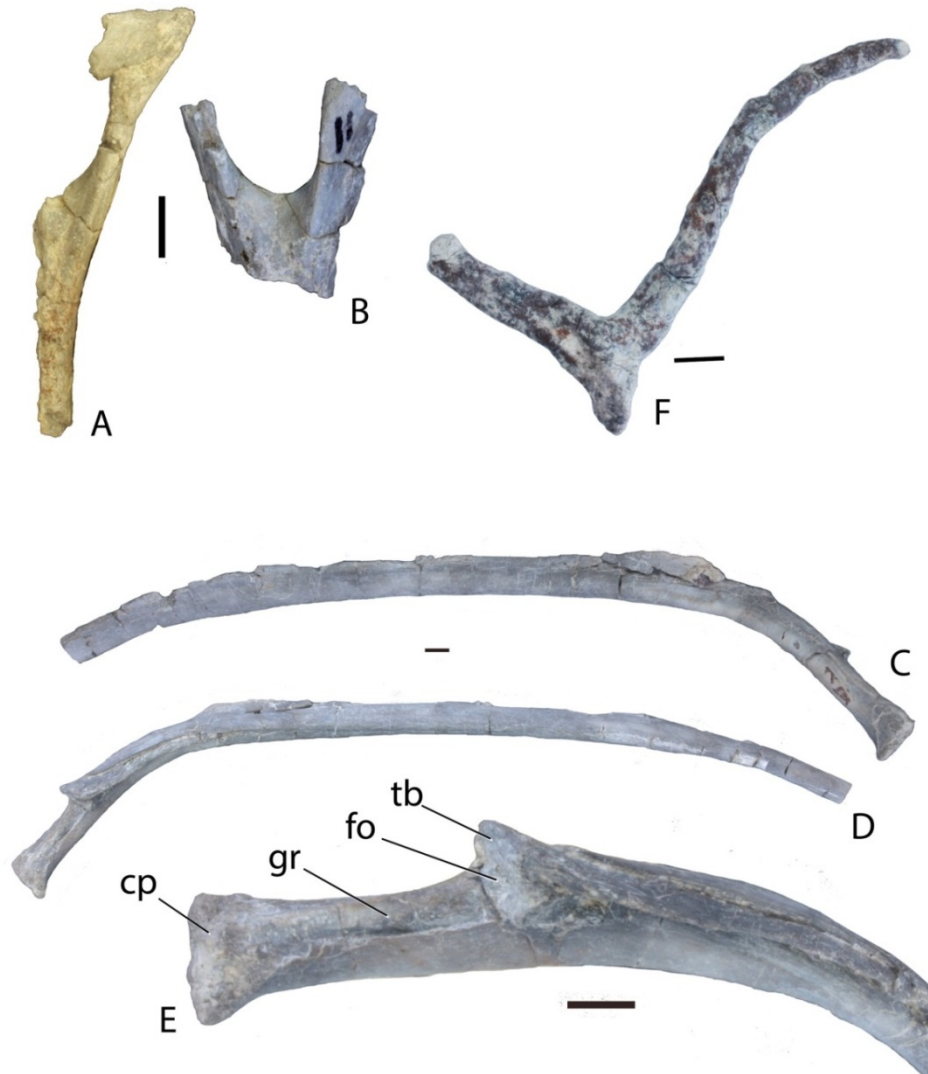


1598

1599

1600 Figure 16. Mid-caudal vertebrae of *Scutarx deltatylus*. A-C, anterior mid-caudal vertebra (PEFO  
 1601 34919) in lateral (A), anterior (B), and posterior (C) views. D, posterior mid-caudal  
 1602 vertebra (PEFO 34045) in lateral view. Scale bar = 1 cm. Abbreviations: cf,  
 1603 chevron facet; cr, caudal rib; ns, neural spine; prez, prezygapophysis; posz,  
 1604 postzygapophysis.

1605



1606

1607

1608 Figure 17. Chevrons and ribs of *Scutarx deltatylus*. A-B, partial anterior chevrons from

1609 PEFO 34045 in posterior view; C-D, left trunk rib from PEFO 34045 in posterior (C) and

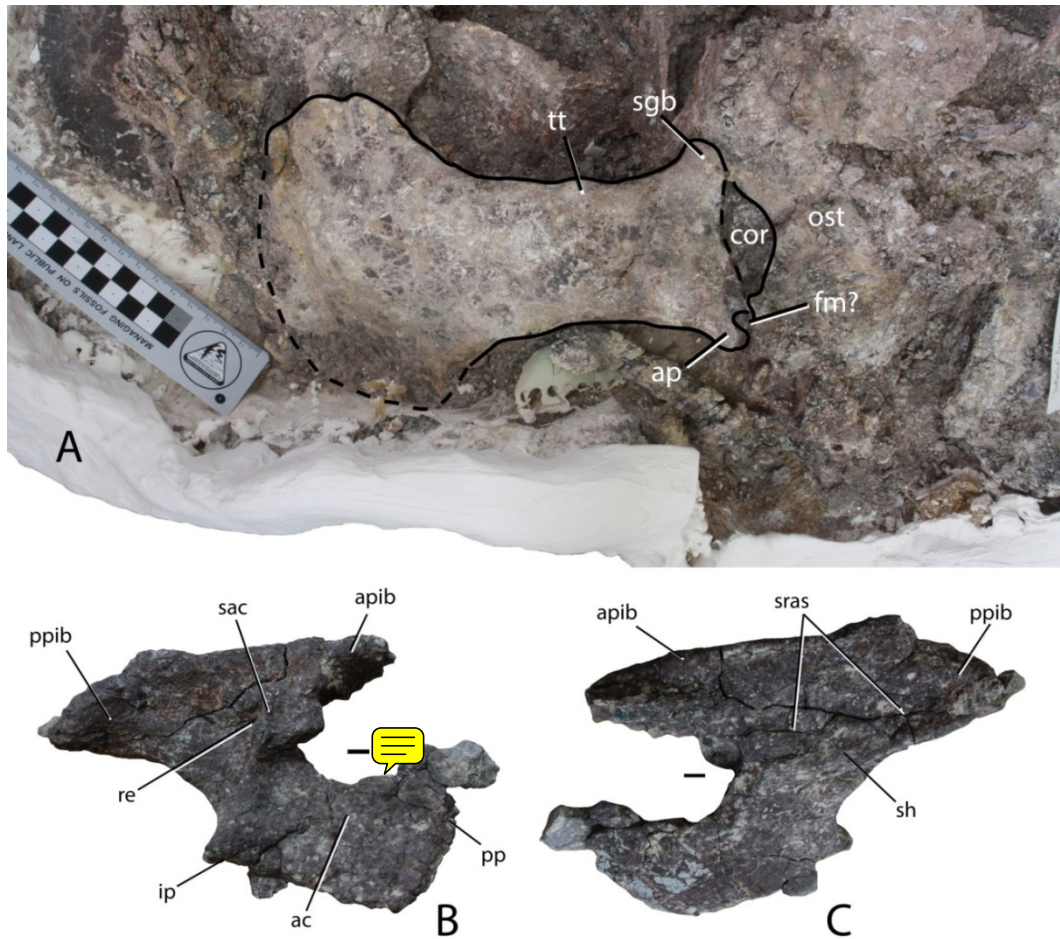
1610 anterior (D) views. E, close-up view of head of trunk rib from PEFO 34045. F, paired gastral ribs

1611 from PEFO 34616. Scale bars equal 1 cm. Abbreviations: cp, capitulum; fo, fossa; gr, groove; tb,

1612 tuberculum.

1613

1614



1615

1616

1617 Figure 18. Girdle elements of *Scutarx deltatylus*. A, left scapulocoracoid of PEFO 31217

1618 in lateral view. B-C, right ilium of PEFO 34919 in 'lateral' and 'medial' views (see text for

1619 discussion regarding anatomical direction of the ilium). Scale bars equal 10 cm (A) and 1 cm (B-

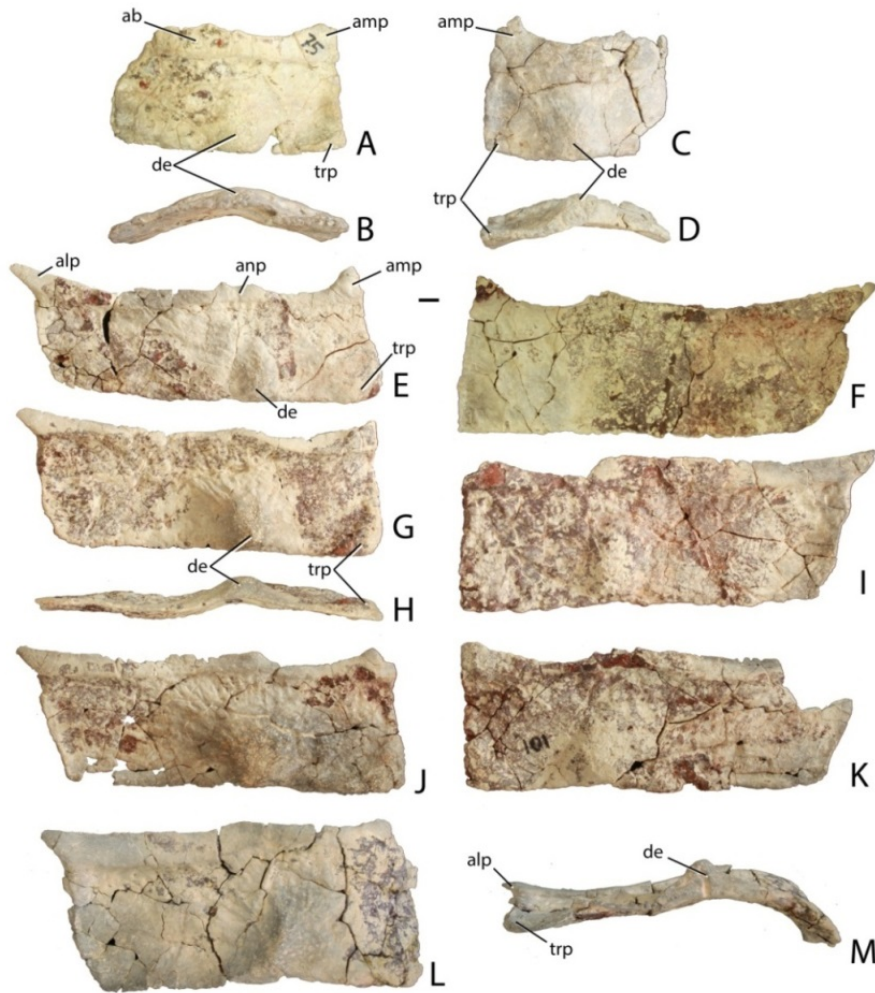
1620 C). Abbreviations: ac, acetabulum; ap, acromion process; apib, anterior process of the iliac

1621 blade; cor, coracoid; fm, foramen; ip, ischiadic peduncle; ost, osteoderms; pp, pubic peduncle;

1622 ppib, posterior process of the iliac blade; re, recess; sac, supraacetabular crest; sgb, supraglenoid

1623 buttress; sh, shelf; sras, sacral rib attachment surfaces; tt, triceps tubercle.

1624



1625

1626

1627

1628 Figure 19. Cervical and dorsal trunk paramedian osteoderms of *Scutarx deltatylus* from

1629 PEFO 34045. A-B, left mid-cervical osteoderm in dorsal (A) and posterior (B) views. C-D, right

1630 mid-cervical osteoderm in dorsal (C) and posterior (D). E-F, left (E) and right (F) dorsal trunk

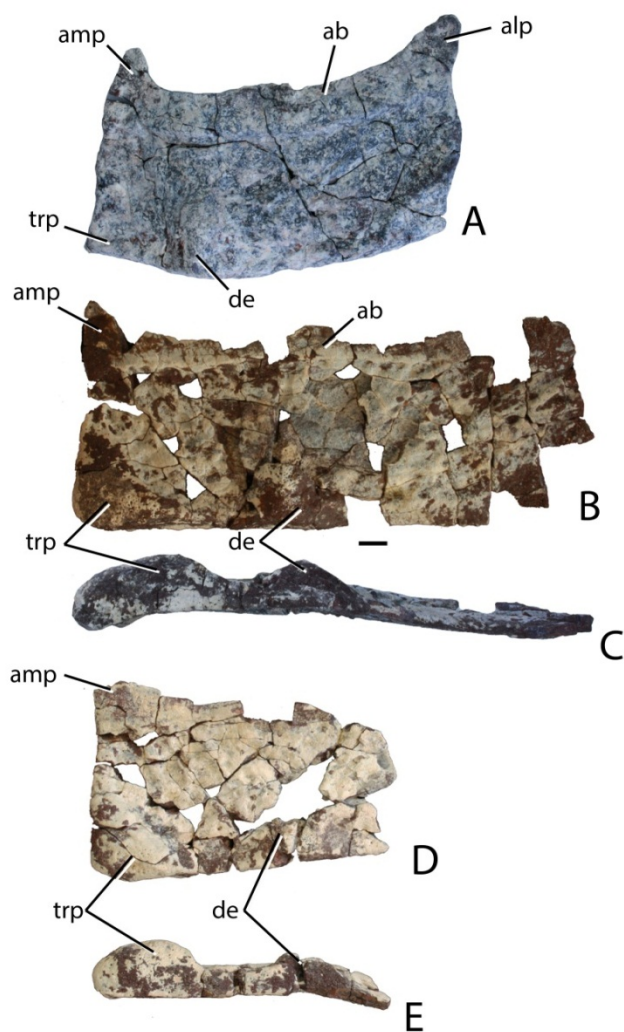
1631 osteoderms in dorsal (G, I) and posterior (H) views. J-K, left (J) and right (K) dorsal trunk osteoderms in dorsal view. L-M,

1632 posterior dorsal trunk osteoderm in dorsal (L) and posterior (M) views. Scale bar = 1 cm.

1633 Abbreviations: ab, anterior bar; alp, anterolateral process; amp, anteromedial process; anp,

1634 anterior process; de, dorsal eminence; trp, triangular protuberance.

1635



1636

1637

1638 Figure 20. Holotype paramedian osteoderms of *Scutarx deltatylus* from PEFO 34616. A,

1639 posterior cervical osteoderm in dorsal view. B-C, right dorsal trunk paramedian osteoderm in

1640 dorsal (B) and posterior (C) views. D-E, partial right dorsal trunk paramedian osteoderm in

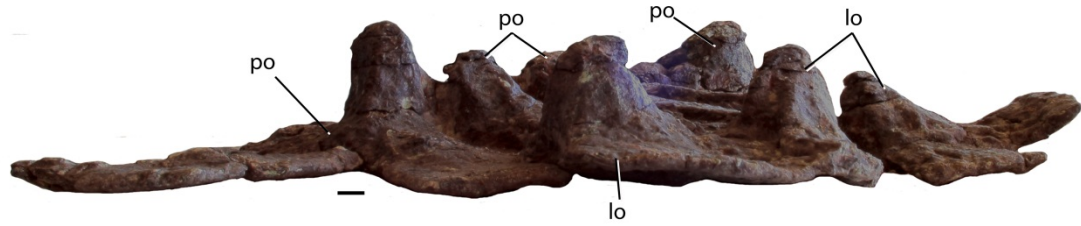
1641 dorsal (D) and posterior (E) views. Note the prominence of the triangular protuberance in the

1642 posterior views. Scale bar equals 1 cm. Abbreviations: ab, anterior bar; alp, anterolateral process;

1643 amp, anteromedial process; de, dorsal eminence; trp, triangular protuberance.

1644

1645

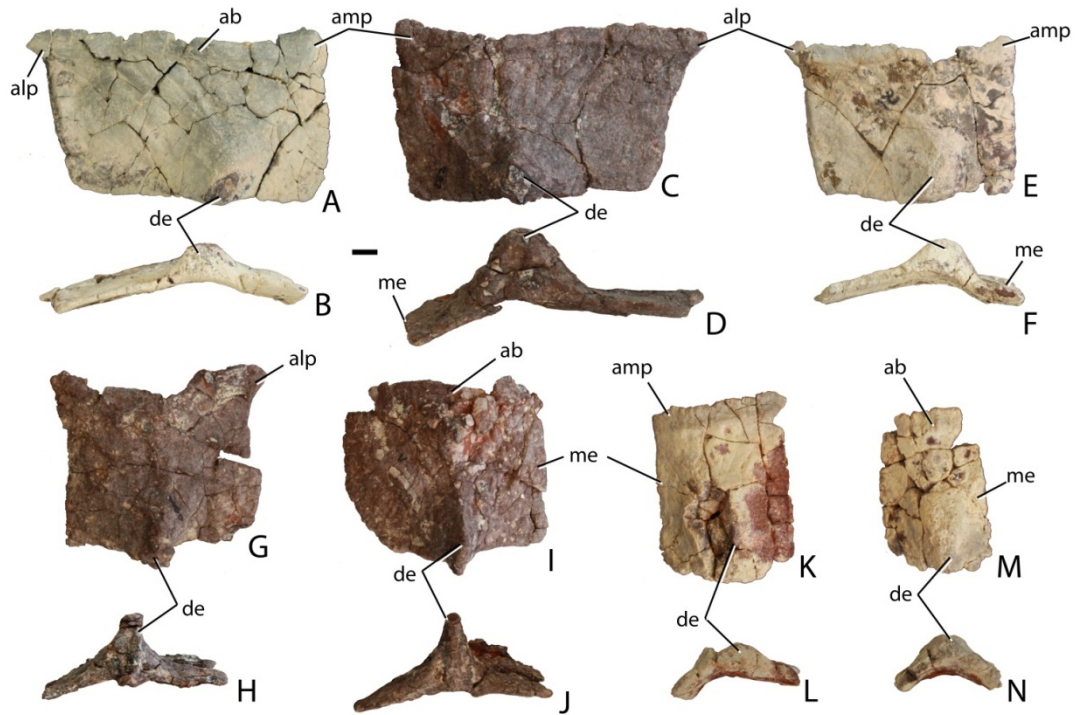


1646

1647

1648 Figure 21. Fused semi-articulated anterior dorsal caudal paramedian and dorsal caudal lateral  
1649 osteoderms of *Scutarx deltatylus* (PEFO 34919) in a lateral view showing extreme  
1650 development of the dorsal eminences. Scale bar equals 1 cm. Abbreviations: lo,  
1651 lateral osteoderm; po, paramedian osteoderm.

1652



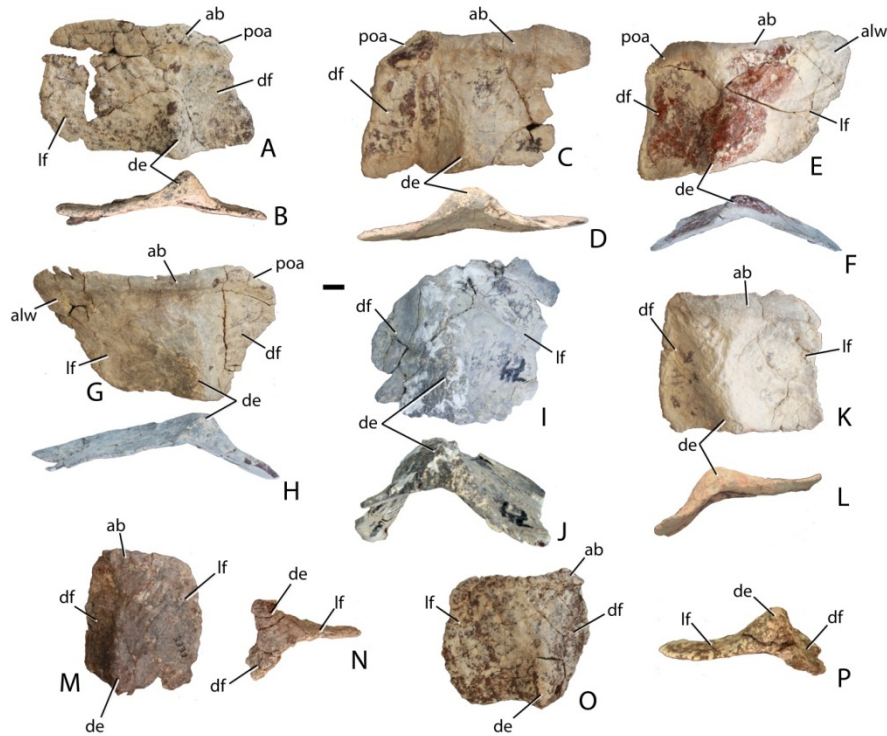
1653

1654

1655 Figure 22. Dorsal caudal paramedian osteoderms of *Scutarx deltatylus*. A-B, left anterior mid-  
 1656 caudal osteoderm (PEFO 34045) in dorsal (A) and posterior (B) views. C-D, right  
 1657 anterior mid-caudal osteoderm (PEFO 34919) in dorsal (C) and posterior (D) views;  
 1658 E-F, left mid-caudal osteoderm (PEFO 34045) in dorsal (E) and posterior (F) views.  
 1659 G-H, right mid-caudal osteoderm (PEFO 34919) in dorsal (G) and posterior (H)  
 1660 views. I-J, left mid-caudal osteoderm (PEFO 34919) in dorsal (I) and posterior (J)  
 1661 views. K-L, right posterior caudal osteoderm (PEFO 34045) in dorsal (K) and  
 1662 posterior (L) views. M-N, left posterior caudal osteoderm (PEFO 34045) in dorsal  
 1663 (M) and posterior (N) views. Scale bar equals 1 cm. Abbreviations: ab, anterior  
 1664 bar; alp, anterolateral process; amp, anteromedial process; de, dorsal eminence; me,  
 1665 medial edge.

1666

1667



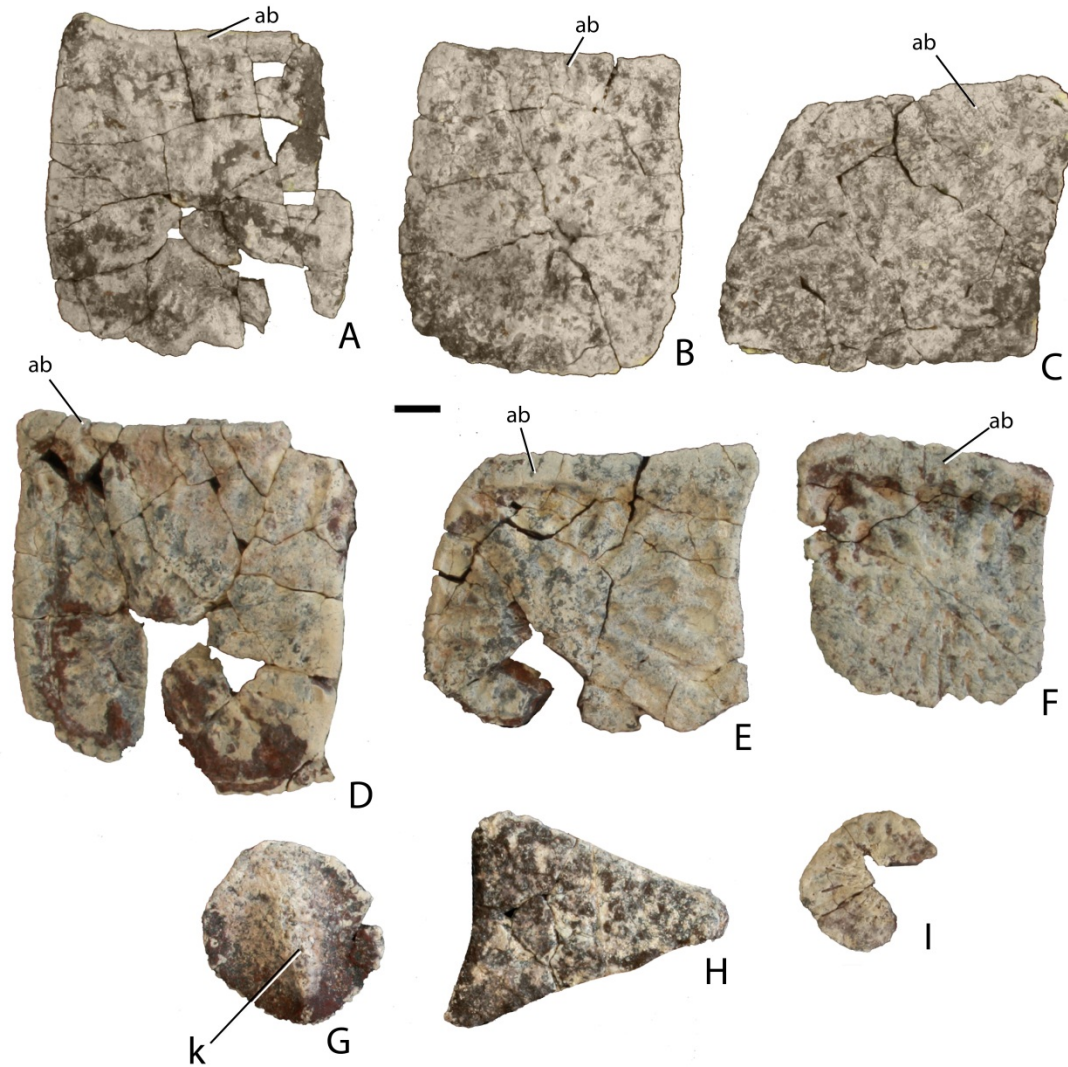
1668

1669

1670 Figure 23. Lateral osteoderms of *Scutarx deltatylus*. A-B, left anterior trunk osteoderm (PEFO  
 1671 34616) in dorsal (A) and posterior (B) views; C-D, right anterior trunk osteoderm  
 1672 (PEFO 34045) in dorsal (C) and posterior (D) views; E-F, right posterior mid-trunk  
 1673 osteoderm (PEFO 34045) in dorsal (E) and posterior (F) views; G-H, left posterior  
 1674 mid-trunk osteoderm (PEFO 34045) in dorsal (G) and posterior (H) views; I-J, right  
 1675 posterior trunk osteoderm (PEFO 34045) in dorsal (I) and posterior (J) views; K-L,  
 1676 right anterior dorsal caudal osteoderm (PEFO 34045) in dorsal (K) and posterior (L)  
 1677 views; right posterior dorsal mid-caudal osteoderm (PEFO 34919) in dorsal (M) and  
 1678 posterior (N) views; O-P, left dorsal mid-caudal osteoderm (PEFO 34616) in dorsal  
 1679 (O) and posterior (P) views. Scale bar equals 1 cm. Abbreviations: ab, anterior bar;  
 1680 alw, anterolateral wing; de, dorsal eminence; df, dorsal flange; mf, medial flange;  
 1681 poa, paramedian osteoderm articular surface.

1682

1683



1684

1685

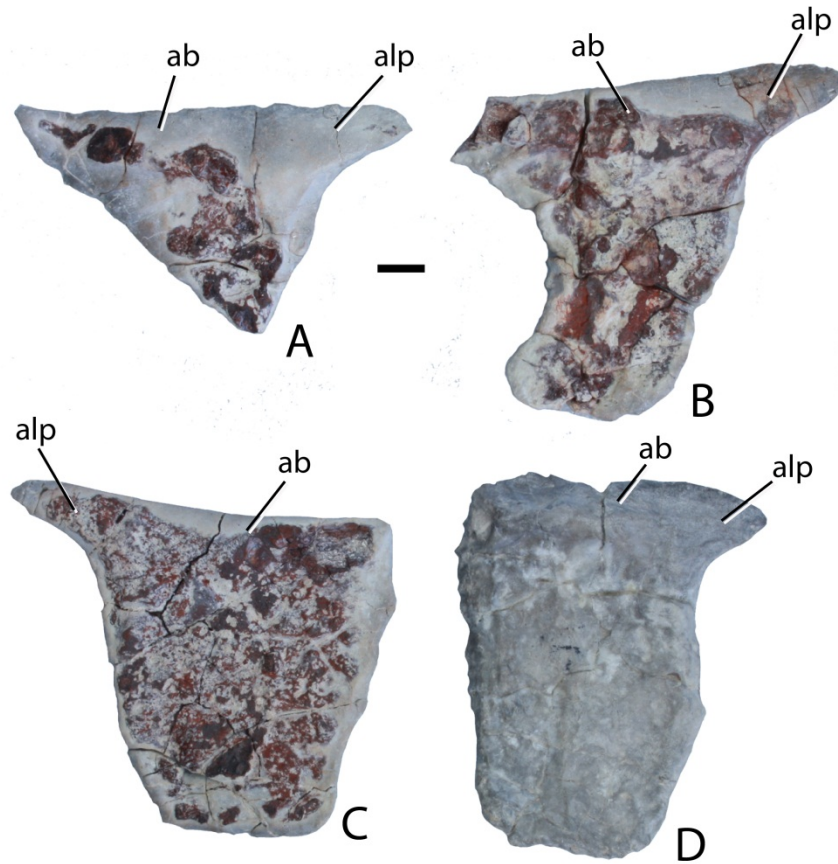
1686 Figure 24. Ventral trunk and appendicular osteoderms of *Scutarx deltatylus* from PEFO 34616.

1687 A-F, square ventral osteoderms. G, round, keeled appendicular osteoderm. H,

1688 triangular ventral or appendicular osteoderm. I, round, ornamented appendicular

1689 osteoderm. Scale bar equals 1 cm. Abbreviations: ab, anterior bar; k, keel.

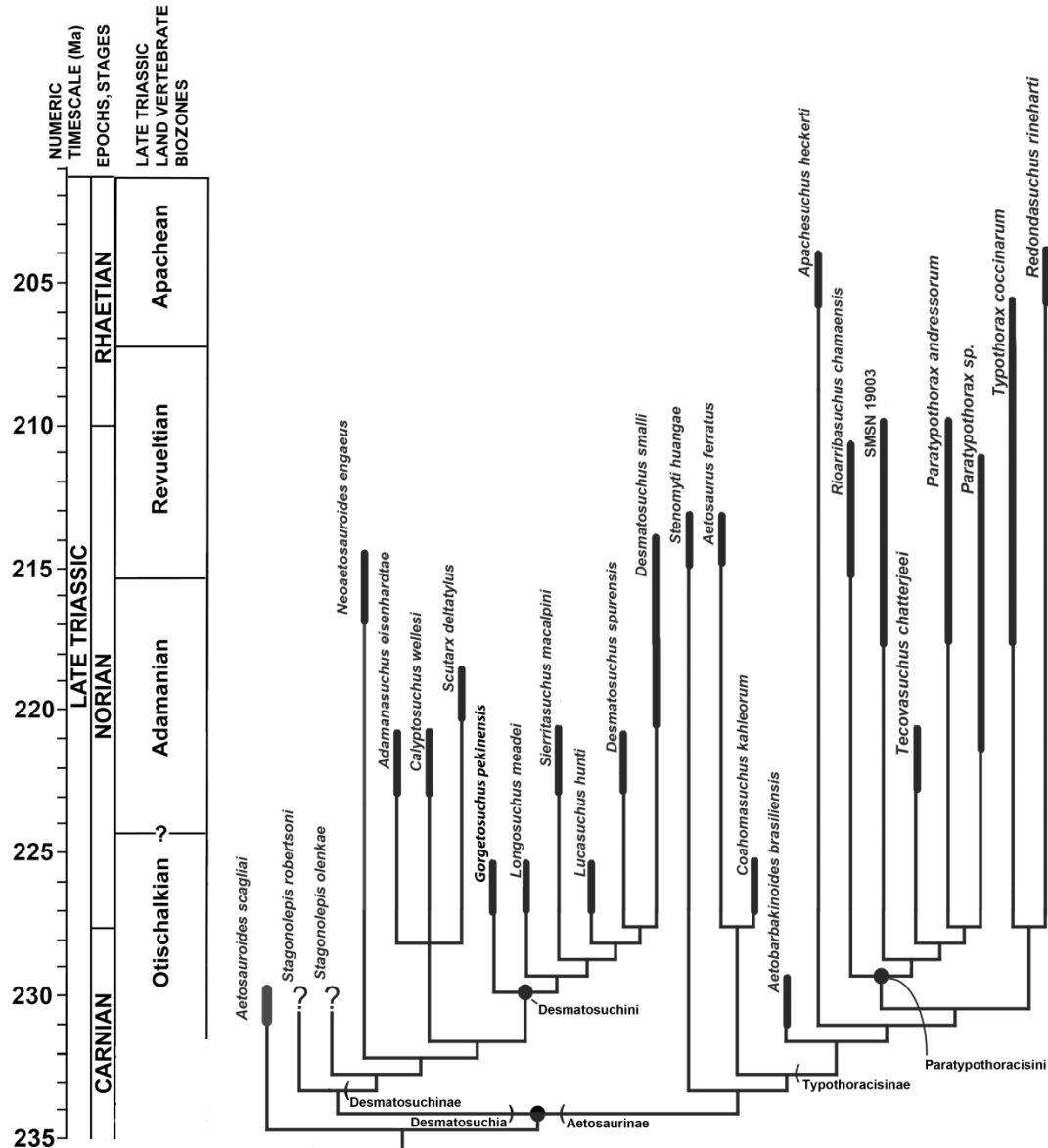
1690



1691

1692

1693 Figure 25. Incompletely formed trunk paramedian osteoderms from PEFO 34045. A-B, right  
1694 osteoderms in dorsal view; C, left osteoderm in dorsal view; D, right osteoderm in  
1695 dorsal view. Scale bar equals 1 cm. Abbreviations: ab, anterior bar; alp,  
1696 anterolateral process.



1698

1699

1700 Figure 26. Time-calibrated phylogeny of the Aetosauria showing estimated ranges of taxa in the  
 1701 Triassic stages and associated vertebrate biozones.

1702

1703

1704

1705